

Dissertation
submitted to the
Combined Faculties for the Natural Sciences and for Mathematics
of the Ruperto-Carola University of Heidelberg, Germany
for the degree of
Doctor of Natural Sciences

Presented by

M.Sc. (Animal Biotechnology) Raga Deepthi Ediga
Born in Kurnool, India

Oral-examination: November 2018

Identification of effective drug targets in treating Glutaric aciduria type 1 disease

Referees: Prof. Dr. Marc Freichel
Dr. rer. nat. Sven Wolfgang Sauer

*This thesis is dedicated to my better half **Dr.rer.nat. Jagadeesh Gandla**. You are incredible....*

Table of Contents

Summary	1-2
Zusammenfassung	3-4
Abbreviations	5-6
1. Introduction	7-30
1.1 Lysine	
1.1.1 Metabolism of Lysine	
1.1.1.1 Anabolism of Lysine	
1.1.1.2 Catabolism of Lysine	
1.1.1.2.1 Saccharopine pathway of lysine degradation	
1.1.1.2.2 Pipecolate pathway of lysine degradation	
1.1.1.2.3 Convergence of pipecolic acid pathway and saccharopine pathway	
1.2 Inborn errors of lysine metabolism	
1.2.1 Hyperlysinemia	
1.2.2 2-aminoadipic 2-oxoadipic aciduria	
1.2.3 Zellweger syndrome	
1.2.4 Glutaric aciduria type I	
1.2.4.1 Biochemical features of GA-I	
1.2.4.2 Clinical features of GA-I	
1.2.4.3 Neuropathology of GA-I	
1.2.4.4 Gcdh knockout mouse model	
1.2.4.5 Treatment strategies followed for GA-I patients	
1.2.4.6 Alternate therapeutic strategies	
1.2.4.6.1 Target 1, DHTKD1	
1.2.4.6.2 Target 2, AADAT	
1.3 Objectives of the thesis	
2. Materials and Methods	31-56
2.1 Materials	

- 2.1.1 Chemicals used
- 2.1.2 Consumables used
- 2.1.3 List of Primers
- 2.1.4 List of antibodies
- 2.1.5 Inhibitors used
- 2.1.6 Commercially available kits used
- 2.1.7 General Buffers used
- 2.1.8 Instruments used

2.2 Methods

- 2.2.1 Cloning of DHTKD1 into pGEX4T1 vector
 - 2.2.1.1 PCR amplification of DHTKD1
 - 2.2.1.2 Restriction digestion of vector and insert
 - 2.2.1.3 Ligation of vector and insert
 - 2.2.1.4 Transformation and positive clone confirmation
- 2.2.2 DHTKD1 protein expression and purification using Glutathione sepharose beads
 - 2.2.2.1 Transformation, starter culture preparation and protein expression
 - 2.2.2.2 Preparation of Glutathione sepharose beads and purification of protein (protocol from GE healthcare, modified)
 - 2.2.2.3 Western blotting and confirmation of purified DHTKD1 protein
- 2.2.3 DHTKD1 enzyme activity assay
- 2.2.4 Determination of K_m and V_{max} for DHTKD1
 - 2.2.4.1 DHTKD1 inhibitor studies
- 2.2.5 Western blotting of Dhtkd1 in mouse tissue samples
 - 2.2.5.1 Preparation of tissue homogenates
 - 2.2.5.2 Determining the concentration of protein
 - 2.2.5.3 SDS-PAGE, immunoblotting and detection by enhanced chemiluminescence
- 2.2.6 Analysis of Glutaric acid (GA), 2-oxoadipic acid (OA) and 2-aminoadipic acid (AA) quantitatively
- 2.2.7 Measurement of Glutaryl carnitine levels
- 2.2.8 Culturing of fibroblasts, HEK 293T and HeLa cells

- 2.2.9 AADAT siRNA treatment
- 2.2.10 CRISPR/Cas9 method for the generation of GCDH and AADAT
 - Knockouts
 - 2.2.10.1 Designing gRNAs
 - 2.2.10.2 Oligo annealing and cloning into PX459 vector
 - 2.2.10.3 Determining the cytotoxicity of puromycin for HEK and HeLa cells
 - 2.2.10.4 Transfection of PX459-gRNA constructs into HEK and HeLa cells
 - 2.2.10.5 Confirmation of Knockout cells by western blotting
 - 2.2.10.6 Generation of single cell clones of GCDH Knockout and AADAT knockout cells
- 2.2.11 Inhibitor treatment of patient fibroblasts and measurement of glutaric acid (GA) levels using GCMS
- 2.2.12 Establishing enzyme activity assay for AADAT in patient fibroblasts
- 2.2.13 Effect of PF-04859989 inhibitor on HEK and HeLa GCDH Knockout cells and GA detection using GCMS
- 2.2.14 Detection of DNA damage in fibroblasts
 - 2.2.14.1 Seeding of patient and control cells
 - 2.2.14.2 Immunofluorescence staining
 - 2.2.14.3 Image analysis
- 2.2.15 Statistical analysis

3. Results

57-87

- 3.1 Can targeting DHTKD1 rescue the clinical and biochemical phenotype of GA-I?
 - 3.1.1 Cloning, expression and purification of DHTKD1 protein
 - 3.1.2 Determining the substrate specificity and enzyme kinetics of purified DHTKD1 protein
 - 3.1.3 Pharmacological inhibition of DHTKD1
 - 3.1.4 Murine model for targeting DHTKD1
 - 3.1.4.1 Generation of Dhtkd1 Knockout (Dhtkd1^{-/-}/Gcdh^{+/+}) mice
 - 3.1.4.2 Behavioral and biochemical characterization of Dhtkd1^{-/-}/Gcdh^{+/+} mice

3.1.4.3	Knockout of Dhtkd1 was not able to rescue the clinical and biochemical phenotype seen in Gcdh-deficient mice	
3.1.4.3.1	Generation and characterization of double Knockout (Dhtkd1-/-/Gcdh-/-) mice	
3.1.4.3.1.1	The clinical phenotype of Dhtkd1-/-/Gcdh-/- mice contradicts our current hypothesis	
3.1.4.3.1.2	The biochemical phenotypes of Dhtkd1-/-/Gcdh-/- and Gcdh-/- mice do not differ	
3.2.	AADAT as an alternative target for treating GA-1 patients?	
3.2.1	siRNA mediated knockdown of AADAT	
3.2.2	Inhibition of AADAT by PF-04859989 <i>in vitro</i>	
3.2.3	Effect of lysine stress induction on GA levels of GA-I patient and control Fibroblasts	
3.2.4	Effect of AADAT inhibitor on GA levels of patient and control fibroblasts	
3.3	Generation of alternative GA-I cell culture models	
3.3.1	CRISPR/Cas9-mediated generation of knockout cells	
3.3.2	Analysis of GA levels in GCDH Knockout and control cells after inhibitor treatment	
4.	Discussion	88-97
4.1	Inhibiting of DHTKD1 function does not rescue the clinical and biochemical phenotype of Gcdh-/- mice	
4.2	Development of an alternative therapeutic strategy	
4.3	Outlook 1. Novel mechanism of chronic GA-induced toxicity	
4.4	Outlook 2, Role of DHTKD1 in Diabetes	
5.	Conclusions	98
6.	References	99-115
7.	Original publications	116
8.	Acknowledgements	117

Summary (English)

Glutaric aciduria type I (GA-I) is an autosomal recessive cerebral organic aciduria, caused by a defective GCDH enzyme. This protein lies in the common final catabolic pathway of L-lysine, L-hydroxy lysine and L-tryptophan. Individuals possessing GCDH enzyme deficiency are biochemically characterized by the accumulation of neurotoxic metabolites glutaryl-CoA, GA, 3-OH-GA as well as non-toxic C5DC in their tissues and body fluids. If untreated, most of the individuals develop an acute encephalopathic crisis causing striatal damage during a finite period of brain growth, resulting in complex movement disorder with predominant dystonia, most commonly between 3 months to 3 years of age. Individuals, diagnosed before the onset of irreversible neurologic symptoms can be prevented from striatal damage, if they are treated with a special diet consisting of low L-lysine content, supplementation with carnitine and essential amino acids as well as emergency treatment on demand. Even though the currently followed metabolic treatment is predicted to be safe and effective, a significant number of patients still suffer from striatal damage despite early diagnosis and treatment. In addition, recent findings report on extra-striatal, extra cerebral and non-neurologic abnormalities despite the current regimen followed. This highlights the prerequisite for the discovery of novel, safe and more efficient long-term treatment strategies. In this thesis, we hypothesize that pharmacological inhibition of upstream enzymatic steps of the lysine degradation pathway, prior to GCDH, will prevent toxic metabolite accumulation and, consequently, induction of clinical disease phenotype in Glutaric aciduria Type I. To this end, Dehydrogenase E1 and transketolase domain containing 1 (DHTKD1) (approach1) and Amino adipate amino transferase (AADAT) (alternate approach 2) are targeted and our hypothesis is tested in genetically modified cell models, Glutaric aciduria type I patient cell lines, and knockout mouse models. We therefore, developed a *Dhtkd1*^{-/-}/*Gcdh*^{-/-} mouse model and studied its characteristics biochemically and clinically after giving high lysine (4.7% (w/w) or 235mg of L-lysine in food) in diet. Our studies showed that DHTKD1 knockout was unable to rescue GA-I phenotype in *Dhtkd1*^{+/+}/*Gcdh*^{-/-} mice as seen by the accumulated GA levels on GCMS measurement. Since our in vivo data strongly suggested that DHTDK1 is not a suitable drug target in GA-I, we did not proceed with drug testing.

Next, we evaluated the commercially available, patented AADAT inhibitor PF04859989 in GCDH-deficient cells. Indeed, the inhibitor treatment significantly reduced GA accumulation in these cells. Overall this thesis suggests that, pharmacological inhibition of AADAT is a novel therapeutic strategy for GA-I. .

Zusammenfassung (Deutsch)

Die Glutarsäure-Azidurie Typ I (GA-I) ist eine autosomal-rezessive zerebrale Organoazidurie, die durch einen genetischen Defekt der Glutaryl-CoA-Dehydrigenase (GCDH) verursacht wird. Dieses Protein liegt in dem gemeinsamen Abbauweg von L-Lysin, L-Hydroxylysin und L-Tryptophan. Patienten, die einen GCDH-Defekt aufweisen, sind biochemisch durch die Akkumulation der neurotoxischen Metaboliten Glutaryl-CoA, GA, 3-OH-GA sowie nicht toxische Glutarylcarnitin in Geweben und Körperflüssigkeiten charakterisiert. Wenn sie unbehandelt sind, entwickeln die meisten Individuen eine akute encephalopathische Krise, die während einem zeitlich begrenzten Abschnitt der kindlichen Gehirnentwicklung (zwischen 3 Monaten bis 3 Jahren) eine striatale Schädigung verursacht und zu einer komplexen Bewegungsstörung mit vorherrschender dystonie führt. Patienten, die vor dem auftreten irreversibler neurologischer symptome diagnostiziert wurden, können vor einer Schädigung des Striatums bewahrt werden, wenn sie mit einer Diät bestehend aus niedrigem L-lysingehalt, Supplementierung mit Carnitin und essentiellen Aminosäuren sowie Notfallbehandlung während kataboler Krisen behandelt werden. Auch wenn die derzeit durchgeführte metabolische Behandlung als sicher und wirksam gilt, erleiden trotz einer rechtzeitigen Diagnose und Behandlung immer noch eine signifikante Anzahl von Patienten Schäden des Striatums. Darüber hinaus berichten neuere Studien über extrastriatale, extra-zerebrale und nicht-neurologische Veränderungen trotz Einhaltung der Therapieleitlinien. Dies verdeutlicht die Notwendigkeit der Entwicklung neuer, sicherer und effizienterer Langzeitbehandlungsstrategien. In dieser Arbeit stellen wir die Hypothese auf, dass die pharmakologische Inhibition eines enzymatischen Schritts, der dem defekten Protein GCDH vorangeschaltet ist, die Produktion toxischer Metabolite und damit die Induktion des klinischen Phänotyps der GA-I verhindert. Zu diesem Zweck wurden die Proteine D Dehydrogenase E1 And Transketolase Domain Containing 1 (DHTKD1) (Ansatz 1) und Aminoacidat-Aminotransferase (AADAT) (Ansatz 2) ausgewählt und unsere Hypothese in genetisch modifizierten Zellmodellen, GA-I-Patientenzelllinien und knockout-Mausmodellen getestet. Wir entwickelten daher ein *Dhtkd1*^{-/-}/*Gcdh*^{-/-} Mausmodell und untersuchten seine biochemischen und

klinischen Eigenschaften nach Gabe einer Hochlysin-Diät (4,7% (w / w) oder 235 mg L-lysin in der Nahrung). Unsere Studien zeigten, dass DHTKD1-Knockout nicht in der Lage war, den GA-I-Phänotyp in *Dhtkd1^{+/+} / Gcdh^{-/-}* Mäusen zu therapieren, da die Tiere weiterhin hohe GA-Spiegel und einen klinischen Phänotyp aufwiesen. Von einer Inhibitor-Testung für DHTKD1 haben wir daher abgesehen. Eine pharmakologische Inhibierung der AADAT unter Verwendung des patentierten und kommerziell erhältlichen Wirkstoffs PF04859989 in GCDH-defizienten Zelllinien keinen Effekt, führte hingegen zu einer stark verminderten GA-Produktion.

Insgesamt zeigen diese Arbeiten, dass die AADAT ein neues und vielversprechendes Drug Target für die Behandlung der GA-I ist.

Abbreviations

AA	α -Aminoadipate
AAS	α -Aminoadipatesemialdehyde
AASDH	α -Aminoadipatesemialdehyde-Dehydrogenase
AASS	α -Aminoadipatesemialdehyde-Synthase
ADP	Adenosin 5'-Diphosphate
AADAT	α -Aminoadipateaminotransferase
ATP	Adenosin 5'-Triphosphate
d	day
BSA	Bovine Serum Albumin
C5DC	Glutaryl-carnitine
C0	free L-Carnitine
CoA	Coenzyme A
Da	Dalton
DAPI	4',6-Diamidino-2-phenylindol
DCPIP	Dichlorophenolindophenol
DMSO	Dimethylsulfoxid
EDTA	Ethylendiamintetraaceticacid
GA	Glutaricacid
GC/MS	Gaschromatography/Massspektrometry
GCDH	Glutaryl-CoA-Dehydrogenase
h	hours
3-OH-GA	3-Hydroxyglutaricacid
H ₂ O	distilled water
min	Minute
ml	Milliliter
μ g	Microgram
μ l	Microliter
LOR	Lysine oxido reductase
n	number
NaCl	Sodium chloride
NAD	Nicotinamide Adenine dinucleotide, oxidised
NADH	Nicotinamide Adenine dinucleotide, reduced
NADP	Nicotinamide Adenine dinucleotide phosphat,oxidised
NADPH	Nicotinamide Adenine dinucleotide

NMDA	phosphate reduced N-Methyl-D-Aspartate
PBS	Phosphate Buffer saline
P6C	1-Piperidin-6-Carboxylate
OA	Oxo adipic acid
OGDHc	2-Oxoglutarate dehydrogenase- complex
RT	Room temperature
s	Seconds
SD	standard deviation = Standardabweichung
SDH	Saccharopine-Dehydrogenase
Tris	Tris(hydroxymethyl)aminomethan
Triton-X-100	t-Octylphenoxypolyethoxyethanol
U/mg	Units per mg [$\mu\text{mol min}^{-1}$], specific Activity
O/N	over night
WT	Wildtype
vs.	versus

1. INTRODUCTION

1.1. Lysine

Lysine (α , ϵ -diaminocaproic acid), a positively charged amino acid is indispensable for growth and maintenance in mammals (Anthony A. Albanese Selma E. Snyderman Marilyn Lein Emilie M. Smetak Betty Vestal, 1949; Jansen, 1962; Neuberger & Webster, 1945; Thomas B. Osborne & Wakeman, 1914). It was for the first time discovered by E. Drechsel in 1889 (G. Wu, 2010). It falls under the category of essential amino acids because of the inability of mammals to synthesize inherently and hence is to be necessarily taken through diet. The average dietary intake of lysine in order to maintain the nitrogen balance and growth, as proposed by the Food and Nutrition Board is 30 mg/kg/day for young adults above 18 years (Tomé & Bos, 2007). Infants above 0.5 years of age need 64 mg/kg/day lysine and are at a higher range of lysine requirement when compared to adults (Tomé & Bos, 2007). The individuals falling under the age groups between the infants and adults require lysine of range 45-34 mg/kg/day (Tomé & Bos, 2007). Lysine is present at a lower concentration in plant-derived foods when compared to animal-derived foods. However, legumes harbor high amounts of lysine and cereals; usually, the staple source of energy, harbor the least (Young, 1994).

The chemically reactive ϵ -ammonium group (NH_3^+) containing amino acid lysine (Tomé & Bos, 2007), plays a significant role in providing essential nitrogen for the synthesis of proteins and other biological molecules (Friedman, 1996). It is of paramount importance in the production of many precursor molecules like the neurotransmitters glutamate (Fabio Papes, Surpili, Langone, Trigo, & Arruda, 2000), carnitine; a key player in the metabolism of fatty acids (Vaz & Wanders, 2002), etc. Modification of lysine residues in different proteins via methylation (Lanouette, Mongeon, Figeys, & Couture, 2014), acetylation (Tapias, Wang, & Yang, 2017), hydroxylation (Slyke & Sinext, 1958), glutarylation (Tan et al., 2014) or sumoylation (Zhang et al., 2014) is a very important process happening after translation to build a functionally active protein. Metabolism of lysine is complex and differs from other amino acids in that it cannot reversibly accept α -amino nitrogen from any other sources. Weisman and co-workers using isotope

exchange method have shown that the α -hydroxy analog of lysine does not support the growth of rats on a lysine-free diet, suggesting lysine as an inert indispensable amino acid (Weissman & Schoenheimer, 1941).

1.1.1. Metabolism of Lysine

1.1.1.1. Anabolism of Lysine

Lysine, amongst the other 20 Proteinogenic amino acids is unique, since, evolutionarily, its synthesis occurs *de novo* via two well distinct, independent pathways: 1) The diaminopimelic acid (DAP) pathway (fig: 1) which begins with L-aspartate and includes nine enzymatic steps leading to L-lysine synthesis. This Pathway occurs in most bacteria, certain lower fungi and green plants. 2) The α -amino adipic acid (AAA) pathway (fig: 1) is preceded by 2-oxoglutarate giving rise to L-lysine, following nine enzymatic steps. This pathway occurs only in a few groups of organisms such as fungi, bacteria such as *Thermus thermophilus* and *Deinococcus radiodurans* and the Archaea *Pyrococcus*, *Thermoproteus*, and *Sulfolobus*. Certain higher fungi and euglenoids were typically shown to possess a distinct variant of the AAA pathway for lysine synthesis (Fondi, Brilli, Emiliani, Paffetti, & Fani, 2007). Since mammals are deprived of lysine synthesis, they depend on lysine producers for their dietary lysine needs.

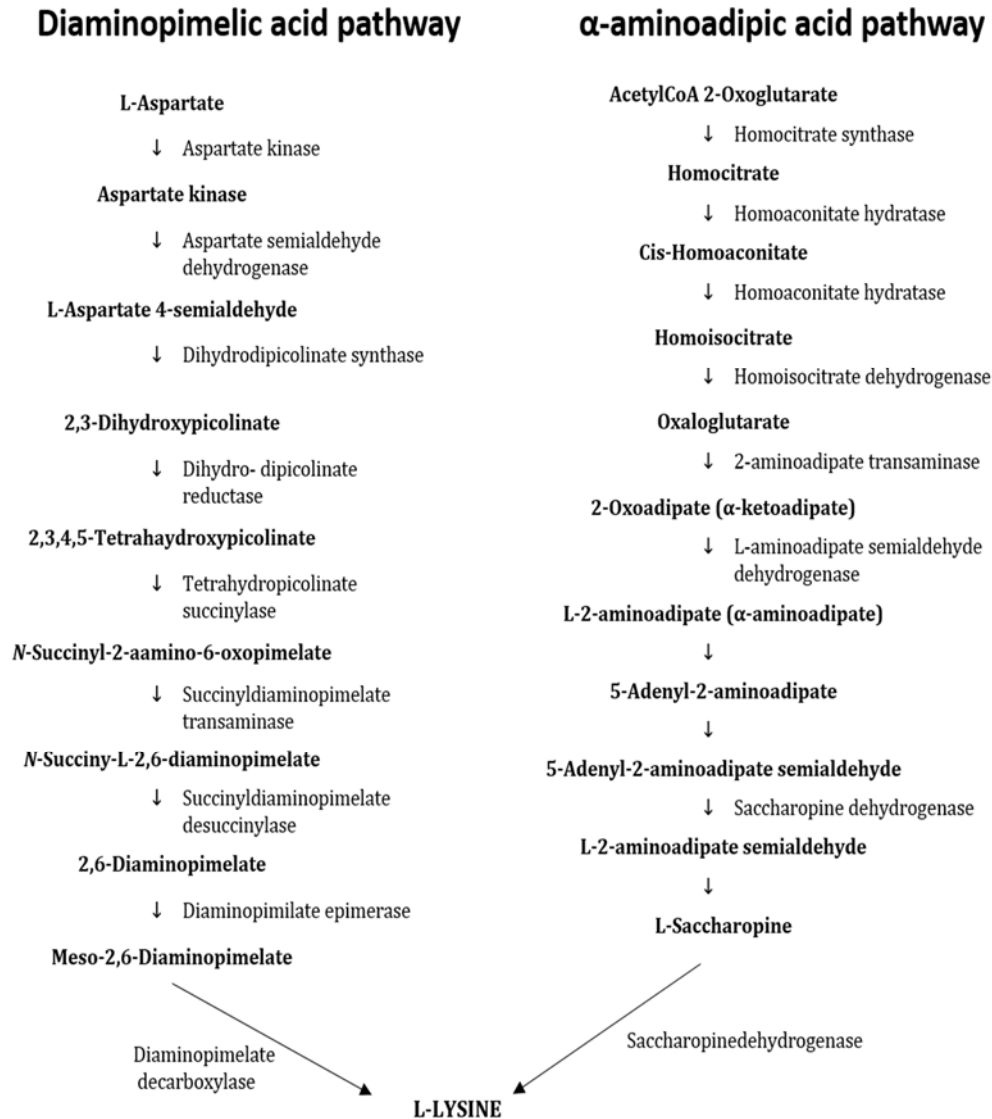


Figure 1: Lysine biosynthesis via DAP and AAA pathway (Source: modified from Kobashi, Makoto, & Tanokura, 1999)

1.1.1.2. Lysine Catabolism

Breakdown of lysine is important to maintain the general nitrogen balance and essential ketone body production (Hutzler & Dancis, 1968, 1975). Lysine catabolism is very diverse and distinct among different organisms and nine catabolic fates of lysine have been discovered so far (Zabriskie & Jackson, 2000). In mammals, lysine degradation is complex and is shown to occur mainly via two different pathways. The saccharopine pathway, which is the mitochondrial

means of lysine degradation, operates predominantly in the fetal brain and extra-cerebral tissues, while the pipercolate pathway, which localizes in the peroxisomes and cytosol, occurs mostly in the adult brain (Hallen, Jamie, & Cooper, 2013). In the saccharopine pathway, the ϵ -ammonium group (NH_3^+), which resides in the side chain of lysine is converted to an aldehyde group, while in the pipercolate pathway, the α -amino group of lysine is converted to the α -keto group (Hallen et al., 2013). Both pathways converge into a common degradative pathway finally giving rise to two molecules of acetyl CoA and CO_2 .

1.1.1.2.1. Saccharopine pathway of lysine degradation

Saccharopine (ϵ -N- [glutaryl-2]-L-lysine) pathway or the mitochondrial pathway of lysine degradation is considered to be the major route for the breakdown of lysine. It is shown to occur in the liver and kidney of mammals. The existence of this pathway was first experimentally demonstrated by Higashino and co-workers in the rat liver mitochondria, where the formation of saccharopine from L-lysine was shown in the presence of α -ketoglutarate (α -KG) (Higashino, Fujioka, Aoki, & Yamamura, 1967; Higashino, Tsukada, & Lieberman, 1965). The enzyme catalyzing the conversion of L-lysine to saccharopine in humans was subsequently identified by Hutzler and Dancis as a NADPH dependent lysine α -KG reductase (LKR) (Hutzler & Dancis, 1968). However, an enzyme with a higher specific activity that converts L-lysine to saccharopine was later identified as saccharopine dehydrogenase (SDH), using liver tissue samples from herbivores (pig ox, sheep), carnivores (rat, dog, cat) and omnivores (human). Such observations from Fellows and Lewis showed that herbivores have a higher specific activity of SDH when compared to carnivores and omnivores (Fellows & Lewis, 1973). Additionally, SDH activity was further confirmed by performing complementary experiments by Fellow and Lewis. They observed the activity of saccharopine oxidoreductase in Ox and human liver, that catalyses the hydrolysis of saccharopine to lysine and α -ketoglutarate (Fellows & Lewis, 1973). Carson and co-workers identified patients with saccharopinuria, who were characterized with abnormal levels of saccharopine in their physiological fluids (CARSON, SCALLY, NEILL, & CARRÉ, 1968). This discovery eventually led

to the identification of the next step of saccharopine pathway i.e; the conversion of saccharopine to α -aminoadipate δ -semialdehyde (AAS) and glutamate (Fellows & Lewis, 1973). Interestingly, both LKR and SDH activities were shown to be catalyzed by a bi-functional enzyme in the liver mitochondrial extracts of baboon and bovine, which was named as aminoadipate semialdehyde synthase (AASS) (P. J. Markovitz, Chuang, & Cox, 1984; Paul J Markovitz & Chuang, 1987). Other eukaryotes, including *C. elegans* and plants (Epelbaum, Mcdevitt, & Falco, 1997), also seem to have evolved a single-gene locus for these two activities. But, in lower eukaryotes like in *S. cerevisiae*, LKR and SDH are encoded by two distinct genes, LYS1 and LYS9 respectively (Kobashi et al., 1999) . Papes and co-workers moved a step further and identified two mRNA variants in the mouse liver and kidney samples by northern blot analysis, in which the longer transcript corresponds to a bi-functional mitochondrial LKR/SDH and the shorter encodes a mono-functional SDH (F Papes, Kemper, Cord-Neto, Langone, & Arruda, 1999). In humans, however, LKR and SDH are shown to be encoded by a single gene (Sacksteder et al., 2000). By performing LKR/SDH enzyme activity measurements, Rao et al experimentally demonstrated that saccharopine pathway is the major contributor of L-lysine metabolism, in the liver of adult rats. Findings from Hutzler and Dancis showing low LKR/SDH activity in adult rat brain, were further strengthened by Chang et al, who demonstrated that adult rat brain harbors pipecolate pathway as the major route for lysine degradation (Chang, 1976, 1978, Hutzler & Dancis, 1968, 1975; Rao & Chang, 1992). Further confirmation was given by Sauer et al. using adult mouse brain samples, where they detected low LKR/SDH mRNA expression along with no detectable enzyme activity (Sauer et al., 2011). Although adult rat brain shows low LKR/SDH activity, Rao and co-workers experimentally showed that in the embryonic rat brain, LKR/SDH activity was high and gradually decreases through development. This establishes the fact that saccharopine pathway is the major lysine degradation pathway in the fetal brain (Rao, Pan, & Chang, 1992). The saccharopine pathway converges with the pipecolate pathway at the level of aminoadipate semialdehyde (AAS), which is the product of oxidative deamination, catalyzed by AASS enzyme (fig 2). AAS is in equilibrium with its cyclic ketamine form Δ^1 -piperidine-6-carboxylate (P6C) (Soda, Misono, &

Yamamoto, 1968). Inter-conversion between AAS and P6C occurs spontaneously without any enzyme involved and the equilibrium favors P6C.

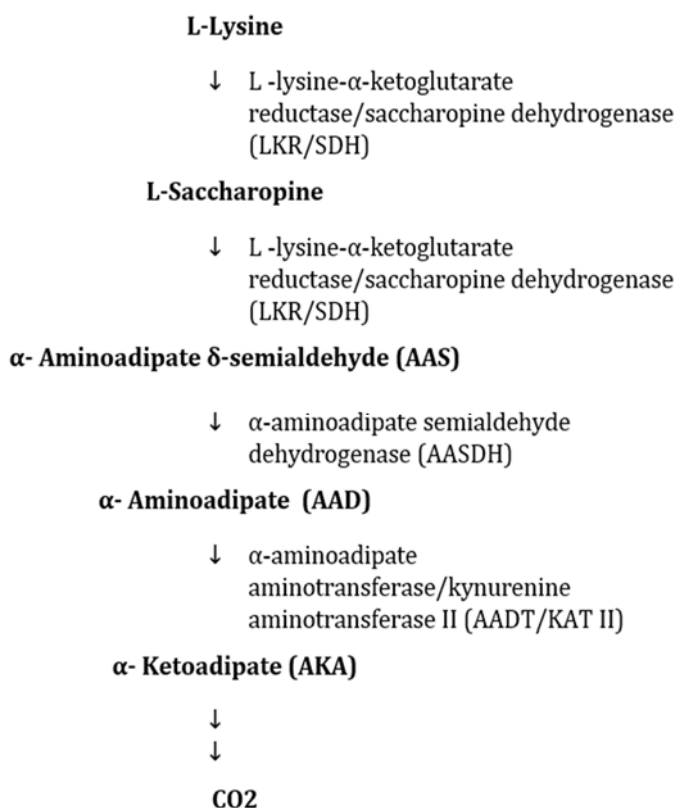


Figure 2: Saccharopine pathway, Source: (Hallen et al., 2013)

1.1.1.2.2. Pipecolate pathway of lysine degradation

The existence of an alternate route for lysine degradation has been an interesting topic of high speculation and a challenging experimental question for over many years. For the first time, Rothstein and Miller demonstrated that pipecolic acid is a major metabolite of lysine and it lies on the pathway between lysine and α -aminoadipic acid, by using the metabolite-overloading procedure in intact rats (Rothstein & Miller, 1954a). Reports showing the clinical cases of hyperpipecolic acedemia indicate the essential role of lysine degradation via the pipecolic acid forming pathway (Gatfield et al., 1968). Knowing that the mammalian brain is inactive in terms of degrading lysine via the saccharopine pathway (Hutzler & Dancis, 1968, 1975), in turn, highlights the speculations about the functional

existence of pipercolic acid pathway. These speculations were further confirmed by Chang via intra-cerebroventricular administration of ^{14}C labeled L- and D-lysine enantiomers, which subsequently metabolized to L-pipercolic acid but not saccharopine, thus emphasizing the concept of the separate existence of saccharopine pathway and pipercolate pathway for L-lysine metabolism (Chang, 1976, 1978). Findings from Woody and Pupene about the abnormal levels of pipercolate excretion in case of hyperlysinemia patients in comparison to unaffected controls also indicate the existence of L-pipercolate pathway of lysine degradation (Woody & Pupene, 1970). In the developing fetal brain, the saccharopine pathway is highly active and predominates. However, during development, the capacity of the pipercolate pathway increases, becoming the major catabolic pathway for lysine degradation in adult brain (Rao et al. 1992). This relationship suggests a specific neuronal developmental role for the pipercolate pathway and its intermediate metabolites. The existence of regional differences in the concentrations of L-pipercolate in the dog brain and causal of cerebral dysfunction due to hyperpipercolic acidemia in infants specifies the significant role of L-pipercolate neurobiologically (Y. Kasé, Kataoka, Miyata, & Okano, 1973; Yoshitoshi Kasé et al., 1980).

Many speculations about the conversion of D-lysine and L-lysine to pipercolate in brain came into existence. According to Grove and Henderson, in rats, D-lysine is converted to L-pipercolate by D-amino acid oxidase (DAAO), a peroxisomal enzyme (Grove & Henderson, 1968). D-lysine is oxidatively deaminated to α -keto- ϵ -amino caproate (KAC) in the first step, which instantly cyclizes to ketamine P2C, that in turn is reduced to L-pipercolate by the action of cytosolic P2C reductase (Meister, 1962; Scannone, Wellner, & Novogrodsky, 1964). However, when it comes to L-lysine conversion to KAC and then to L-pipercolate, it was shown to be via the loss of α -amino group of lysine from the metabolite overloading experiments in the rat (Rothstein & Miller, 1954b). However, little is known about the enzymes involved in this conversion (L-lysine to KAC/P2C). Many theories about the involvement of an L-amino acid oxidase (LAAO) (Murthy & Janardanasarma, 1999) or an aminotransferase (Fabio Papes, Surpili, Langone, Trigo, & Arruda, 2001) or an acetyltransferase (Neuberger & Sanger,

1943) in the conversion of L-pipecolate to KAC/P2C came into picture. However, KATIII/GTL, which is present in cytosolic fractions of mammalian brain, appears to be the most likely option for the source of KAC in brain, even though its efficacy in transaminating lysine at physiological pH values is still not clear (Han, Robinson, Cai, Tagle, & Li, 2009). Further studies and confirmation are markedly essential to unravel the mechanism behind the conversion of L-lysine to KAC/P2C. The second step of the pipecolate pathway is also cytosolic and involves the reduction of P2C via μ -crystallin (CRYM)/ Ketimine reductase (KR) to L-pipecolate. Interestingly, CRYM/KR is shown to be strongly regulated by Thyroid hormone T₃ (Beslin, Vie, Blondeau, & Francon, 1995; Mori et al., 2002). The third step of the pipecolate pathway, however, occurs in the peroxisomes (Hallen et al., 2013). Studies about the patients with Zellweger syndrome who have increased plasma pipecolate levels suggests that oxidation of L-pipecolate occurs in liver peroxisomes and indeed these patients are defective in L-pipecolate oxidation (Wanders et al., 1988; Wanders, Romeyn, Schutgens, & Tager, 1989). Zellweger syndrome is an autosomal recessive disorder, where the affected individuals are characterized by a defect in the formation of peroxisomes (Versmold et al., 1997) leading to the improper development of the brain and mental retardation. Studies from Wanders and co-workers about the oxidation of L-pipecolate in human liver peroxisomes were further confirmed by Rao and Chang (Rao & Chang, 1990; Rao, Tsai, Pan, & Chang, 1993). They, in turn, identified the product formed from L-pipecolate oxidation as the cyclic ketimine Δ^1 -piperidine-6-carboxylate (P6C), which is in close equilibrium with its open-chain aldehyde form α - amino adipate δ -semialdehyde (AAS) (Rao & Chang, 1990). It is also reported that in humans, Δ^1 -piperidine-6-carboxylate (P6C) can, in turn, generate L-pipecolic acid by the action of enzyme pyrroline-5-carboxylate reductase (PYCR1) (Struys, Jansen, & Salomons, 2014). However, few studies also identified the enzyme involved in the oxidation of L-pipecolate to P6C/AAS as L-pipecolate oxidase (L-pox), whose subcellular localization differs amongst several mammalian species (Mihalik, S.J., Rhead, 1991; S J Mihalik & Rhead, 1989; Rao et al., 1993). The pipecolate pathway, thus, is considered to be operative predominantly in the cytosol, with a peroxisomal component involved.

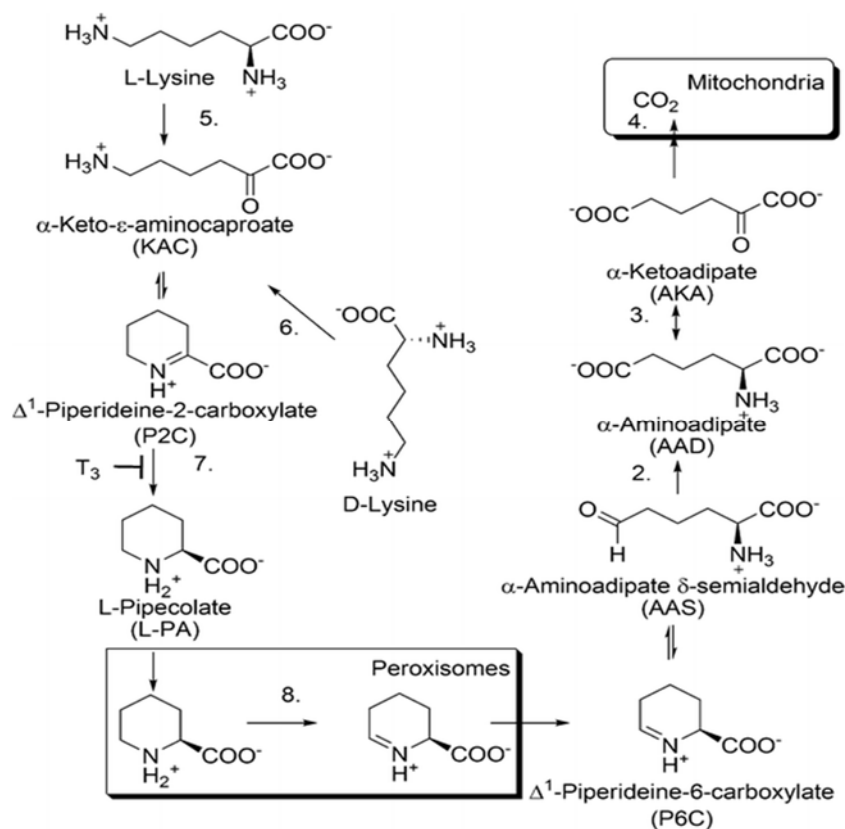


Figure 3: Pipecolate pathway, Source: (Hallen et al., 2013).

1.1.1.2.3. Convergence of pipecolic acid pathway and saccharopine pathway

The pipecolate pathway and the saccharopine pathway both converge at the step, where 2-amino adipate semialdehyde (AAS) is oxidized to α-amino adipate (AA) via amino adipate semialdehyde dehydrogenase enzyme (AASDH), which resides in cytosolic compartment (Chang et al., 1990; Okuno et al., 1993). The next step in the lysine degradation is transamination of AA to 2-oxoadipate (OA). The enzymes that catalyze the reversible transamination between AA and 2-oxoglutarate (OG) to form OA and glutamate were identified in yeast and were named as glutamate-α-keto adipate transaminase I and II (GKAT I and GKAT II) (Matsuda & Ogur, 1969). Mammalian amino adipate aminotransferase (AADAT) that has the capacity to catalyze the transamination between AA and OG was first discovered in rat liver mitochondria (Nakatani, Fujioka, & Higashino, 1970) and was shown to possess activity in both cytosolic and mitochondrial fractions of

rat liver and kidney (Tobes & Mason, 1975, 1977). Aminotransferases exhibit a broad range of specificity and so does AADAT. Namely, kynurenine aminotransferase II (KAT II), an enzyme that catalyzes the transamination between L-kynurenine (Kyn) and OG was discovered (Mason, 1954; Miller, Tsuchida, & Adelberg, 1953) which was subsequently shown to be identical to AADAT in the rat by Tobes and Mason (Tobes & Mason, 1975, 1977). It is noteworthy to know that OA formed here is a common metabolic intermediate in both L-lysine and L-tryptophan degradation pathways (Wass et al., 2011). The OA formed is oxidatively decarboxylated to glutaryl-CoA by dehydrogenase E1 and transketolase domain containing 1 (DHTKD1), which is the E1 like subunit of oxoglutarate dehydrogenase complex enzyme (OGDHc), (V. Bunik & Degtyarev, 2008). Glutaryl CoA is then dehydrogenated to form glutaconyl CoA, which in turn is decarboxylated to form Crotonyl CoA and CO₂. Both the steps are catalyzed by glutaryl CoA dehydrogenase enzyme (Gomes, Fendrich, & Abeles, 1981). Crotonyl CoA is further degraded to 2 molecules of acetyl CoA and CO₂ (Benevenga & Blemings, 2007; Varadkar & Surtees, 2004).

1.2. Inborn errors of lysine metabolism

Till now, a variety of inborn errors of lysine metabolism have been delineated. Though these disorders are considered rare, collectively they account for a substantial portion of childhood deformities and mortality rate (Dasgupta, Wahed, Dasgupta, & Wahed, 2014). Most of these inborn errors are inherited as autosomal recessive traits. Up to date, several disorders linked to lysine metabolism are known, i.e., hyperlysinemia, saccharopinuria, 2-amino adipic and 2-oxoadipic aciduria, Pyridoxine-dependent epilepsy or antiquitin deficiency, Zellweger syndrome, glutaric aciduria type-I (Divry, Vianey-Liaud, & Mathieu, 1991).

1.2.1. Hyperlysinemia

Hyperlysinemia I (MIM # 238700) was first described in 1964 when two siblings were shown to have reduced capacity to degrade lysine, after radioactive lysine

administration (WOODY, 1964). Fibroblasts from the affected individuals were detected to have a defect in the first enzymatic step of major route of lysine degradation, catalyzed by AASS (Dancis, Hutzler, Woody, & Cox, 1976). Hyperlysinemia type I patients have defects in both LKR and SDH activities of AASS resulting in hyperlysinemia, hyperlysinuria and a relatively mild saccharopinuria. Patients with hyperlysinemia I are characterized by abnormally high levels of lysine in the body fluids (Dancis et al., 1976) resulting in accumulation of homoarginine, N- ϵ -acetyl-L-lysine, N- α -acetyl-L-lysine and pipercolic acid as a result of usage or activation of alternate detoxifying biochemical pathways (vd Heiden et al., 1978; Woody & Pupene, 1970). Hyperlysinemia I/ Saccharopinuria is generalized as a benign metabolic variant and hence is not associated with any increase in mortality (Dancis et al., 1983; Gelderen & Teijema, 1973; Georg F Hoffmann, 2006; Houten et al., 2013; Tondo et al., 2013).

In hyperlysinemia II or saccharopinuria (MIM # 268700) as described by Carson (1968), a defect in SDH activity of AASS is observed with residual LKR activity resulting in increased excretion of saccharopine (CARSON et al., 1968). Patients with saccharopinuria show elevated levels of saccharopine, citrulline, lysine (Houten et al., 2013). Hyperlysinemia II/ Saccharopinuria follows an autosomal recessive inheritance and appears to be a non-disease. About 50% of the patients described were discovered accidentally and reported to be healthy (Dancis et al., 1983). Clinical characteristics of some of the patients include psychomotor retardation, microcephaly, developmental delay, spastic diplegia, epilepsy, ataxia, nonspecific seizures and short stature (Houten et al., 2013; Tondo et al., 2013), yet a causal link between deficient AASS activity and clinical phenotypes is lacking. Till now, only a few studies explain about the therapeutic approach to be followed and one treatment option includes long-term dietary regimen with lysine restriction, which is of no benefit (Tondo et al., 2013). Since the patients do not suffer from any metabolic crisis, specific interventions during intercurrent illnesses are not needed.

1.2.2. 2-aminoadipic 2-oxoadipic aciduria

2-aminoadipic and 2-oxoadipic aciduria (MIM # 204750) is an autosomal recessive inborn error. Affected individuals are characterized by the accumulation of 2-aminoadipic acid and 2-oxoadipic acid in their body fluids (Duran, Beemer, Wadman, Wendel, & Janssen, 1984). Till now, not more than 30 individuals are reported with this disorder, out of which half are asymptomatic and the other half presented with mild neurological phenotype like intellectual disability, ataxia, epilepsy, muscular hypotonia and developmental delay (Biagosch et al., 2017; Duran et al., 1984; Przyrembel et al., 1975). Since this disease conditions are not lethal, dietary lysine restrictions and administration of Vitamin B1 and B6 were followed but has proven no long-term effects (Casey, Zaleski, Philp, Mendelson, & MacKenzie, 1978; Duran et al., 1984). By performing whole exome sequencing of two patients with 2-aminoadipic and 2-oxoadipic aciduria, Danhauser and colleagues have identified mutations in Dehydrogenase E1 and transketolase domain containing 1 (*DHTKD1*) (EC 1.2.4.2) gene to cause 2-aminoadipic and 2-oxoadipicaciduria (Danhauser et al., 2012a). Findings from Hagen et al. further delineates additional mutations in *DHTKD1*, confirming the studies of Danhauser and co-workers (Hagen et al., 2015).

1.2.3. Zellweger syndrome

Cerebrohepatorenal syndrome or Zellweger syndrome (MIM # 214100) is an autosomal recessive severe congenital disorder characterized by a defect in the development of functional peroxisomes (Stephanie J. Mihalik et al., 1989). Patients with Zellweger syndrome are associated with an impairment in brain development, neuronal positioning, neuronal migration and several other characteristics like loss of myelin in the central nervous system, loss of hearing, vision, etc. (Versmold et al., 1997). Matsumoto et al., have observed a reduction in neuronal viability and also an increase in neuronal apoptosis in the affected patients (Matsumoto et al., 2003). Patients with Zellweger syndrome do not survive more than one year after birth. Biochemically, patients are characterized among other abnormal metabolite patterns by elevated levels of pipecolic acid

excretion in body fluids, indicating a defect in a pathway related to pipecolate breakdown (Danks, Tippett, Adams, & Campbell, 1975; Trijbels, Monnens, Bakkeren, Van Raay-Selten, & Corstiaensen, 1980).

Studies from different groups on Zellweger syndrome were supportive in understanding the role of peroxisomes in the oxidation of L-pipecolate, which is an alternate route of lysine degradation.

1.2.4. Glutaric aciduria type I

Glutaric aciduria/acidemia type I (GA-I; MIM # 231670) was for the first time discovered by Goodman and co-workers in the year 1975 (Goodman, Markey, Moe, Miles, & Teng, 1975b). Affected individuals were reported to have defective oxidation of glutaryl-CoA in their peripheral leukocytes. By giving oral lysine administration to the affected patients, they demonstrated glutaric acid accumulation and interestingly they also identified that by lowering the intake of protein, glutaric acid accumulation was decreased. Subsequent findings from different groups described this neurodegenerative disorder as an autosomal recessive inherited deficiency of glutaryl-CoA dehydrogenase (GCDH) (Borsook H, Deasy CL, Haagen-Smit A J, Keighley G, 1948; Gholsoi, Sanders, & Henderson, 1959; Goodman & Kohlhoff, 1975; Goodman et al., 1975b). GCDH (EC 1.3.8.6) is a flavin adenine dinucleotide (FAD) dependent mitochondrial enzyme that catalyzes the oxidative decarboxylation of glutaryl-CoA to crotonyl-CoA and CO₂ in the common downstream catabolic pathway of L-lysine, L-hydroxy lysine and L-tryptophan. It is encoded by the *GCDH* gene, in humans, it is located on chromosome 19p13.2 with 7kb in length spanning 11 exons (C. R. Greenberg, Duncan, .Gregory, Singal, & Goodman, 1994). Till now, the prevalence of GA-I is approximated to be about 1:110,000 newborns (Heringer et al., 2010), it is significantly widespread in certain genetically isolated ethnic groups like the Pennsylvania Amish, Canadian Ojibway-Cree aboriginals of Manitoba, Lumbee heritage of eastern North Carolina and the Irish travellers (Basinger et al., 2006; B. L. Greenberg & Glick, 2012; C. R. Greenberg et al., 2002a; Naughten et al., 2004; Strauss, Puffenberger, Robinson, & Morton, 2003; van der Watt et al., 2010). So

far, close to 200 disease-causing mutations are identified in the *GCDH* gene with missense mutations being the most common type (Aishah et al., 2016).

1.2.4.1. Biochemical features of GA-I

Individuals possessing a defective GCDH enzyme are biochemically characterized by the accumulation of neurotoxic glutaryl-CoA, glutaric acid (GA), 3-hydroxyglutaric acid (3-OH-GA), low levels of glutaconic acid as well as non-toxic glutaryl carnitine (C5DC) in their tissues and body fluids (Goodman, Markey, Moe, Miles, & Teng, 1975a; Hoffmann et al., 1991; Georg F. Hoffmann et al., 1996), which are detectable by organic acid (GA, 3-OH GA, glutaconic acid) and acyl carnitine analysis (C5DC) (Chace, Kalas, & Naylor, 2003; Schulze et al., 2003). Reports from different groups suggest that a significant number of GA-I patients have differential (either very low or normal or even highly elevated) levels of GA excretion (Bergman et al., 1989; Campistol, Ribes, Alvarez, Christensen, & Millington, 1992; Superti-Furga, 1997). Among the disease-causing mutations identified in GA-I patients, R402W is the most frequent mutation reported and patients with this mutation were shown to excrete high amounts of glutaric acid (GA) and 3-hydroxyglutaric acid (3-OH-GA) (Busquets, Merinero, & Christensen, 2000; Christensen, Ribes, Merinero, & Zschocke, 2004a; Schwartz, Christensen, Niels, & Brandt, 1998; Zschocke, Quak, Guldborg, & Hoffmann, 2000). Two bio-chemically demarcated groups were defined, based on the GA levels detected in urine and serum samples using gas chromatography-mass spectrometry (GC/MS). The individuals having complete loss of GCDH activity and as a result excrete high amounts of GA (GA in urine > 100 mmol/mol creatinine) are categorized into the group of high excretors; whereas the individuals who possess residual enzyme activity (up to 30% in fibroblasts or leucocytes; (Christensen, Ribes, Merinero, & Zschocke, 2004b)) and as a result excrete no to low levels of GA (GA in urine < 100 mmol/mol creatinine) are categorized into the group of low excretors (Baric et al., 1999a). Interestingly, a correlation exists between the genotype and the biochemical phenotype, but the severity of the clinical phenotype is not predicted by the biochemical phenotype, i.e. low excretors and high excretors can exhibit the

same severity in the clinical phenotype and low excretors are not to be considered to have a mild clinical phenotype. (Baric et al., 1999b; Busquets et al., 2000; Christensen et al., 2004b; S. Kölker, Sauer, Surtees, & Leonard, 2006; Stefan Kölker, Sauer, Okun, Hoffmann, & Koeller, 2006; Mühlhausen et al., 2003). However, high excretors were recently proposed to be at risk to have severe clinical phenotype progressing with age (Harting et al., 2015) and all late-onset GA-I (definition see chapter 1.2.4.2) patients were shown to be high excretors (Boy, Heringer, et al., 2017).

1.2.4.2. Clinical features of GA-I

Clinically, although some GA-I patients are asymptomatic (Monavari & Naughten, 2000; Strauss, Lazovic, Wintermark, & Morton, 2007), macrocephaly, usually the early symptom of the disease, can be seen immediately after birth or after the 30th week of pregnancy. Neurological malformations begin *in utero*, and in exceptional cases might lead to severe abnormalities like optic hypoplasia, agenesis of corpus callosum, lissencephaly (G F Hoffmann & Zschocke, 1999). If untreated, approximately around 90% of the affected individuals develop clinical symptoms during a finite period of brain growth, i.e. during the first six years of life (most commonly between 3 months-3 years of age), as a result of acute encephalopathic crisis that is induced by incidents like gastroenteritis, fever, routine vaccinations or surgical interventions resulting in irreversible striatal damage and eventually, a complex movement disorder with predominant dystonia. These patients fall into the early onset category (Hoffmann et al., 1991; S. Kölker et al., 2006; Stefan Kölker et al., 2007, 2011). With increasing age, the infants progressively suffer from intellectual deterioration, feeding problems, hyperpyrexia, regression of midbrain structures during the course of additional encephalopathic crises which are mostly linked with catabolic events further increasing the degree of morbidity and mortality (G F Hoffmann & Zschocke, 1999; Stefan Kölker, Garbade, et al., 2006; Kyllerman et al., 2004). Most of the above-stated symptoms are reduced and of less prognostic value if the affected infants are diagnosed early and treated successfully (Heringer et al., 2016; Georg F. Hoffmann et al., 1996).

Two clinical subsets of GA-I patients (10-20%) were diagnosed, in which the neurological disease state was demonstrated even in the absence of an encephalopathic crisis and were categorized under insidious-onset (Busquets et al., 2000; Georg F. Hoffmann et al., 1996; Strauss et al., 2007) and late-onset groups (Külkens et al., 2005).

The insidious onset group of GA-I patients differs from the acute onset or early onset group in that they develop dystonia even in the absence of an acute event (Boy, Garbade, et al., 2018). Few patients were also shown to develop distinct perinatal striatal lesions, followed by latency over several months before the actual signs of permanent disability become clinically apparent (Boy, Garbade, et al., 2018; Strauss et al., 2007; Strauss & Morton, 2003). Observations from Heringer and co-workers suggested that insidious onset symptoms are particularly developed in the neonatally diagnosed individuals deviating from the metabolic dietary management, in particular, from lysine restricted diet (Heringer et al., 2010). This was in turn confirmed by the observations from Strauss et al. who observed the disappearance of insidious onset of dystonia in a genetic cohort following improved dietary treatment (Strauss et al., 2011). Overall, insidious onset GA-I patients differ from the early or acute onset group in terms of the lesser extent of striatal lesions followed by less severe dystonia and are categorized by symptomless latency phase regardless of the previously prevailing dorsolateral lesions of the putamen (Boy, Garbade, et al., 2018). Apparent changes in white matter with increasing age is also a common feature observed in this group of GA-I patients (Harting et al., 2009).

The clinical sub-set of GA-I patients who are diagnosed after the age of six years come under the late-onset or adult-onset group. Their clinical manifestation is shown to be non-specific with more severe neurologic symptoms in older patients compared to younger patients who are either asymptomatic or commonly presented with a headache, vertigo, etc (Boy, Heringer, et al., 2017). Interestingly, all the reported late onset patients so far were shown to be high excretors and were devoid of striatal necrosis (Tuncel et al., 2018). The late

onset patients do not show any particular differences in genotypes and biochemical phenotypes to that of the early onset group (childhood-onset), however, severe leukencephalopathy (Bähr, Mader, Zschocke, Dichgans, & Schulz, 2002), changes in white matter (spongiform myelinopathy) (Külkens et al., 2005), frontotemporal hyperplasia, sub-ependymal mass lesions (Herskovitz, Goldsher, Sela, & Mandel, 2013a; Korman et al., 2007; Pierson et al., 2015) are the striking neuroradiologic hallmarks observed in these patients. According to Boy et al., the extra-striatal abnormalities observed in late-onset GA-I patients are a result of the chronic neurotoxicity caused due to the cerebral accumulation of toxic metabolites over several years. Thus, in the case of late-onset group of GA-I patients who are high excretors, the biochemical phenotype is responsible for determining the clinical outcome (Boy, Heringer, et al., 2017).

All clinical subsets of GA-I patients were shown to be prone to extra-striatal abnormalities despite neonatal treatment (as in case of acute onset) or despite lack of susceptibility to striatal damage (as in case of late-onset group) (Tuncel et al., 2018). Few GA-I patients were reported to have extra cerebral and non-neurologic abnormalities (Boy, Heringer, et al., 2017) like peripheral polyneuropathy (Herskovitz, Goldsher, Sela, & Mandel, 2013b), chronic renal disease (du Moulin et al., 2017) showing that the GA-I disease is not restricted to brain alone.

1.2.4.3. Neuropathology of GA-I

The toxic metabolites, GA, 3-OH GA and glutaryl-CoA, have been shown to be of high significance in the pathophysiology of the disease (Sauer et al., 2011). The basis behind the metabolite mediated neuropathogenesis in GA-I is attributed to different synergistic pathomechanisms, based on the results of many *in vitro* and *in vivo* studies. They include primarily, the excitotoxicity mediated cell damage and oxidative stress involving nitric oxide production stimulated by cytokines (Stefan Kölker, Koeller, Okun, & Hoffmann, 2004), impairment of the energy metabolism due to inhibition of oxoglutarate dehydrogenase complex (OGDHc) and the dicarboxylic acid shuttle between the astrocytes and neurons by the

accumulating GA, 3-OH GA and glutaryl CoA (Sauer et al., 2005; Sauer, Okun, Fricker, Mahringer, et al., 2006), and the disturbance of cerebral hemodynamics leading to expansion in the cerebrospinal fluid volume (Strauss, Donnelly, & Wintermark, 2010). Interestingly, reports from several groups via *in vitro*, *in vivo* and postmortem findings identified that the blood-brain barrier (BBB) is a major player in the neuropathogenesis of GA-I (S. Kölker et al., 2006; Sauer et al., 2010; Sauer, Okun, Fricker, Mahringer, Müller, et al., 2006). The toxicity inducing metabolites GA, 3-OH GA and glutaryl-CoA are synthesized within the brain compartment and subsequently trapped due to limited permeability across the BBB, further enhancing the toxic effects of accumulating metabolites (Jafari, Braissant, Bonafé, & Ballhausen, 2011; S. Kölker et al., 2008, 2006).

1.2.4.4. *Gcdh* knockout mouse model

In order to understand the pathophysiological mechanisms which drive the neuropathology of glutaric aciduria type I, a clinically relevant *Gcdh* knockout (*Gcdh*^{-/-}) mouse model was generated via targeted deletion of the *Gcdh* gene in mouse embryonic stem cells by Koeller and co-workers (Koeller et al., 2002). The murine *Gcdh* gene shares a high degree of homology to that of humans and is located on chromosome 8 with 11 exons, spanning a region of 7kb of the total genomic DNA (Koeller et al., 1995). The knockout mice are characterized by the loss of GCDH activity in all the tissues and organs. Biochemically, the knockout mouse model replicated the GA-I patients, as seen via the accumulation of toxic metabolites in tissues urine and blood (Sauer, Okun, Fricker, Mahringer, et al., 2006) and also showed vulnerability to striatal damage during the early neonatal period, when exposed to striatal toxins (Bjugstad, Crnic, Goodman, & Freed, 2006). However, the KO mouse showed a substantial difference clinically and histopathologically to GA-I patients, i.e., the absence of acute encephalopathic crises induced by catabolism or inflammatory cytokines as well as the absence of gliosis and neuronal loss in the striatum (Koeller et al., 2002). Interestingly, studies from Zinnanti et al., showed that *Gcdh*^{-/-} mice exposed to high dietary lysine develop severe neurological phenotype induced by increased cerebral accumulation of toxic metabolites (Zinnanti et al., 2006). *Gcdh*^{-/-} mice showed

age-dependent susceptibility to increased lysine and GA accumulation in the developing brain, which was similar to the human GA-I disease. This work provided a basis for utilizing the *Gcdh*^{-/-} mouse model as a valuable tool in understanding the GA-I pathophysiology during critical stages of brain development and eventually advancing towards the development of novel treatment strategies (Zinnanti & Lazovic, 2010).

1.2.4.5. Treatment strategies followed for GA-I patients

The treatment strategies followed for GA-I patients primarily focus on reducing the accumulation of neurotoxic metabolites GA, 3OH-GA and glutaryl-CoA. This can be achieved by following age-dependent dietary lysine restriction along with ensuring the supplementation of essential amino acids in combination with carnitine (S. Kölker et al., 2007). The outcome of GA-I patients was best and patients remained asymptomatic when they were diagnosed neonatally and received all the three interventions and an emergency treatment during catabolism-inducing episodes. However, the outcome was poor and the dietary treatment was not helpful when diagnosed after the manifestation of the neurological disease (Boy, Mühlhausen, et al., 2017). Apart from dietary treatment, GA-I patients were also treated with different pharmacological agents, but there was no evidence to confirm the beneficial role of neuroprotective agents like N-acetyl cysteine, phenobarbitone, creatine monohydrate, glutamate receptor antagonists (C. R. Greenberg et al., 2002b; Kyllerman et al., 2004; Strauss & Morton, 2003). Although the c-factor Riboflavin was previously used as a pharmacotherapeutic agent, responsiveness in patients was shown to be rare (Chalmers, Bain, & Zschocke, 2006) and no firm evidence was reported about improvement in the neurological outcome of patients upon its administration (Stefan Kölker, Garbade, et al., 2006). Even though the dietary treatment is effective, a relevant number of patients who were known to be 'metabolically stable', still suffer from extra-striatal (namely, frontotemporal hypoplasia (Boy, Heringer, et al., 2017), white matter changes (Pierson et al., 2015), subependymal mass lesions (Herskovitz et al., 2013)), extra cerebral and non-neurologic abnormalities (like peripheral polyneuropathy (Herskovitz et al.,

2013) and renal disease (S Kölker, Cazorla, et al., 2015; S Kölker, Valayannopoulos, et al., 2015) respectively), thus debating on our current understanding about the prediction and prevention of late GA-I complications using conventional metabolic treatment. This in turn questions the efficacy of the therapeutic strategies followed in treating GA-I, further strengthening the need for more effective and novel treatment options (Tuncel et al., 2018).

1.2.4.6. Alternate therapeutic strategies

Since the current treatment strategies for GA-I do not protect patients from late-onset disorders, there is an urgent need to develop safe and state of the art treatment regimen to address the severe complications associated with GA-I. Hence, we hypothesize a new treatment strategy for treating GA-I based on the approach established and followed for treating the metabolic disorder Tyrosinaemia type I (Lock et al., 1998). Tyrosinaemia type I (MIM # 27670) is an autosomal recessive disorder caused due to the deficiency of fumaryl acetoacetase (FAH) that catalyzes the final step in the degradation of Tyrosine. Defective FAH leads to accumulation of fumarylacetoacetate, maleylacetoacetate and succinylacetone. Accumulation of these metabolites lead to liver and kidney damage and eventually hepatocellular carcinoma (Kvittingen, Bergan, & Berger, 1993). Interestingly, as a treatment option for Tyrosinaemia type-I, Lindstedt et al, have targeted 4-hydroxyphenylpyruvate dioxygenase an enzyme lying two metabolic steps ahead of fumaryl acetoactate hydrolase in Tryptophan catabolism (Lindstedt, Holme, Lock, Hjalmarson, & Strandvik, 1992) by using a drug named 2-(2-nitro-4-trifluoro- methylbenzoyl)-1,3-cyclohexanedione (NTBC) or Nitisinone (INN). This drug was branded in the name of Orfadin and is a potent inhibitor of 4-hydroxyphenylpyruvate dioxygenase (Lock et al., 1998). By targeting 4-hydroxyphenylpyruvate dioxygenase, they prevented the formation of maleylacetoacetate and fumaryl acetoacetate. This treatment option is still a gold standard treatment available for Tyrosinaemia type-I patients preventing liver transplantation and other side effects. Similarly, the strategy of blocking 4-hydroxyphenylpyruvate dioxygenase enzyme using Nitisinone is also studied in an inherited metabolic disorder called Alkaptonuria, in which patients

lack the capability of metabolizing Phenylalanine and Tyrosine (Ranganath, Jarvis, & Gallagher, 2013).

In line with the above strategy followed for treating tyrosinaemia type-I and alkaptonuria, we aim to find a pharmaceutical inhibitor for GA-I patients targeting enzymatic steps prior to GCDH.

1.2.4.6.1. Target 1, DHTKD1

DHTKD1 is one of the two known isoforms of E1 subunit of 2-oxoglutarate dehydrogenase complex (OGDHC) enzyme that catalyzes the conversion of 2-oxoadipate to glutaryl-CoA (Danhauser et al., 2012). Defective DHTKD1 activities results in accumulation of metabolites 2-oxoadipic acid and 2-aminoadipic acid which are considered less toxic resulting in a very mild clinical phenotype in the affected patients. Since glutaryl-CoA is the main substrate of GCDH and the precursor of toxic GA and 3-OH-GA, pharmacological inhibition of DHTKD1 in GA-I affected individuals could be a new potential drug target preventing the accumulation of toxic metabolites (Danhauser et al., 2012a).

1.2.4.6.2. Target 2, AADAT

Amino adipate amino transferase (AADAT) (EC 2.6.1.39) mediates the transamination of 2-amino adipate to 2-oxoadipate (Nakatani et al., 1970) and lies upstream of GCDH and DHTKD1 (Biagosch et al., 2017). AADAT is also called as kynurenine aminotransferase II (KAT II), which is a pyridoxal phosphate-dependent enzyme and is well reported in the transamination of kynurenine to kynurenic acid in tryptophan catabolism (Goh et al., 2002). Kynurenic acid (KYNA) is a neuroactive metabolite elevated in the brain of patients with psychiatric and neurological disorders (Linderholm et al., 2016). There are two known inhibitors of AADAT available that however have only been tested regarding their effect on Tryptophan metabolism but not on Lysine metabolism. Nematollahi et al, have observed that NS-1502 is a reversible and competitive inhibitor of AADAT (Nematollahi, Sun, Jayawickrama, Hanrahan, & Church,

2016). Similarly, PF-04859989 a blood-brain barrier penetrating AADAT inhibitor was shown to effectively reduce brain KYNA levels, thereby decreasing firing activity of midbrain dopamine neurons and, consequentially, having a potential to treat hyper dopaminergic conditions that are characteristic of schizophrenia and bipolar disorder (Linderholm et al., 2016). PF-04859989 forms a covalent adduct with pyridoxal phosphate (PLP), which is the cofactor of KAT II, in its active site, thus inhibiting its activity (Dounay et al., 2012). Till date, no disease-causing mutations in AADAT have been identified with and similarly, KAT-II knockout mice were reported to remain asymptomatic (Potter et al., 2010; Yu et al., 2004).

Figure 4: Kynurenine pathway of Tryptophan metabolism (Source: Schwarz 2017)

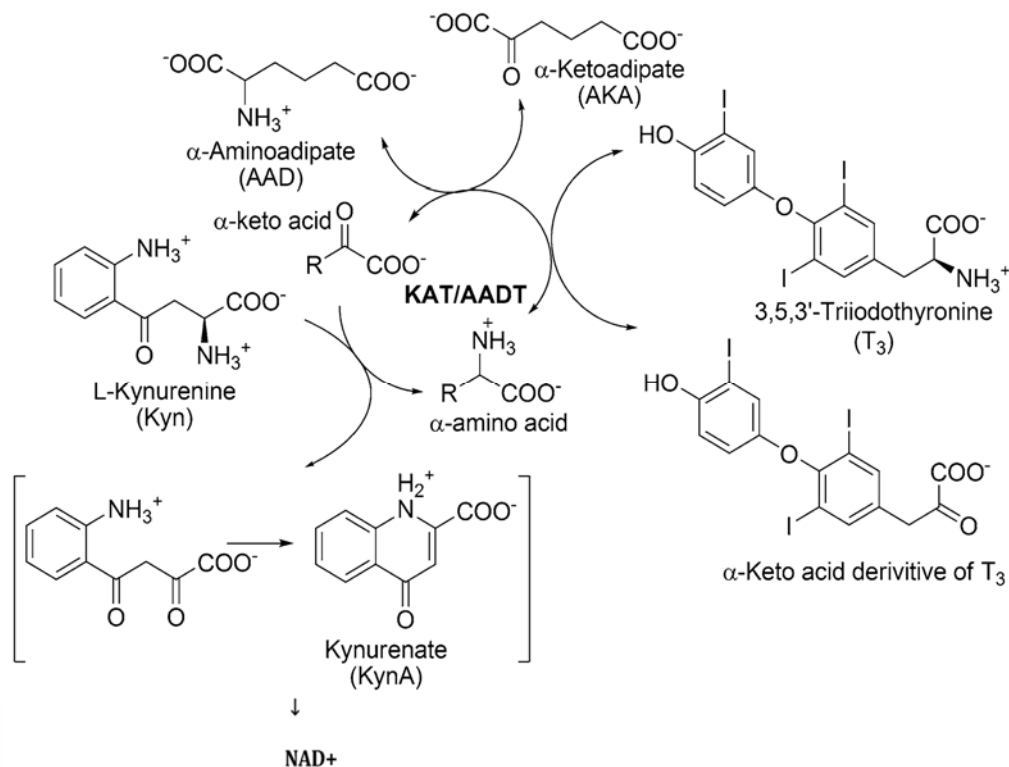


Figure 4: KAT II/Amino adipate aminotransferase (AADAT) (Hallen et al., 2013)

1.3. Objectives of the thesis

GA-I disease treatment and management involve reducing the toxic metabolite accumulation by the implementation of age-dependent dietary lysine restriction, supplementation of carnitine including the essential amino acids along with intermittent emergency treatment. However, the metabolic treatment proved of no help for patients who showed frequent deviations from the proposed treatment guidelines. Moreover, patients treated according to the current treatment recommendations are still prone to develop extra-striatal, extra cerebral and non-neurologic abnormalities clearly depicting the need for more effectual and novel therapeutic interventions to answer the long-term complications of GA-I disease. Hence, we intend to identify alternative therapeutic strategies in treating GA-I disease. Thus, we hypothesize to pharmacologically inhibit the enzymatic steps prior to GCDH in the lysine catabolic pathway, eventually preventing the toxic metabolite accumulation and the clinical phenotype of GA-I patients.

On the basis of our proposed hypothesis, in this thesis, we concentrated on investigating the following steps.

- 1) Pharmacological inhibition of DHTKD1 in DHTKD1 patient and control fibroblasts using the available inhibitors and biochemical assessment of GA and OA levels using GCMS.
- 2) Clinical and biochemical characterization of the generated *Dhtkd1*^{-/-}/*Gcdh*^{-/-} mouse model after giving standard diet (1.7% (w/w) or 85mg) of L-lysine in food and high lysine diet (4.7% (w/w) or 235mg of L-lysine in food) using GCMS.
- 3) Alternative therapeutic approach involving AADAT by,
 - A) Inhibition of AADAT using siRNA and further proceeding for GA level measurement using GCMS.
 - B) Inhibition of AADAT in GA-I patient and control fibroblasts using the inhibitor PF-04859989 and quantitative detection of GA levels using GCMS.

- 4) Generation of alternate GA-I cell culture models (GCDH and AADAT) using CRISPR/Cas9 technology and further analysis of GA levels in knockout cells and controls using GCMS.

2. MATERIALS AND METHODS

2.1. Materials

2.1.1. Chemicals used

Agarose	Applichem
40% Acrylamide/Bis Solution	Bio Rad
APS, Ammoniumpersulfate (H ₈ N ₂ O ₈ S ₂)	Applichem
Acetone (C ₃ H ₆ O)	Roth
Acetic acid (C ₂ H ₄ O ₂)	Carl Roth
Ampicillin - Natriumsalz	AppliChem
Amphotericin 250 UG/ml (Fungi Zone)	Life technologies
Bromophenol blue sodium salt (C ₁₉ H ₉ Br ₄ NaO ₅ S)	Sigma-Aldrich
Bacteriological agar for molecular biology	Sigma-Aldrich
BSA	Santa Cruz
	Biotechnology
β-2-Mercaptoethanol (C ₂ H ₆ OS)	Merck
Bacillol	Hartmann AG
Biozidal	MIT- Diagnostics
Bad stabil	Neo lab
Citric acid (C ₆ H ₈ O ₇)	Roth
Citric acid monohydrate (C ₆ H ₈ O ₇ x H ₂ O)	Sigma-Aldrich
DAPI, 10 mg	Sigma-Aldrich
DIG RNA Labeling Mix	Sigma-Aldrich
Dimethyl Sulfoxide (DMSO), cell culture reagent	Santa Cruz
	Biotechnology
DTT (dithiothreitol)	Thermo Scientific
Dodecylsulfate·Na-salt in Pellets	SERVA
dNTP mix 10mM	Thermo fischer
scientific	
DEPC, diethylpyrocarbonate (C ₆ H ₁₀ O ₅)	Sigma-Aldrich
DNase I recombinant, RNase-free from bovine pancreas	Sigma-Aldrich
DMEM high w. Glutmax-1	Life Technologies
EDTA disodium-ethylenediaminetetra-acetate	Sigma-Aldrich
Ethanol (C ₂ H ₆ O) 99.8% PA	Roth
Ethidium bromide (C ₂₁ H ₂₀ N ₃ Br)	Sigma-Aldrich
Fetal calf serum	GIBCO
FastAP Thermosensitive Alkaline Phosphatase (1 U/μL)	Thermo Fisher
Scientific	
Gene Ruler 1Kb DNA Ladder	Thermo Fisher
Scientific	
Glycerol, 1,2,3 -propanetriol (C ₃ H ₈ O ₃)	Sigma-Aldrich
Glucose	Sigma-Aldrich
Glutaric acid	Sigma-Aldrich
Glutathione sepharose TM 4B	GE health care

Hydrochloric acid, 37% (HCl)	Sigma-Aldrich
Hepes, N-2-hydroxyethylpiperazine-N'-2-ethanesulfonic acid (C ₈ H ₁₈ N ₂ O ₄ S)	Sigma-Aldrich
IPTG	Sigma-Aldrich
Isopropanol 70%	Bioline
	Sigma-Aldrich
Kanamycin sulphate	Sigma-Aldrich
Lipofectamine® 2000 Transfection Reagent Scientific	Thermo Fisher
Lysozyme human recombinant	Sigma-Aldrich
L-lysine (monohydrochloride)	Sigma-Aldrich
6X Loading dye Scientific	Thermo Fisher
Magnesium sulphate anhydrous	Sigma-Aldrich
MyTaq™ HS Red Mix	Bioline
Milchpulver	Carl Roth
Methanol (CH ₄ O)	Carl Roth
Mowiol® 4-88	Merck
Magnesium chloride (MgCl ₂)	Sigma-Aldrich
NotI-HF Biolabs	New England
NEB® 5-alpha Competent E. coli (High Efficiency) Biolabs	New England
NBT/BCIP Stock Solution	Sigma-Aldrich
β-nicotinamide adenine dinucleotide	Sigma-Aldrich
Nonidet™ P-40	Sigma-Aldrich
2-Oxoadipic acid	Sigma-Aldrich
Protector RNase Inhibitor 2000 U	Roche
Protein Assay Reagent A	Bio-Rad
Protein Assay Reagent B	Bio-Rad
Protease inhibitor cocktail	Sigma-Aldrich
Proteinase K	Carl roth
Penicillin Streptomycin (100 ml)	Life Technologies
PMSF	Sigma-Aldrich
Phusion High-Fidelity DNA Polymerase Scientific	Thermo Fisher
Phosphate buffered saline Dulbecco's w.o Ca &Mg	Life Technologies
Potassium chloride (KCl)	Sigma-Aldrich
Potassium hydroxide (KOH)	Sigma-Aldrich
Puromycin	Sigma-Aldrich
Ponceau S (C ₂₂ H ₁₂ N ₄ Na ₄ O ₁₃ S ₄) Darmstadt	Applichem,
Protease-Inhibitor complete mini Diagnostics	Roche
RNase inhibitor	Sigma-Aldrich
Sodiumdeoxycholate	Sigma-Aldrich
Sodium chloride	Roth
SDS, sodium dodecyl sulphate (C ₁₂ H ₂₅ NaO ₄ S)	Sigma-Aldrich
SP6 RNA Polymerase	Sigma-Aldrich

SensiFAST™ SYBR® Hi-ROX Ki	Bioline
SuperSignal™ West Pico Chemiluminescent Substrate 1L	Thermo Fisher Scientific
sodium azide	Sigma-Aldrich
sodium cyanide	Sigma-Aldrich
sheep serum	Sigma-Aldrich
T7 RNA Polymerase	Sigma-Aldrich
TRizol® Reagent	Life Technologies
Tween 20 (C58H114O26)	Carl roth
TRIS	Carl Roth
Triton™ X-100 (Alkylphenylpolyethylenglykol)	Sigma-Aldrich
(C14H22(C2H4O) _n O)	Sigma-Aldrich
Tris, Hydrochloride	Santa Cruz Biotechnology
Trypton	Roth
T4 Polynucleotide Kinase - 500 units	New England Biolabs (NEB)
T4 DNA Ligase - 100000 units	New England Biolabs (NEB)
Thiamine pyrophosphate (TPP)	Sigma-Aldrich
N, N, N', N'-Tetramethylethylenediamine (TEMED)	Sigma-Aldrich
Tryphan blue	Sigma-Aldrich
Trypsin 0.25% EDTA	Life technologies
Yeast extract	Sigma-Aldrich

2.1.2. Consumables used

Blotting paper 580 x 600 mm	Neo Lab
Cryotubes	NeoLab
Cell scraper 25 cm	Sarstedt
Centrifuge tubes (15 ml, 50 ml)	Sarstedt
96 well cell culture plates	Sarstedt
6 well cell culture plates	Neolab/Falcon
24 well cell culture plates	Sarstedt
Eppendorf tubes (2 ml, 1.5 ml, 0.5 ml)	Starstedt & Neolab
Gloves	VWR
Microscope slide (24 x 50 mm)	Carl Roth, Karlsruhe
Microseal 'B' Adhesive Seals	Bio-Rad
Pasteur pipettes	Stein
Pipette tips (1-10 µl, 10-200 µl, 100-1000 µl)	Sarstedt
PCR tubes (0.2 ml, 8 strip)	Star Lab
Petri plates	Sarstedt
Sterile disposable pipettes (2 ml, 5 ml, 10 ml, 25 ml)	Corning Costar
Sealing film Parafilm	Stein
Skalpel	Pfm medical
T75 cell culture flasks for adherent cells	Sarstedt
T175 cell culture flasks	Sarstedt

2.1.3. List of primers

All the primers were ordered from Life technologies

Name of the primer	Sequence	application
DHTKD1 Eco RI fwd	ccggaattccagaccgagcggggcggt tacggctaccgg	Cloning
DHTKD1 Not I rev	aaggaaaaactcgagtcaagcgaag gtcttggcgagg	
Exon5 hum gRNA GCDH fwd	caccgatgcacctatctatgccta	CRISPR cloning
Exon5 hum gRNA GCDH Rev	aaactaggcatagatagggtgcatc	
Exon1 hum gRNA GCDH fwd	caccgcctgcacgtccttcgcacg	
Exon1 hum gRNA GCDH Rev	aaaccgtgcgaaggacgtgcaggc	
GCDH hum gRNA1 F	caccgtctcgtcggcggcgagac	
GCDH hum gRNA1 R	aaacgtctgcgccgacgagac	
GCDH hum gRNA2 F	caccgcctgcacgtccttcgcacg	
GCDH hum gRNA2 R	aaaccgtgcgaaggacgtgcaggc	
GCDH hum gRNA3 F	caccctgacgagtatcacgtgatc	
GCDH hum gRNA3 R	aaacgatcacgtgatactcgtcag	
hAADAT sgRNA1 Fwd	caccgaattacgcacggtcatca	
hAADAT sgRNA1 Rev	aaactgatgaaccgtgcgtaattc	
hAADAT sgRNA2 Fwd	caccgccaaggagatcatcgattt	
hAADAT sgRNA2 Rev	aaacaaatcgatgatctccttggc	
hAADAT sgRNA3 Fwd	caccgtgattacggcagtccttaa	
hAADAT sgRNA3 Rev	aaacttaagactgccgtaatcac	
hAADAT sgRNA4 Fwd	caccgtactggaaactcattaacca	

hAADAT sgRNA4 Rev	aaactggtaatgagttccagtac	
hAADAT sgRNA5 Fwd	caccgtaagagacatactttccaga	
hAADAT sgRNA5 Rev	aaactctggaaagatgtctcttac	
hAADAT sgRNA6 Fwd	caccgagatgaacctgcttattcag	
hAADAT sgRNA6 Rev	aaacctgaataagcaggttcatctc	
hAADAT sgRNA7 Fwd	caccgtcacatctggcagccaaca	
hAADAT sgRNA7 Rev	aaactgttgctgccagatgtgac	
Human U6 seq	actatcatatgcttaccgtaac	Sequencing primers
T7 Reverse primer	aaaagcaccgactcgggtgcc	

2.1.4. List of antibodies

Name	Primary (1°)/ Secondary (2°)	Species	type	Manufacturer
DHTKD1 N17	1°	donkey		Santa Cruz Biotechnology
DHTKD1 (F-11)	1°			Santa Cruz Biotechnology
KAT II (G-4)	1°	goat		Santa Cruz Biotechnology
Gamma H2Ax	1°			
Actin (C4) HRP	1° and 2°			Santa Cruz Biotechnology
GCDH	1°			proteintech
Anti-rabbit IgG HRP	2°	Donkey		Santa Cruz Biotechnology
Anti-mouse IgG HRP	2°	Goat		Santa Cruz Biotechnology
Anti-goat IgG HRP	2°	Donkey		Santa Cruz Biotechnology

2.1.5. Inhibitors used

Name	Target	Source
PF-04859989	AADAT/KAT II	Pfizer
Acetyl phosphonate (AP)	DHTKD1	Obtained from Collaboration partners in Munich
Glutaryl phosphonate (GP)		
Diethyl ester of glutaryl phosphonate (DEGP)		
Triethyl ester of glutaryl phosphonate (TEGP)		
Tri methyl acetyl phosphonate (TMAP)		

2.1.6. Commercially available kits used

Name	Manufacturer
ECL Western Blotting System	GE Healthcare
Nucleo spin plasmid Mini/Midi Prep Kit	Machery & Nagel (M&N)
Nucleo spin gel and PCR Clean-up Kit	Machery & Nagel (M&N)
Maxima first strand cDNA synthesis kit	Thermo Fischer scientific
TOPO TA Dual Promoter cloning kit	Thermo Fischer scientific

2.1.7. General Buffers used

General buffers and solutions were prepared with autoclaved double-distilled water. For all RNA work, nuclease-free water was used. Buffers were autoclaved at 121 °C for one hour or sterile filtered through a 0.22 µm membrane of a vacuum-driven disposable filter unit. If not listed here, buffer compositions are given in the text.

Name	Components added	Remarks
1) 10X LB medium:	Trypton 100 g NaCl 100 g Yeast extract 50 g dd H ₂ O to 1 liter	pH was adjusted to 7 using 1 M NaOH
2) PBS (10X, 1L)	NaCl 80 g KCl 2 g Na ₂ HPO ₄ x 7H ₂ O 26.8 g KH ₂ PO ₄ 2.4 g	pH was adjusted to 7.4
3) TAE buffer	Tris-HCl 40 mM Acetic acid 20 mM	pH was adjusted to 8.0

	EDTA 2 mM	
Western blotting related buffers		
1) RIPA buffer (10 ml)	NaCl 150 mM Triton X 100 1% Sodium deoxycholate 0.5% SDS 0.1% TRIS 50 mM Protease inhibitor mini- 1 tablet	pH was adjusted to 8.0
2) 6X SDS loading dye 10 ml	TRIS pH 6.8 1 M- 3.75 ml SDS- 1.2 g Glycerol(100%)- 6 ml Bromophenol Blue- 0.006 g DTT- 0.462 g ddH ₂ O to 10 ml	
3) SDS-gel running buffer	Tris-HCl, pH 8.3 0.25 M Glycine 1.92 M SDS 1 M	
4) Ponceau S	Ponceau S 0.2% Glacial acetic acid 1%	
5)TBST (10X, 1L)	Tris-HCl, pH 7.5 NaCl 100 mM Tween 150 mM	
6) Blotting buffer (Transfer buffer)	Tris base 25 mM Glycine 192 mM SDS 0.01 % Methanol 10 %	
7) Lamelli buffer (4X) (protein gels)	Tris-HCl, pH 6.8 0.28 M SDS 5.7 % EDTA 0.01 M Glycerol 100 % Bromophenol blue 0.28 g/ml 2-Mercaptoethanol 0.06 ml/ml	
Protein purification related buffers		
1) Lysis Buffer for lysing the bacterial cell pellet	50 mM Tris-HCl pH 7.5 50-200 mM NaCl 5 mM DTT 1 mM PMSF	
2) Binding Buffer	PBS, PH 7.3 (140 mM NaCl 2.7 mM KCl 10 mM Na ₂ HPO ₄ 1.8 mM KH ₂ PO ₄)	pH was adjusted to 7.3
3) Elution Buffer	50 mM Tris-HCl 10 mM reduced glutathione	pH was adjusted to 7.3

2.1.8. Instruments used

Name	Manufacturer
CFX96 Touch™ Real-Time PCR Detection system	Bio-RAD
C1000 Touch™ Thermal Cycler	Bio-RAD
Light Microscope	Leica GmbH, Wetzlar
Mini-PROTEAN Tetra Cell Electrophoresis apparatus	Bio-RAD
Spectramax 340 PC Plus Microplate Reader	Molecular Devices, Sunnyvale, USA

2.2. Methods

2.2.1. Cloning of *DHTKD1* into pGEX4T1 vector

2.2.1.1. PCR amplification of *DHTKD1*

To clone *DHTKD1* gene, we have utilized the already available commercial plasmid Lentiviral vector (Ex-H4610-LV21) containing *DHTKD1* insert, obtained from Genecopoeia. It was kindly provided by Dr. Holger Prokisch, Helmholtz Zentrum, Munich. Primers specific for the 5' and 3' terminus of the construct, containing restriction enzyme overhangs were generated (Forward primer containing EcoRI overhang and NotI overhang in the reverse primer) and used to amplify the DNA sequence. A non-template control reaction which included only ddH₂O without the plasmid was included to determine the specificity of the primers. Automated DNA thermal cycler was used to load the reaction mixtures for further amplification of the DNA. Each PCR amplification contained a 50 µl reaction setup as in the table below (table 1a&1b).

1a Master Mix per reaction	
5X HF Buffer	10 μ l
10 mM dNTP Mix	1 μ l
10 μ M F+R Primers	2 μ l
<i>DHTKD1</i> insert containing vector (100 ng)	1 μ l
dd H ₂ O	35 μ l
Phusion Polymerase	0.5 μ l
50 mM Mgcl ₂	0.5 μ l
Total per Reaction	50 μ l

1b PCR conditions	
98 °C	5 min
98 °C	30 sec
65 °C	45 sec
72 °C	3 min
72 °C	10 min
12 °C	pause

Table 1a & 1b: PCR reaction set up and amplification conditions used for cloning *DHTKD1*

After the completion of the PCR reaction, few microliters of sample was loaded on to a 2% agarose gel to check for the required size of the amplified product. The reaction mix was then purified using the Nucleospin gel and PCR clean-up kit (M&N). Briefly, the sample was mixed with 2 volumes of column binding buffer, loaded on to the matrix containing column and centrifuged at 11,000 \times g for 30 sec at room temperature (RT). Flow through was discarded and the column was washed with washing buffer, centrifuged at 11,000 \times g for 30 sec at RT followed by dry spinning for 2 min (at 11,000 \times g RT). Finally, DNA was eluted into a clean tube using 35 μ l nuclease free water which was directly added on to the column, incubated for 1 min at RT and then centrifuged at 11,000 \times g, 1 min. The concentration of insert (dsDNA) was determined using nanodrop at 260 nm.

2.2.1.2. Restriction digestion of vector and insert

Both the vector (pGEX4T1) and the insert (PCR product) were digested at 37 °C overnight (O/N) using EcoRI and NotI restriction enzymes separately in the 1X compatible buffer. The reaction mixture was set up according to table 2a&2b. The vector and the insert were first digested with EcoRI enzyme in different tubes followed by enzyme heat inactivation @ 80 °C for 20 min and PCR purified (as per 2.2.1.1 Nucleospin gel and PCR clean-up kit (M&N)). The digested vector

and insert were again used in the same reaction setup as above where Not I enzyme is used instead of EcoRI.

<u>2a EcoRI digestion</u>		<u>2b. NotI digestion</u>	
DNA (vector or insert)	Upto 30 μ l	DNA (vector or insert)	Upto 30 μ l
Cut smart Buffer (10X)	5 μ l	Cut smart Buffer (10X)	5 μ l
EcoRI (NEB)	1 μ l	NotI (NEB)	1 μ l
dd H ₂ O	14 μ l	dd H ₂ O	14 μ l
Total Reaction volume	50 μ l	Total Reaction volume	50 μ l

Table 2a& 2b: Reaction set up for Restriction digestion

Restriction enzyme digested insert and vector were analysed by running them on 2% agarose gel. Following the gel electrophoresis, the prominent (correct) size band was excised using a sharp disposable scalpel. The excised DNA band was weighed on a tarred balance and processed as per the instruction manual of Nucleospin gel and PCR clean-up kit (M&N). Briefly, the gel slice was melted in 2 volumes (to 100 mg of gel 200 μ l of buffer was added) of gel solubilization buffer and incubated on dry bath maintained at 50 °C for at least 10 min. The melted sample was then loaded onto the binding column, followed by centrifugation at 11,000 \times g for 30 sec at RT. After binding of DNA, the flow through was discarded and the column was washed twice using 500 μ l of wash buffer, centrifuged at 11,000 \times g for 30 sec RT. The column was again dry spun for 2 min at high speed to remove the left over the buffer. Finally, DNA was eluted with nuclease-free water and the concentration was measured using nanodrop at 260 nm and the quality of elution was determined by agarose gel electrophoresis.

2.2.1.3. Ligation of vector and insert

The purified vector and insert DNA samples obtained after gel elution were further used for ligation. The ligation reaction was carried out using T4 DNA ligase as shown in table 3. Different molar ratios of vector: insert for ligation (1:3, 1:5, 1:6, 1:10) were used along with a negative control (only vector without insert). The insert molar ratios were calculated using the ligation calculator shown below. For example, a ratio of 3:1 can be calculated as,

$$\frac{ng\ of\ Vector\ \times\ size\ of\ Insert\ in\ kb}{size\ of\ Vector\ in\ kb} \times \frac{3}{1} = ng\ of\ Insert$$

(vector in ng- 50; Size of *DHTKD1* insert= 2688 bp; Size of pGEX4T1 vector= 4969 bp).

Components	1:3	1:5	1:6	1:10	-ve control
10X DNA ligation buffer	2 ul	2 ul	2 ul	2 ul	2 ul
Vector (digested)	50 ng	50 ng	50 ng	50 ng	50 ng
Insert (Digested)	81.1 ng	135 ng	162.2 ng	270.5 ng	0.0 ul
T ₄ DNA Ligase	1.0 ul	1.0 ul	1.0 ul	1.0 ul	1.0 ul
ddH ₂ O added upto	10 ul	10 ul	10 ul	10 ul	10 ul

Table 3: Ligation reaction set up with different ratios of pGEX4T1vector and *DHTKD1* insert concentrations

The ligation reaction was incubated O/N at 16 °C.

2.2.1.4. Transformation and positive clone confirmation

Following the next day after ligation, transformation procedure was continued. Briefly, 25 µl of DH5α competent bacteria were mixed with 2 µl of the above

ligation reaction mix and incubated for 30 min on ice followed by heat shock at 42 °C for 45 sec and immediate cooling for 2 min on ice. To this 900 µl of LB medium was added and incubated at 37 °C for 1 hr in a bacterial shaker incubator. The recovered bacteria were then plated onto ampicillin-containing LB agar plates and incubated in a bacteriological incubator maintained at 37 °C for 16–18 h. The well-grown single colonies were selected for screening by inoculating in 5.0 ml of LB medium containing 5 µl of ampicillin (100 mg/ml) and were grown individually for 14-16 h. The turbid bacterial culture was then used for the preparation of plasmid DNA using NucleoSpin plasmid mini-prep kit (Macherey-Nagel). A selected number of clones were further confirmed using restriction digestion and PCR amplification (colony PCR) using specific primers. The positive clones were then sequence verified using vector-specific primers from Thermo Fischer Scientific. The positive clones were further selected for protein expression and purification.

2.2.2. DHTKD1 protein expression and purification using Glutathione sepharose beads

2.2.2.1. Transformation, starter culture preparation and protein expression

DHTKD1 gene without the mitochondrial target sequence was cloned into a pGEX4t1 vector as explained above (2.2.1). This vector was transformed into BL21DE3 Lys bacteria, which can express the protein when induced. The bacteria were transformed with 2 µl of plasmid DNA (80 ng/µl) and rest of the procedure as 2.2.1.4. The turbid bacterial culture grown after inoculating a single colony was then used to cultivate large culture (500 ml LB medium containing 500 µl of ampicillin (100 mg/ml)) in an Erlenmeyer flask. The culture was allowed to shake for 2-3 h at 37 °C until the OD @600 reached 0.6. Frequent measuring of OD for every half an hour was done. After the OD has reached 0.6, 2 ml of culture was taken and stored, which was used as a un-induced control. The culture was then induced for protein expression by adding 0.3 mM isopropyl

thiogalactoside (IPTG) and set for shaking at 37 °C for 3½ to 4 h. From this, 2 ml of culture was stored to be used as an induced sample. The bacterial culture was pelleted at 4000 rpm for 15 min at 4 °C and immediately proceeded for the next steps of purification. A part of pellet and supernatant were stored for western blot analysis. Optionally, the pellet could be stored at -80 °C and used for purification following the next day. To the pellet, chilled lysis buffer was added, resuspended and cooled on ice for 10 min (ratios of cell wet weight to buffer volume of 1:1 to 1:4 were used). The cell suspension was then sonicated with 10 short bursts of 10 sec each followed by intervals of 30 sec for cooling. The cell debris was removed by ultracentrifugation at 4 °C for 30 min at 45,000 rpm using a 45Ti rotor (Beckman). The lysate obtained was then used for loading on to the beads and 1 ml of lysate was stored for SDS analysis.

2.2.2.2. Preparation of Glutathione sepharose beads and purification of protein (protocol from GE healthcare, modified)

The volume of the Glutathione Sepharose 4B beads required for purification was primarily determined. In the current procedure, 5 ml of lysate was used per 1 ml of beads. Beads were centrifuged at 500×g for 5 min to remove the supernatant followed by washing with 5 ml of binding buffer and centrifugation at 500×g for 5 min. The supernatant was carefully removed and the washing step was repeated twice to make sure that the beads are clean. To the washed beads cell lysate was added and incubated for at least 30 min at RT using gentle agitation such as end-over-end rotation. The supernatant (=flow through) obtained by centrifugation at 500×g for 5min was stored to measure the binding efficiency of the lysate via SDS PAGE. The beads were washed by adding 5 ml binding buffer to each 1 ml slurry and inverting up and down for 30 sec. Centrifugation was done at 500×g for 5min and the supernatant (=wash 1) obtained was collected for SDS PAGE analysis. Wash steps were repeated thrice and the supernatants (wash 2 and wash 3) were collected by centrifugation. Bound protein was eluted by adding 0.5 ml of elution buffer per 1 ml slurry of Glutathione sepharose beads. The mixture was gently agitated at RT for 10 min followed by centrifugation at 500×g for 5 min. The supernatant obtained was the eluted protein. Three elution

steps were performed separately to obtain the purified protein. The purified protein was flash frozen in liquid nitrogen and stored at -80 °C.

2.2.2.3. Western blotting and confirmation of purified DHTKD1 protein

All the collected samples during the protein purification procedure were run through SDS PAGE to confirm the presence of DHTKD1 protein. To visualize the protein expression, Coomassie staining and silver staining were done using standard methods according to Maniatis and Sambrook et al.

2.2.3. DHTKD1 enzyme activity assay

DHTKD1 (EC 1.2.4.2) pure protein used for the assay was a kind gift provided by Dr. Wyatt Yue, Oxford University, UK. It was purified by nickel resin based affinity chromatography and gel filtration using ACTA purifier, GE Health care. The activity of DHTKD1 (the so-called E1 like subunit of OGDHc) was assayed in α -keto glutarate dehydrogenase complex buffer (buffer A) (table 4) and was determined as a reduction in 2,6 dichlorophenol indophenol (DCPIP) at $\lambda = 610-750$ nm (Sauer et al., 2005). The activity was measured in buffer with and without 2-oxoadipate or with and without 2-oxoglutarate to check for the specificity of the substrate. The buffer contains dichlorophenolindophenol (DCPIP), which is a colored dye that can be employed as a substrate in redox reactions. DCPIP is blue in color in oxidized conditions and becomes colorless in reduced conditions when measured at wavelength range 610-750 nm (VanderJagt, Garry, & Hunt, 1986).

α- keto glutarate dehydrogenase complex buffer (buffer A)			
Name of the reagent	Stock concentration	Final concentration used	Remarks
Potassium phosphate (KH ₂ PO ₄)	1 M	35 mmol/liter	5 ml of buffer was prepared

EDTA	0.5 M	0.5 mmol/liter	and the pH was adjusted to 7.4
MgSO ₄	1 M	0.5 mmol/liter	
Oxoadipate/alpha keto glutarate	100 mM	2 mmol/liter	
TPP		1mmol/ liter (23 mg taken)	
2,6 Dichlorophenol indophenol (DCPIP)	3 mM	60 μM DCPIP	
sodium azide	1 M	5mM	
triton X 100	20%	0.01%	

Table 4: α - keto glutarate dehydrogenase complex buffer (buffer A)

2.2.4. Determination of Km and Vmax for DHTKD1

To determine the Km & Vmax for DHTKD1, different concentrations of the substrate 2-oxoadipate (0.1 mM, 0.05 mM, 0.1 mM, 0.25 mM, 0.5 mM, 0.75 mM, 1 mM, 2 mM and no substrate) and constant amount of enzyme were analyzed in buffer A without Triton X 100 (table 4), in a 96 well micro titer plate and the OD was measured at $\lambda = 610-750$ nm. The OD values obtained for different substrate concentrations were plotted on a graph and Vmax and Km were calculated using Hanes Woolf equation.

$$\frac{[S]}{V_o} = \frac{[S]}{V_{max}} + \frac{km}{V_{max}}$$

Vo= initial velocity; [S]= substrate concentration; Vmax = maximum velocity; 1/Vmax= Slope; Y intercept= Km/Vmax

2.2.4.1. DHTKD1 inhibitor studies

In order to test the effect of inhibitor on the function of DHTKD1, we used 1mmol/l concentration of each the several synthetic analogues of 2-oxoglutarate namely, glutaryl phosphonate (GP), triethyl ester of glutaryl phosphonate (TEGP), trimethyl acetyl phosphonate (TMAP), acetyl Phosphonate (AP) and diethyl ester of glutaryl phosphonate (DEGP) and incubated DHTKD1 patient and

control fibroblasts for 2.5h and 24h with them. Subsequently, cells pellets were lysed in RIPA buffer and GA and OA levels were analyzed using GCMS.

2.2.5. Western blotting of *Dhtkd1* in mouse tissue samples

2.2.5.1. Preparation of tissue homogenates

Liver and brain tissues of *Dhtkd1* and *Gcdh* single (*Dhtkd1*^{-/-}/*Gcdh*^{+/+}; *Dhtkd1*^{+/+}/*Gcdh*^{-/-}) and double KOs (*Dhtkd1*^{-/-}/*Gcdh*^{-/-}) along with wild-type (*Dhtkd1*^{+/+}/*Gcdh*^{+/+}) mice were obtained from the collaboration partners in Helmholtz Zentrum, Munich. The tissues were chilled on ice in RC buffer (0.1 ml/0.1 mg of tissue) (table 5) and were homogenized with a Potter-Elvehjem system (Fisher Scientific, Schwerte, Germany) using a size that allows the disruption of cell membranes but not organelles, and subcellular fractions were prepared.

RC buffer composition			
Reagent	Stock concentration	Stock concentration	Remarks
sucrose	1 M	1 M	pH adjusted to 7.4
KCl	1 M	1 M	
MgCl ₂	500 mM	500 mM	
Tris-HCl	500 mM	500 mM	

Table 5: Composition of RC Buffer used for the homogenization of tissues

For the preparation of “mitochondrial-enriched” fractions, first cell debris and nuclei were removed by centrifuging the homogenates at 600×g, 4 °C for 10 min. Next, the 600×g supernatant obtained was centrifuged for 10 min, 4 °C at 3,500×g and the pellet used as “mitochondria-enriched” fractions (Kaminski et al., 2010).

2.2.5.2. Determining the concentration of protein

Protein concentration was determined using protein assay kit containing Reagent A and Reagent B from Bio-Rad which is similar to the colorimetric method for protein determination (Lowry, Rosebrough, Farr, & Randall, 1951) described by Lowry. BSA solutions of different concentrations were used as a standard. BSA and samples were diluted in a 1% SDS solution followed by addition of 25 μ l of reagent A and 200 μ l of reagent B. After 10 min of incubation at RT, the absorbance was measured at 750 nm using a spectrophotometer, and the respective protein concentration was calculated depending on the BSA standard curve.

2.2.5.3. SDS-PAGE, immunoblotting and detection by enhanced chemiluminescence

Mitochondrial-enriched fractions (refer Section 2.2.5.1) from livers of knockout and wild-type mice were prepared (in RC buffer) and used for Western blotting. An equal amount of protein was loaded and was separated by sodium dodecyl sulfate-polyacrylamide gel electrophoresis (SDS-PAGE) and transferred to nitrocellulose membranes by electroblotting. After blotting, the membranes were incubated for 1 hr in blocking buffer (5% milk in TBST) followed by incubation with goat polyclonal antibody generated against human DHTKD1 (diluted in 5% milk in TBST; 1:500) O/N at 4 °C with continuous shaking. Non-specific binding was then removed by washing the membrane (1x TBST, 3 times, 10 min each) followed by incubation with horseradish peroxidase-conjugated secondary antibody (diluted in 5% milk in TBST 1:2000) at RT for 1 hr. Unbound antibody was cleared by washing the membrane (1X TBST, 3 times, 10 min each) and visualized by enhanced chemiluminescence according to the manufacturer's instructions (GE Healthcare, Germany).

2.2.6. Analysis of Glutaric acid (GA), 2-oxoadipic acid (OA) and 2-aminoadipic acid (AA) quantitatively

The metabolites GA, 2-OA, and 2-AA were quantitatively measured in tissue homogenates from mice using GC-MS with stable-isotope dilution assay as described by (Sham et al; 2012) with some modifications. Thousand micro liters of the suspension was used for liquid-liquid extraction. In brief, as internal standards, 10 all each of 1 mmol/L stable isotope-labeled d4-nitrophenol and d4-GA were added respectively. The samples were acidified using 300 μ L of 5 M HCl. Following this solid sodium chloride was added and extracted twice with 5 mL ethyl acetate. The obtained fractions were dried initially over sodium sulfate and followed by drying down at 40 °C under nitrogen stream. Samples were further derivatized using N-methyl-N-(trimethylsilyl) heptafluorobutyramide for 1 h at 60 °C. For performing GCMS analysis, MSD 5975A, the quadrupole mass spectrometer was used and run in the selective ion-monitoring mode along with electron impact ionization. A capillary column was used to achieve gas chromatographic separation using helium as a carrier gas. One micro liter of the sample that was derivative was injected in split less mode. The temperature parameters used for GC were as follows; 80 °C for 2 min, ramp 50 °C/min to 150 °C, ramp 10 °C/ min to 300 °C, and hold for 2 min at 300 °C. Interface temperature was set to 290 °C and injector temperature to 280 °C. For quantification of the metabolites, the fragment ions at m/z 261 (GA), m/z 265 (d4- GA) and m/z 302 (2-oxoadipic acid) were analyzed. A dwell time of 50 ms was used. The obtained GCMS results were normalized to the total protein content.

2.2.7. Measurement of Glutaryl carnitine levels

Glutaryl carnitine (C5DC) levels were measured in the liver and brain tissue homogenates (600 \times g supernatant) using ESI-MS/MS as described previously (Sauer, Okun, Fricker, Mahringer, Müller, et al., 2006). Briefly, tissue homogenates (100 μ g) were placed in a single well of a 96- well plate and 100

μL of a methanol stock solution of internal deuterated standards were added and incubated for 20 min. Samples were centrifuged and the supernatant obtained was evaporated until dry, reconstituted in 60 μL of 3 N HCl/butanol, placed in sealed microtiter plates, and incubated at 65 °C for 15 min. The obtained mixtures were then dried and reconstituted in a 100 μL solvent of acetonitrile/water/formic acid (50:50:0.025 v/v/v). A PE 200 auto sampler transferred 20 μL of each into the collision cell at a solvent flow rate of 40 $\mu\text{L}/\text{min}$ using a PE 200 HPLC pump. For measuring acylcarnitines a positive precursor ion scan of m/z 85 (scan range m/z : 225–502) was used and quantified against appropriate deuterated standards with concentrations expressed as $\mu\text{mol}/\text{L}$.

2.2.8. Culturing of fibroblasts, HEK 293T and HeLa cells

Human Embryonic kidney cells (HEK 293T), Human cervix epithelioid carcinoma cells (HeLa) and Normal human dermal fibroblast cells (NHDFC; patient cells and controls) were cultured in T75 flasks using 15 ml Dulbeccos modified eagle medium (DMEM, 500 ml bottle) containing 10% FCS, 1% Penicillin-Streptomycin antibiotic and 1% Amphotericin B (250 UG/ml) at 37 °C and 5% CO₂. After reaching 80-90% confluence, cells were sub cultured in a ratio of 1:15 ml of DMEM.

2.2.9. AADAT siRNA treatment

To knockdown *AADAT* gene in fibroblasts, ONTargetPlus siRNA pools of 5nmol concentration from Dharmacon were ordered and resuspended in 250 μl of RNase-free water to obtain a final concentration of 20 μM , as recommended in the protocol provided by the manufacturer. Lipofectamine RNAimax was used as a transfection reagent and transfections were done according to the manufacturer's instructions. Briefly, cells were grown in 6 well plate, until 70% confluence. Required concentration of siRNA was resuspended in 150 μl Opti-MEM in a 1.5 ml Eppendorf tube. In another tube, 5 μl of Lipofectamine RNAimax

was dissolved in 150 μ l Opti-MEM. Contents of both tubes were mixed and incubated for 5 min at RT. The incubated transfection reaction was carefully added to cells dropwise. Forty-eight hours after transfection western blot was performed to check the efficiency of knockdown.

2.2.10. CRISPR/Cas9 method for the generation of GCDH and AADAT Knockouts

2.2.10.1. Designing gRNAs

For designing gRNAs, CCTop-CRISPR/Cas9 target online predictor tool (Stemmer, Thumberger, Del Sol Keyer, Wittbrodt, & Mateo, 2015) was used and gRNAs specific to the human *GCDH* gene and *AADAT* gene were generated in different exons and synthesized from Thermo Fischer scientific. The gRNAs were designed in such a way that they are unique with no off targets and they are present immediately upstream of the proto spacer adjacent motive sequence (PAM) which will be recognized by the Cas9 protein of *Streptococcus pyogenes*. gRNAs were designed approximately 20 to 23 bp in length with overhangs containing BsmBI restriction sites. The gRNAs having leading G nucleotides at the 5' end (single G for the T7 promoter and two G's for U6 promoter) will be more efficient in inducing the double-stranded breaks (DSBs). So additional G nucleotides were added at the 5' end of the gRNAs in case of their absence. The gRNA oligos were then directly used for the next steps of cloning.

2.2.10.2. Oligo annealing and cloning into PX459 vector (Ran et al., 2013) (modified).

PX459, a mammalian expression vector having a human U6 promoter, Cas9 gene and a puromycin resistance gene was used to clone the gRNAs. Briefly, 1 μ g of plasmid was digested using BbsI enzyme for 30 min at 37 $^{\circ}$ C (table 6). The cut vector was then gel purified (as in 2.2.1.1) using Nucleospin gel and

PCR clean-up kit (M&N). Phosphorylation and annealing of gRNAs was done followed by ligation into the cut PX459 vector (table 7a&7a1) at RT for at least 1 hr. The ligated reaction was then proceeded with transformation (refer 2.2.1.4). Importantly, the ligation reaction and the transformation were included with proper controls, to get rid of false positives. The colonies obtained were selected (10-15 colonies) and mini preparation of plasmid was performed by isolating the plasmid from the O/N cultured colonies. Positive clones were then selected after confirmation by sequencing using human U6 promoter sequencing primer.

Digestion of PX459 vector	
Reagent	Amount
Vector(PX459)	1 µg
FastdigestBsmBI (Thermoscientific)	1 µl
Fast AP (Thermoscientific)	1 µl
10x Fast digest Buffer	2 µl
Nuclease free H2O upto	20 µl

Table 6: Digestion of Px459 vector

b. Ligation reaction		
Reagent	amount	Remarks
BsmBI digested plasmid	50 ng	The reaction was set up at RT for 1 hr
Phosphorylated and annealed oligo duplex (1:200 diluted)	1 µl	
10X T4 DNA ligase buffer	1 µl	
T4 DNA ligase	0.5 µl	
Nuclease free water upto	10 µl	

b1. Thermal cycler conditions
37 °C- 30 min 95 °C- 5 min and then ramp down to 25 °C at 5 °C/min

Table 7 a: Phosphorylation and annealing of oligos; 7 a1: Thermal cycler conditions

2.2.10.3. Determining the cytotoxicity of puromycin for HEK and HeLa cells

The lowest amount of puromycin concentration that causes cell death of HEK and HeLa cells varies among different experimental conditions and cell types. To test this, approximately 25000 cells (HEK and HeLa) were seeded in two different 96 well plates containing 100 μ l DMEM medium and were grown until 70-80% confluence. Different concentrations of puromycin, 0.5 μ g/ml, 1 μ g/ml, 1.5 μ g/ml, 2 μ g/ml, 2.5 μ g/ml, 3 μ g/ml, 4 μ g/ml until 5 μ g/ml were added to different wells of both HEK and HeLa cells from the stock 10 mg/ml. Untreated cells were kept as controls. The medium containing puromycin was changed for every 24 h until 4 days and observed for highest cell death at the lowest concentration. For HEK, 2 μ g/ml and HeLa, 1 μ g/ml of puromycin was observed to be the lowest concentration that could effectively kill all the cells in the culture.

2.2.10.4. Transfection of PX459-gRNA constructs into HEK and HeLa cells

HEK and HeLa cells were cultured in 6-well plates up to 60% confluency. Transfections were done using Lipofectamine 2000 according to manufacturer's protocol. Briefly, 1 μ g plasmid was resuspended in 150 μ l Opti-MEM in a 1.5 μ l Eppendorf tube. In another tube, 5 μ l of Lipofectamine RNA 2000 was dissolved in 150 μ l Opti-MEM. Contents of both tubes were mixed and incubated for 5min at RT. The incubated transfection reaction was carefully added to cells. Twenty four hours after the transfection, cells were kept under antibiotic selection pressure.

2.2.10.5. Confirmation of Knockout cells by western blotting

The transfected cells which survived after puromycin selection were further cultured in T75 flasks and part of those were used to confirm the *GCDH*

Knockout and AADAT knockout. Cells were lysed in RIPA buffer and protein concentration was determined by Lowry method (refer 2.2.5.2). Equal amounts of protein were loaded and the western blotting procedure was performed as in 2.2.5 by using GCDH primary antibody (diluted in 5% milk in TBST; 1:500) and anti-rabbit 2° antibody (diluted in 5% milk in TBST; 1:2000).

2.2.10.6. Generation of single cell clones of GCDH Knockout and AADAT knockout cells

Single cell clones were generated using serial dilution method. Briefly, 100 µl cell culture medium was added to each well of the 96 well plate. To 100 µl medium in well number A1, another 100 µl medium containing 4000 cells were added and mixed well. From this A1 well, 100 µl was taken and mixed into well number A2 and subsequently, serial dilution is done until well no A12. Using a multi-channel pipette, cells from the top wells (A1 to A12) were serially diluted into bottom wells. Each well is checked for the presence of single cells and marked. Single cells were allowed to grow until full confluence and eventually upscaled for the required volume.

2.2.11. Inhibitor treatment of patient fibroblasts and measurement of glutaricacid (GA) levels using GCMS

GA-I patient fibroblasts were used to test the effect of AADAT inhibitor. An equal number of patient fibroblasts (5×10^6 Cells/ T75 flask) were seeded and grown until confluence. Cells were starved overnight in medium without FCS and on the following day, lysine load in DMEM medium (5 mM lysine/5 ml medium) was given, along with different concentrations of inhibitor PF-04859989 (0.1 µM, 1 µM, 10 µM, 50 µM) for every 24 h until three days. After 72 h, cells were washed in PBS, scraped in ddH₂O (1 ml/T75 flask), sonicated and centrifuged at 13,000 rpm for 30 min. Finally, the supernatant was collected and measured for GA levels by GCMS (refer 2.2.6)

2.2.12. Establishing enzyme activity assay for AADAT in patient fibroblasts

GA-I patient fibroblasts were used to establish AADAT enzyme activity assay. Cells were grown to confluence in 10 cm dishes. The medium was removed from cells, washed with PBS twice followed by trypsinization and centrifugation for 10 min at 3000 rpm. The supernatant was removed and cell pellets (1 ml buffer/ 10^7 cells) were lysed in AADAT assay buffer (buffer B) (table 8) with and without AADAT inhibitor (50 μ M) at different time points and immediately flash frozen in liquid nitrogen. Samples were then measured for Oxoadipate levels by GCMS (refer 2.2.6).

AADAT assay buffer (buffer B)		
Reagents	Final concentration	Remarks
2-aminoadipate	1 mM	pH adjusted to 9.5. The buffer was made with and without AADAT inhibitor (50 μ M)
2-oxoglutarate	1 mM	
NADP	0.5 mM	
glutamate dehydrogenase	10 μ l	
RC buffer (refer table 5) up to	10 ml	

Table 8: AADAT enzyme activity assay buffer

2.2.13. Effect of PF-04859989 inhibitor on HEK and HeLa GCDH Knockout cells and GA detection using GCMS

To test the effect of the inhibitor on HEK and HeLa Knockout cells, the same method used for fibroblasts mentioned above in 2.2.11 section was followed.

2.2.14. Detection of DNA damage in fibroblasts

2.2.14.1. Seeding of patient and control cells

GA-I patient and control fibroblasts were seeded (50,000 cells/well) separately in a 24 well plate containing 12 mm coverslips in each well which were just placed before addition of cells. After plating the cells, the coverslips were left undisturbed in the cell culture incubator at 37 °C, 5% CO₂ for 30 min so that they get attached to the surface of the coverslip. 1 ml of DMEM medium was added to the coverslips carefully. After 4 h, the medium was removed and continued with immunofluorescence staining.

2.2.14.2. Immunofluorescence staining

All the incubation steps, before primary antibody addition was carried out on a rocking shaker at RT if unless otherwise stated. The medium was removed after 4 h and cells (refer 2.2.14.1) were washed gently with PBS for 3 x 10 min. The fixation of the cells was done using 4% PFA for 15 min followed by washes with PBS for 2 x 10 min. To permeabilize the cell membranes, 2% Triton-X-100 in PBST was added for 15 min to each well and cells were washed with PBS for 2 x 10 min. Cells were then blocked in blocking buffer containing 5% BSA in PBS for 30 min. After blocking, 100 µl of gamma H2Ax primary antibody (1°Ab) prepared in blocking buffer (1:1000) was added and incubated in the dark at 4 °C O/N with no shaking. On the next day, 1° Ab was removed and washes with PBS were done 3 x 10 min. After washing, 100 µl of Goat anti-mouse IgG Alexa-488 secondary antibody prepared in blocking buffer (1:500) was added and incubated for 1 hr at RT. 2 x 10min washes with PBS were done followed by DAPI staining (1:1000 in PBS) in the dark for 15 min at RT. DAPI was removed and washed with PBS 2 x 10min. Mounting of the coverslips on to the microscopic slides was done by placing 1 drop of mounting medium on the slide and carefully placing the coverslips containing cells (refer 2.2.14.1) on to the mounting medium in such a way that the surface containing cells were

placed downwards and without any air bubble formation. The slides were dried, kept away from exposure to light and finally image analysis was done.

2.2.14.3. Image analysis

Images were acquired by a fluorescence microscope (Nikon) using 60x optics or confocal microscope (Zeiss) using 63x objective. Image analysis was performed using Image J software by counting the number of Foci in the nuclei of cells and comparing them between the GA-I patient and control cells.

2.2.15. Statistical analysis

We performed all statistical tests in Graph pad Prism and data were calculated and presented as mean \pm S.D. Student's T test or ANOVA was used to reveal statistical significance. $P \leq 0.05$ was considered to be statistically significant.

3. Results

3.1. Can targeting DHTKD1 rescue the clinical and biochemical phenotype of GA-I?

In order to identify novel and effective therapeutic interventions as treatment strategies for GA-I, based on our current knowledge from the literature, we tested if inhibition of DHTKD1 can be therapeutically effective in rescuing the clinical and biochemical phenotype shown in GA-I disease.

3.1.1. Cloning, expression and purification of DHTKD1 protein

We initially aimed to clone and purify human DHTKD1 protein to further use it in the pharmacological testing with available inhibitors. In order to achieve this, we employed a pGEX-4T1 vector system (figure 1A). It is a highly suitable heterologous prokaryotic expression system, in which the proteins of interest are expressed as fusion products of Glutathione-S-transferase (GST). This helps in the purification using affinity column based chromatography. *DHTKD1* ORF without the mitochondrial targeting sequence present within the Lentiviral vector pReceiver-Lv21 (Ex-H4610-LV21) was PCR amplified using specific primers and gel purified. Both, the insert and the vector were double digested using NotI and EcoRI restriction enzymes and gel purified. Subsequently, the insert and the vector were ligated using standard molecular biology methods and transformed into chemically competent DH5 α bacterial strain. Positive colonies were selected and cloning was confirmed by sequencing and PCR based amplification (colony PCR), which showed a band at around 2600 bp confirming the presence of *DHTKD1* (figure 1B) insert. Single colonies were inoculated to grow further and pure plasmid containing *DHTKD1* insert was isolated using midi plasmid purification kit. The purified plasmid was then transformed into BL21DE3 Lys chemically competent bacterial strain, which have the ability to express the protein when induced using isopropylthiogalactoside (IPTG). DHTKD1 protein was successfully purified using glutathione sepharose beads using affinity chromatography. The purified DHTKD1 protein (103 KDa) in fused form with GST tag (26 KDa) was observed

at ~130 KDa in silver staining (figure 1C) and the specificity of DHTKD1 protein was further confirmed by western blot (figure 1D). The obtained pure DHTKD1 protein was flash frozen in liquid nitrogen and stored at -80 °C to use in further biochemical and pharmacological studies.

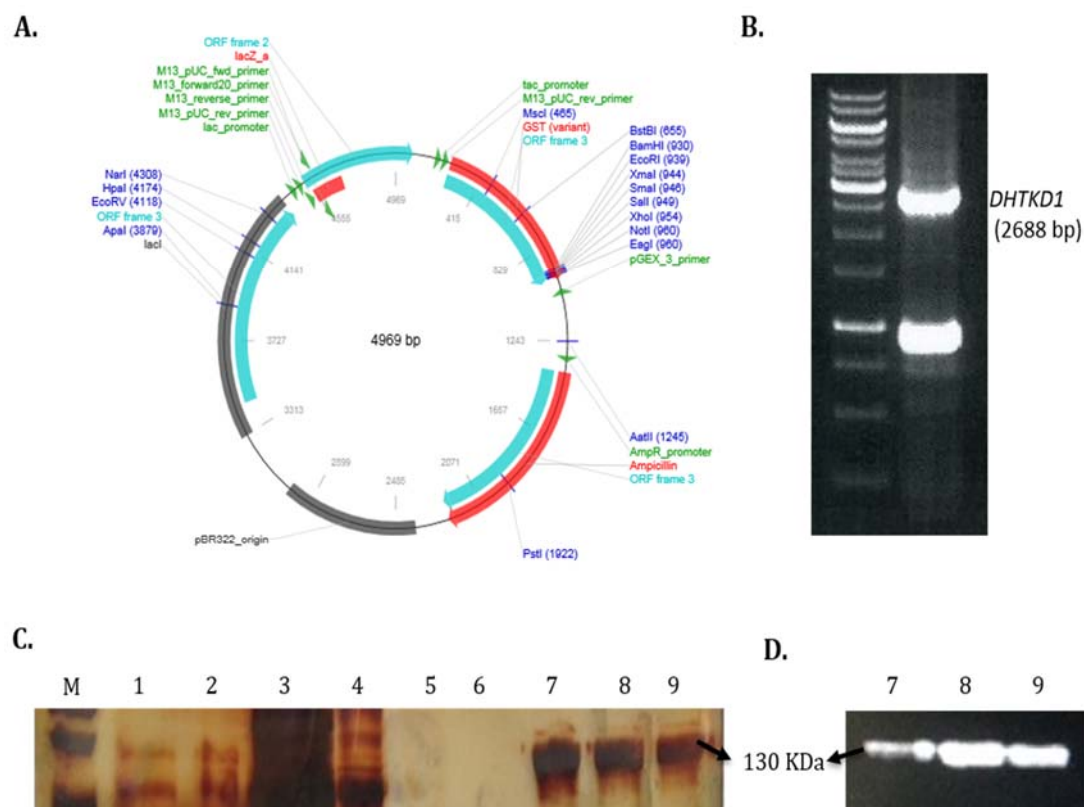


Figure 1: Cloning, expression and purification of DHTKD1 protein: **A.** Schematic representation of pGEX-4T- 1 vector, **B.** Colony PCR showing the presence of *DHTKD1* band (2688 bp), **C.** Silver staining showing DHTKD1 purified protein along with GST fusion tag (130 KDa), **D.** Western blot showing DHTKD1 purified protein (130 KDa) (**M**- marker, **1.** un induced cell pellet, **2.** induced cell pellet, **3.** flow through, **4.** wash-1, **5.** wash-2, **6.** wash-3, **7.** elute-1, **8.** elute-2, **9.** elute-3).

3.1.2. Determining the substrate specificity and enzyme kinetics of purified DHTKD1 protein

We aimed to test the affinity of DHTKD1 towards its substrate 2-oxoadipate using the purified DHTKD1 protein. Unexpectedly, we observed that the

purified DHTKD1 protein (figure 1D) was degraded despite careful and preventive measures employed (figure 2 A). However, purified DHTKD1 protein was generously provided by our collaborator Dr. Wyatt Yue, Oxford University, UK. We obtained highly enriched DHTKD1 protein that was purified using Nickel resin based affinity chromatography and gel filtration using an AKTA purifier, GE Healthcare. The pure DHTKD1 protein has the following sequence (figure 2B). The obtained DHTKD1 protein was incubated with 2-oxoadipate and 2-oxoglutarate in separate reactions in buffer A, which contains the essential components that promote DHTKD1 enzyme activity. 2-Oxoglutarate was used to check the substrate specificity of DHTKD1 using the purified DHTKD1 protein. We observed enzyme activity with incubation with the substrate 2-oxoadipate but not with 2-oxoglutarate (figure 3) suggesting high affinity of DHTKD1 towards 2-oxoadipate.

Additionally, we aimed to assess the kinetic parameters of DHTKD1, providing the necessary K_m and V_{max} values, which are essential for the pharmacokinetic studies. The purified DHTKD1 protein was incubated with different concentrations (0.05 mM, 0.1 mM, 0.25 mM, 0.5mM, 0.75 mM, 1 mM, 2mM and no substrate) of substrate 2-oxoadipate in buffer A and subsequently its kinetic parameters were recorded at wavelength range 610-750 nm. The K_m and V_{max} values for DHTKD1 were determined using Hanes- Woolf equation by plotting (S) on X-axis against $(S)/V$ on Y axis (HALDANE, 1957; Hanes, 1932). The K_m obtained for DHTKD1 was 0.2 mM and the V_{max} was 14.2 $\mu\text{mol}/\text{min}/\text{mg}$ (figure 4).

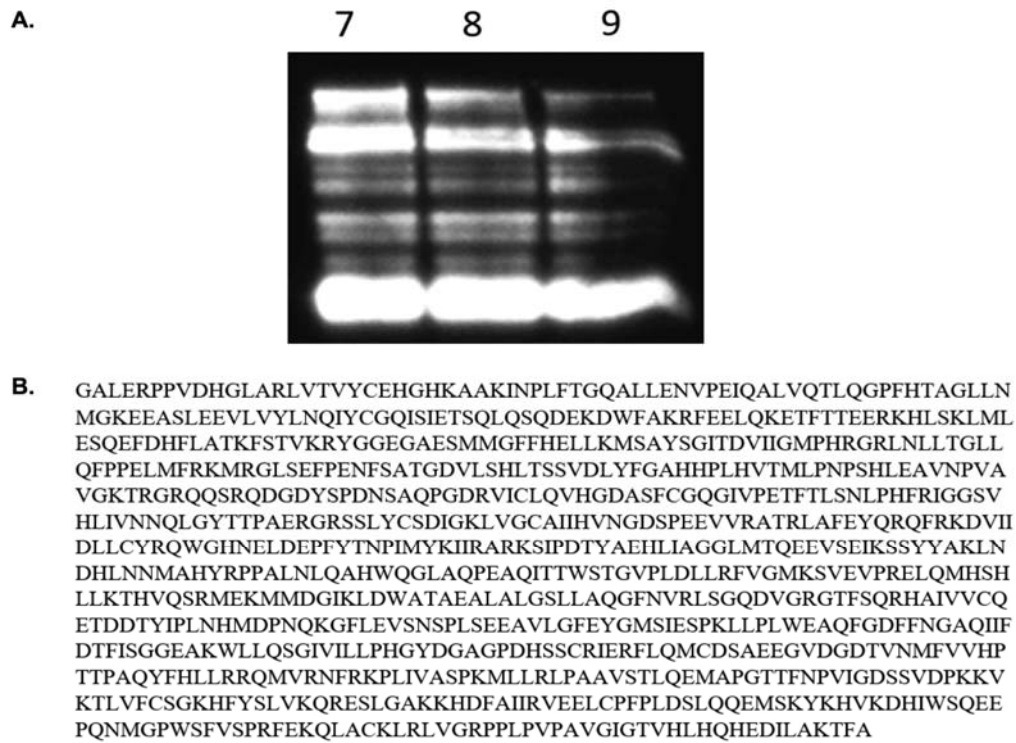


Figure 2: A. Degraded Dhtkd1 protein (7, 8, 9 represents purified protein elutes 1, 2, 3 respectively in degraded form) B. Protein sequence of Dhtkd1 purified protein obtained from Dr. Wyatt Yue's laboratory.

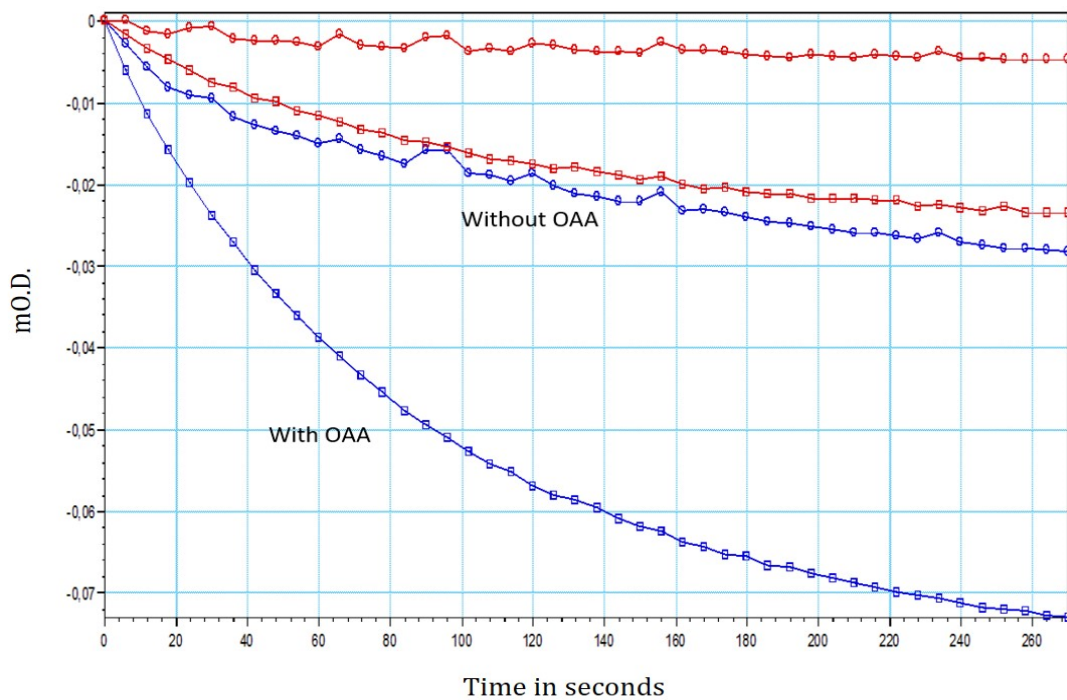


Figure 3: Activity of pure DHTKD1 protein in the presence or absence of its specific substrate, 2-oxoadipate: DHTKD1 enzyme activity was observed in the presence of substrate 2-oxoadipate

(blue squares - with OA), but not in the absence of 2-oxoadipate (blue circles - without OA). Reference line (red).

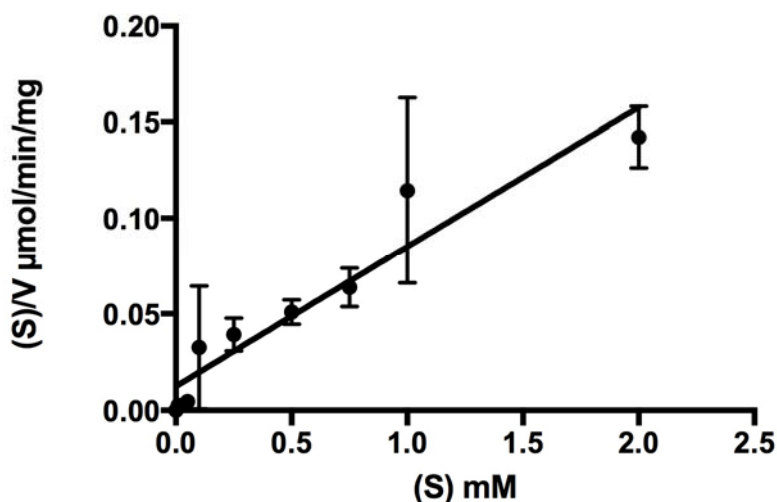


Figure 4: Measurement of K_m and V_{max} for DHTKD1 using Hanes-Woolf plot: Different substrate concentrations (S) plotted on X-axis against the ratio of substrate concentration to initial velocity (S)/V on Y-axis yielded K_m as 0.2 mM and V_{max} as 14.2 $\mu\text{mol}/\text{min}/\text{mg}$ for DHTKD1 protein.

3.1.3. Pharmacological inhibition of DHTKD1

In the next step, we tested the effect of specific synthetic analogues of 2-oxoglutarate on DHTKD1 function *in vitro* by incubating the DHTKD1 patient and control fibroblasts (NHDFC) with phosphonate analogues namely, glutaryl phosphonate (GP), triethyl ester of glutaryl phosphonate (TEGP), trimethyl acetyl phosphonate (TMAP), acetyl Phosphonate (AP) and diethyl ester of glutaryl phosphonate (DEGP). Phosphonate analogues are well known synthetic molecules, reported to inhibit the E1 subunit of OGDHc enzyme (V. I. Bunik et al., 2005).

In brief, we incubated the cells with 1 mmol/l concentration each of the above mentioned phosphonate analogues at two different time points (2.5 h and 24 h) and tested their efficacy in blocking DHTKD1 by measuring the GA and OA levels using GCMS. We observed that the compounds we tested did not show any effect on the GA levels as compared to the basal GA levels. We also found that except for AP, inhibition with other compounds did not show any rise in OA

levels and resembled the basal OA levels (figure 5). Blocking with AP showed an increase in OA levels, in the control cells compared to the basal OA levels, which confirms that AP is able to block DHTKD1 function. Interestingly, DHTKD1 patient cells also displayed increased OA levels in after AP treatment for 24 h. This finding suggests that either residual activity of mutated DHTKD1 or its isoforms (OGDH, OGDHL) partially compensating the loss of DHTKD1 activity are blocked by AP.

Inhibitor			0 (no inhibitor)		GP		TEGP		TMAP		AP		DEGP	
			GA μ M	OA nM	GA μ M	OA nM	GA μ M	OA nM	GA μ M	OA nM	GA μ M	OA nM	GA μ M	OA nM
	Baseline	no cells	0.108	0.007	26.17	0.00	212.534	0.005	0.160	3.961	0.146	1.016	2.118	0.038
2.5 h	NHDF	Medium	0.03	0.05	27.22	0.33	165.99	0.01	1.37	3.60	0.14	1.38	2.10	0.02
	NHDF	Pellet	0.23	1.84	0.26	0.06	0.15	0.09	5.22	0.27	0.18	0.22	0.12	0.12
	Dhtkd1 patient	Medium	0.03	0.02	26.66	0.39	175.77	0.02	0.98	3.22	0.14	1.36	2.33	0.01
	Dhtkd1 patient	Pellet	0.23	1.25	0.26	0.66	3.28	0.46	4.70	0.74	0.27	2.88	0.22	0.66
24 h	NHDF	Medium	0.04	0.03	39.54	0.42	214.96	0.09	3.11	4.73	0.20	5.99	2.88	0.03
	NHDF	Pellet	0.34	0.14	0.34	0.18	4.16	0.02	1.28	0.20	0.42	2.55	0.41	0.00
	Dhtkd1 patient	Medium	0.03	0.33	32.44	0.66	231.25	0.51	2.71	5.16	0.18	2.67	2.30	0.56
	Dhtkd1 patient	Pellet	0.33	1.40	0.33	0.48	2.56	1.18	0.78	1.42	0.39	17.73	0.32	1.47

Figure 5: Measurement of GA and OA levels in DHTKD1^{-/-} patient and control fibroblasts: Different substrate analogues of 2-oxoglutarate were tested on DHTKD1^{-/-} patient and control fibroblasts (medium and pellets). Highlighted shows the levels of GA and OA after AP treatment. NHDF: Normal human derived fibroblasts, taken as a control. Data are presented as n=1.

3.1.4. Murine model for targeting DHTKD1

In order to test the hypothesis of rescuing GA-I phenotype by blocking DHTKD1 *in vivo*, we utilized mice with 4 different genotypes, i.e., *Dhtkd1* Knockout (*Dhtkd1*^{-/-}/*Gcdh*^{+/+}), *Gcdh* Knockout (*Dhtkd1*^{+/+}/*Gcdh*^{-/-}), double Knockout (*Dhtkd1*^{-/-}/*Gcdh*^{-/-}) and control mice (*Dhtkd1*^{+/+}/*Gcdh*^{+/+}) (table A). They were treated with three different diets i.e; standard diet which contains 85mg of L-

lysine, diet with high lysine in chow [contains 235mg lysine in chow] and diet with lysine in both chow and water (376 mg L-lysine in total per day per mouse) (table A1) (Sauer et al., 2015); for GCMS studies, we used tissue homogenates from liver and brain in which the metabolites GA, OA, AA and C5DC were measured.

Type of mice	Genotype	Knockout status
<i>Dhtkd1</i> Knockout mice	<i>Dhtkd1</i> ^{-/-} / <i>Gcdh</i> ^{+/+}	<i>Dhtkd1</i> gene is knocked out, <i>Gcdh</i> gene is normal.
<i>Gcdh</i> Knockout mice	<i>Dhtkd1</i> ^{+/+} / <i>Gcdh</i> ^{-/-}	<i>Gcdh</i> gene is knocked out, <i>Dhtkd1</i> gene is normal.
Double Knockout mice	<i>Dhtkd1</i> ^{-/-} / <i>Gcdh</i> ^{-/-}	Both <i>Dhtkd1</i> gene and <i>Gcdh</i> gene are knocked out.
Control mice	<i>Dhtkd1</i> ^{+/+} / <i>Gcdh</i> ^{+/+}	Both <i>Dhtkd1</i> gene and <i>Gcdh</i> gene are normal.

Table A: Representation of different mouse models along with their genotypes

Diet type	% of L-lysine
No diet or standard diet	1.7% (w/w) or 85mg of L-lysine in food
4.7% chow diet or high lysine diet	4.7% (w/w) or 235mg of L-lysine in food
Chow + water diet	376 mg L-lysine in total in both chow and water

Table A1: Representation of different diets used (Sauer et al., 2015)

Generation of Knockout mice (except of *Gcdh*^{-/-} mice), maintenance, behavioral and clinical characterization were performed in Munich by our collaboration partners (Group of Dr. Holger Prokisch, Helmholtz-Zentrum), whereas the knockout confirmation by western blot (figure 6), biochemical characterization, data analysis were done by me.

3.1.4.1. Generation of *Dhtkd1* Knockout (*Dhtkd1*^{-/-}/*Gcdh*^{+/+}) mice

In brief, the generation of *Dhtkd1*^{-/-}/*Gcdh*^{+/+} mouse was done using Transcription Activator Like Effector Nucleases (TALENs) (wefers et al; 2013). Mutations, which resulted in loss of function of human *DHTKD1*, were identified in exons 1, 7 and 13 (Danhauser et al., 2012a). To knock out *Dhtkd1* in mice, TALENs were designed that are specific for exon 7 and injected into mice. Genotyping of the TALEN injected mice via Sanger sequencing showed a 19 bp deletion in exon 7 of *Dhtkd1*, which predicted to cause frame shift mutations, thereby leading to a premature stop codon, at the amino acid position 431 and giving rise to a truncated protein. The generated *Dhtkd1*^{-/-}/*Gcdh*^{+/+} mice which genetically resembled the patient mutation p.Arg410*, were selected for further characterization (Biagosch et al: 2017).

Liver tissues from the Knockout and control mice were collected and immunoblotting was performed using *Dhtkd1* specific antibody. Western blot analysis showed the presence of *Dhtkd1* protein in samples from control mice, but not in Knockout samples, which confirmed the successful generation of *Dhtkd1*^{-/-}/*Gcdh*^{+/+} mice (figure 6).

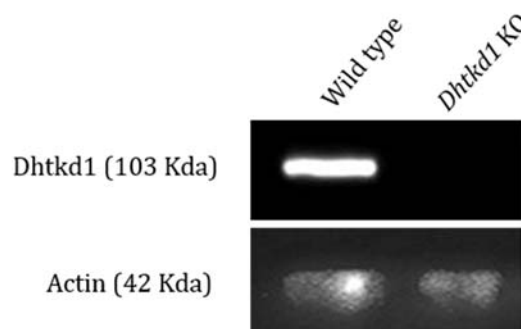


Figure 6: Confirmation of *Dhtkd1*^{-/-}/*Gcdh*^{+/+} by Western blotting: Western blot showing the presence of 103 Kda *Dhtkd1* protein in wildtype sample, but not in *Dhtkd1*^{-/-} sample. Actin (42 Kda) was used as a loading control.

3.1.4.2. Behavioral and biochemical characterization of *Dhtkd1*^{-/-}/*Gcdh*^{+/+} mice

The generated *Dhtkd1*^{-/-}/*Gcdh*^{+/+} mice were characterized by assessing behavioral abnormalities using neurobehavioral experiments like grip strength, inverted grid and balance beam analysis (Biagosch et al., 2017). *Dhtkd1*^{-/-}/*Gcdh*^{+/+} mice did not show any significant differences in its behavior and resembled the control mice, thereby resembling the mild phenotype of patients with *DHTKD1* mutations. Assuming that the knockout of *Dhtkd1* leads to accumulation of OA and AA as seen in patients with mutations of *Dhtkd1*, the *Dhtkd1*^{-/-}/*Gcdh*^{+/+} mice were assessed biochemically via GCMS, by measuring the GA, OA and AA levels in the liver and brain tissue lysates.

Surprisingly, we did not observe any significant rise in OA levels in the liver or brain samples of *Dhtkd1*^{-/-}/*Gcdh*^{+/+} mice on standard diet or high lysine diet compared to *Dhtkd1*^{+/+}/*Gcdh*^{+/+} mice. On the other hand, the AA levels in liver tissue lysates were significantly increased in *Dhtkd1*^{-/-}/*Gcdh*^{+/+} mice to 148.8 ± 69.1 fold compared to *Dhtkd1*^{+/+}/*Gcdh*^{+/+} mice on standard diet ($P \leq 0.05$; two way ANOVA for multiple comparisons; Fisher's LSD). A similar pattern was observed in the *Dhtkd1*^{-/-}/*Gcdh*^{+/+} mice kept on high lysine diet, which showed significantly increased AA levels compared to *Dhtkd1*^{+/+}/*Gcdh*^{+/+} mice in the liver tissue lysates (figure 9B) (10.33 ± 0.21 fold increase; $P \leq 0.05$; two way ANOVA for multiple comparisons; Fisher's LSD). Brain AA levels were similar in both groups (figure 9A). As expected, we did not observe any accumulation of GA levels in the *Dhtkd1*^{-/-}/*Gcdh*^{+/+} mice in both brain and liver tissue lysates under standard diet, high lysine diet and also chow + water diets tested (figure 10 A&B).

3.1.4.3. Knockout of *Dhtkd1* was not able to rescue the clinical and biochemical phenotype seen in *Gcdh*-deficient mice

3.1.4.3.1. Generation and characterization of double Knockout (*Dhtkd1*^{-/-}/*Gcdh*^{-/-}) mice

The *Dhtkd1*^{-/-}/*Gcdh*^{-/-} mice were generated by crossing the well-characterized *Dhtkd1*^{+/-}/*Gcdh*^{-/-} mice with the above described *Dhtkd1*^{-/-}/*Gcdh*^{+/-} mice. At 3 months age, the generated *Dhtkd1*^{-/-}/*Gcdh*^{-/-} mice showed clinical phenotype under standard dietary conditions, similar to the *Dhtkd1*^{+/-}/*Gcdh*^{-/-} mice. For example, we observed a significant reduction in the locomotor activity in both *Dhtkd1*^{-/-}/*Gcdh*^{-/-} and *Dhtkd1*^{+/-}/*Gcdh*^{-/-} mice, as compared to *Dhtkd1*^{-/-}/*Gcdh*^{+/-} mice, which was measured by counting the number of quadrants travelled with in an arena by each animal in 30 sec time (Biagosch et al., 2017). We also observed a more pronounced effect (significant reduction) in transfer arousal of *Dhtkd1*^{-/-}/*Gcdh*^{-/-} mice than *Dhtkd1*^{+/-}/*Gcdh*^{-/-} mice when compared to *Dhtkd1*^{-/-}/*Gcdh*^{+/-} mice, which was measured by placing the mouse into an arena and scoring was given as follows. If the mouse showed freezing behavior after placing into the arena for 5 sec or more, score 0 was given. If the mouse showed a brief freezing, score 1 was given and score 2 was given if the mouse showed immediate movement (Biagosch et al., 2017).

3.1.4.3.1.1. The clinical phenotype of *Dhtkd1*^{-/-}/*Gcdh*^{-/-} mice contradicts our current hypothesis

The generated *Dhtkd1*^{-/-}/*Gcdh*^{-/-} mice along with the *Dhtkd1*^{-/-}/*Gcdh*^{+/-}, *Dhtkd1*^{+/-}/*Gcdh*^{-/-} and *Dhtkd1*^{+/-}/*Gcdh*^{+/-} mice were subjected to high lysine diet or chow + water diet in order to induce a clinical phenotype (Sauer et al., 2015). We defined the clinical endpoints in our study as primarily weight loss, followed by seizures and death. After 24 h of dietary lysine supply, we looked for the clinical phenotype if any and observed that one *Dhtkd1*^{-/-} mice (n=7), four *Dhtkd1*^{+/-}/*Gcdh*^{-/-} mice (n=5) and none of the control mice (n=5) showed

weight loss of >15%, which is a lethal condition, as reported before (Sauer et al., 2015) (figure 7). Surprisingly, all the *Dhtkd1*^{-/-}/*Gcdh*^{-/-} mice (n=7) showed a critical weight loss representing the same clinical characteristics as that of the *Dhtkd1*^{+/+}/*Gcdh*^{-/-} mice (figure 7). We also tested for lethargic behavior, which was estimated by keeping the mice into an arena with four quadrants and mice, which travelled less than two quadrants within 30 sec duration were considered to be lethargic. Four *Dhtkd1*^{+/+}/*Gcdh*^{-/-} mice (n=5) and five *Dhtkd1*^{-/-}/*Gcdh*^{-/-} mice (n=6) showed more lethargic behavior, while only one of the wildtype (*Dhtkd1*^{+/+}/*Gcdh*^{+/+}) (n=7) and two of *Dhtkd1*^{-/-}/*Gcdh*^{+/+} mice (n=7) showed the same phenotype (figure 7).

This unexpected behavioral and clinical characteristics seen in the *Dhtkd1*^{-/-}/*Gcdh*^{-/-} mice in turn questions our initial hypothesis of blocking DHTKD1 function to rescue the clinical phenotype of GA-I.

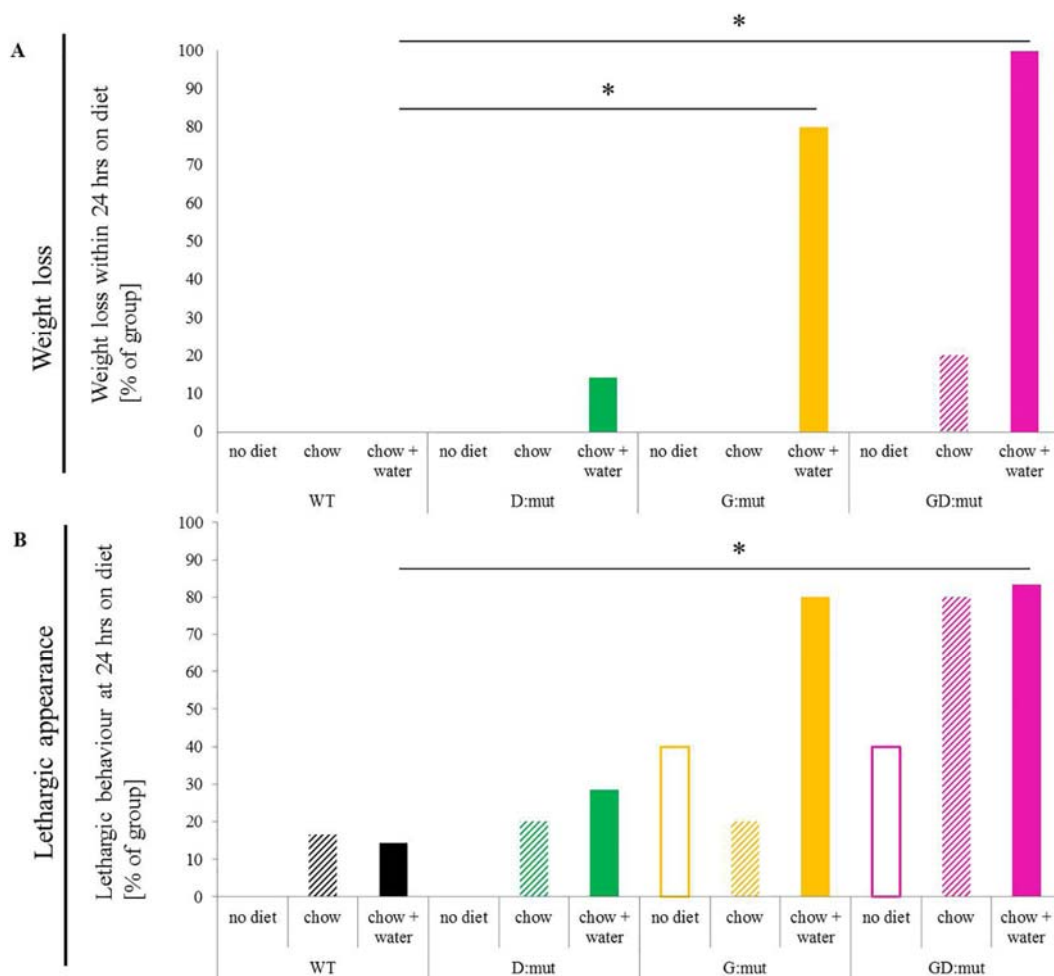


Figure 7: Clinical and behavioral analysis of *Dhtkd1*^{-/-}*Gcdh*^{-/-} mice on different diets: A. weight loss measured after 24 hrs of lysine treatment B. Lethargic behavior was measured by keeping mice into an arena with quadrants and locomotor activity was observed within a time span of 30 sec (no diet; high-lysine in chow; chow and water). WT = *Gcdh*^{+/+}/*Dhtkd1*^{+/+} (n = 8;6;7); D:mut = *Gcdh*^{+/+}/*Dhtkd1*^{-/-} (n = 5;5;7); G:mut = *Gcdh*^{-/-}/*Dhtkd1*^{+/+} (n = 5;5;5); GD:mut = *Gcdh*^{-/-}/*Dhtkd1*^{-/-} (n = 5;5;6). *Fisher's Exact test: *P* < 0.05; Source: Biagosch et al 2017

3.1.4.3.1.2. The biochemical phenotypes of *Dhtkd1*^{-/-}/*Gcdh*^{-/-} and *Gcdh*^{-/-} mice do not differ

Next we tested whether the same holds true biochemically, by measuring different metabolites (GA, OA and AA) in the liver and brain homogenates in all the four different genotypes *Dhtkd1*^{-/-}/*Gcdh*^{+/+}, *Dhtkd1*^{+/+}/*Gcdh*^{-/-}, *Dhtkd1*^{-/-}/*Gcdh*^{-/-} and *Dhtkd1*^{+/+}/*Gcdh*^{+/+} upon standard diet, high lysine diet and chow + water diet, using GCMS. Additionally, we also measured glutaryl carnitine (CD5), which serves as a biological marker for GA-I detection in newborn screening (Sauer, Okun, Fricker, Mahringer, Müller, et al., 2006). Biochemically, we expected a rise in OA and AA levels in *Dhtkd1*^{-/-}/*Gcdh*^{-/-} mice as compared to *Dhtkd1*^{+/+}/*Gcdh*^{-/-} and *Dhtkd1*^{+/+}/*Gcdh*^{+/+} mice. With respect to GA levels, we expected a decrease in *Dhtkd1*^{-/-}/*Gcdh*^{-/-} mice compared to *Dhtkd1*^{+/+}/*Gcdh*^{-/-} mice. We first started with looking for differences in the OA levels. Overall, we did not observe any statistically significant changes of OA levels in *Dhtkd1*^{-/-}/*Gcdh*^{+/+} mice and the *Dhtkd1*^{-/-}/*Gcdh*^{-/-} mice compared to control mice in all the dietary regimens supplied. (figure 8A&B).

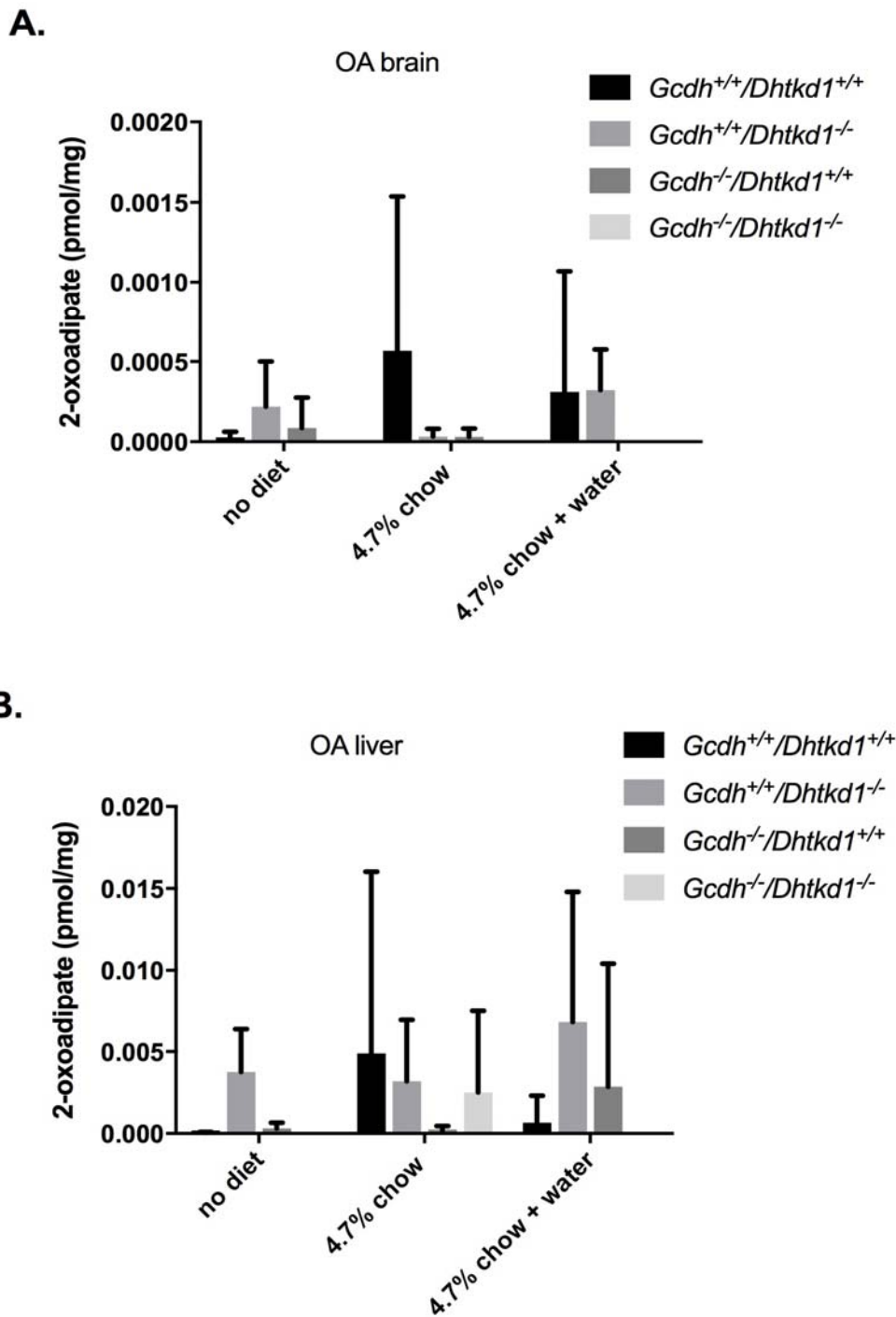
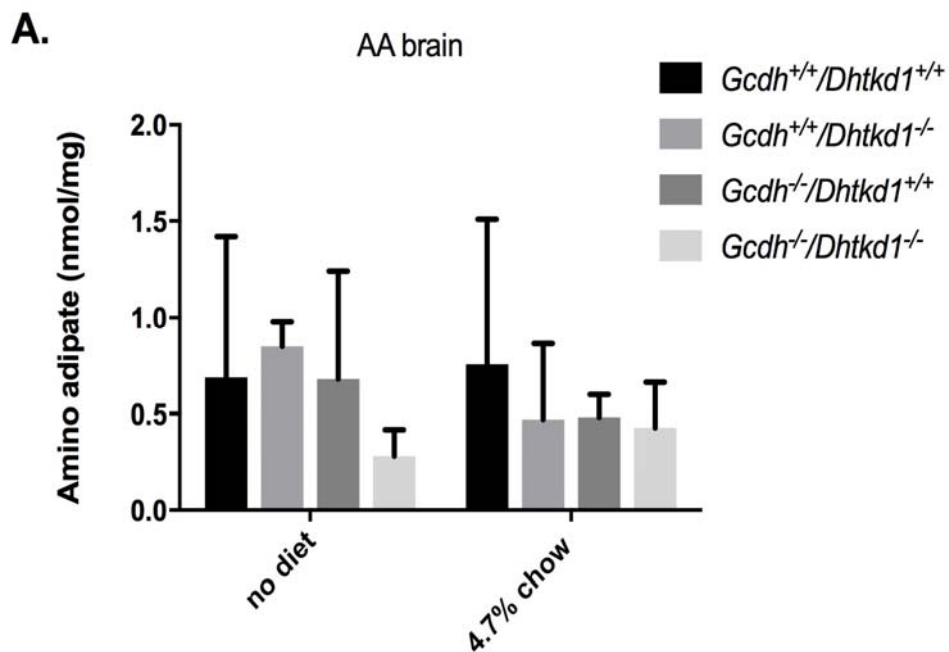


Figure 8: Graphs showing OA levels in brain and liver: Biochemical analyses of OA levels in brain **(A)** and liver tissues **(B)** of double knockout mice (*Dhtkd1*^{-/-}/*Gcdh*^{-/-}), *Dhtkd1* Knockout mice (*Dhtkd1*^{-/-}/*Gcdh*^{+/+}), *Gcdh* Knockout mice (*Dhtkd1*^{+/+}/*Gcdh*^{-/-}) as compared to control mice (*Dhtkd1*^{+/+}/*Gcdh*^{+/+}) on no diet or high-lysine diet or chow + water diet. No diet= standard diet (age of 39.2 days (sd ± 7.7)); chow 4.7%=high lysine in chow (age of 39.7 days (sd ± 3.5)); 4.7%

chow+water=high lysine in chow and water (age of 36.2 days (sd \pm 4.8)); n \geq 5 for OA; Data is presented as mean and error bars indicate standard deviation (sd).

With regard to the AA levels (n=4) in brain, there were no statistically significant differences observed in all the genotypes and diets tested (figure 9A). On the other hand in the liver samples of *Dhtkd1*^{-/-}/*Gcdh*^{+/+} mice, we observed significantly increased ($P \leq 0.05$; two way ANOVA for multiple comparisons; Fisher's LSD) AA levels on standard diet and also after high lysine diet compared to *Dhtkd1*^{+/+}/*Gcdh*^{+/+} mice (see 3.1.4.2) (figure 9B). As expected the *Dhtkd1*^{+/+}/*Gcdh*^{-/-} mice did not show any rise in AA levels on standard diet as well as high lysine diet. The AA levels in the liver tissue lysates of *Dhtkd1*^{-/-}/*Gcdh*^{-/-} mice on high lysine diet showed a increase (5 ± 0.5 fold) as compared to the *Dhtkd1*^{+/+}/*Gcdh*^{+/+} mice $P \leq 0.05$; two way ANOVA for multiple comparisons; Fisher's LSD; figure 9B).



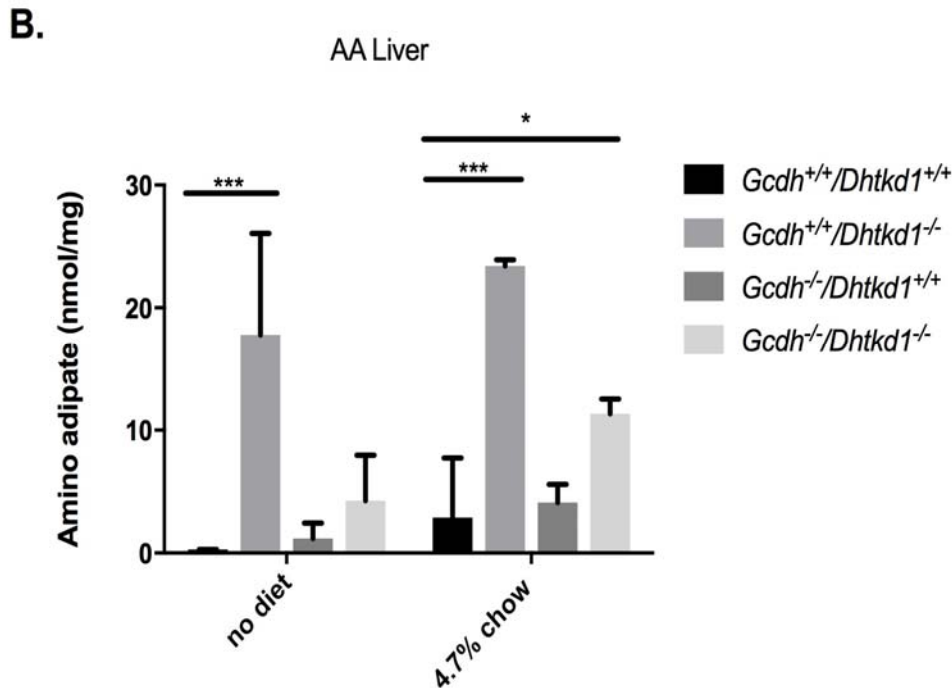


Figure 9: Graphs showing AA levels in brain and liver: Biochemical analyses of AA levels in brain **(A)** and liver tissues **(B)** of double knockout mice (*Dhtkd1*^{-/-}/*Gcdh*^{-/-}), *Dhtkd1* Knockout mice (*Dhtkd1*^{-/-}/*Gcdh*^{+/+}), *Gcdh* Knockout mice (*Dhtkd1*^{+/+}/*Gcdh*^{-/-}) as compared to control mice (*Dhtkd1*^{+/+}/*Gcdh*^{+/+}) on no diet or high-lysine diet or chow + water diet. No diet=standard diet (age of 39.2 days (sd ± 7.7)); chow 4.7%=high lysine in chow (age of 39.7 days (sd ± 3.5)); 4.7% chow+water=high lysine in chow and water (age of 36.2 days (sd ± 4.8)); n=3-4 for AA; Data is presented as mean and error bars indicate standard deviation (sd). (* represents $P \leq 0.05$; two way ANOVA for multiple comparisons; Fisher's LSD).

In the next steps, we determined the GA levels in both brain and liver tissue lysates of the *Dhtkd1*^{+/+}/*Gcdh*^{-/-} mice. As expected, in the brain tissue lysates, *Dhtkd1*^{+/+}/*Gcdh*^{-/-} mice showed a significant accumulation ($P \leq 0.05$; two way ANOVA for multiple comparisons; Fisher's LSD) of GA levels on standard diet (60.23 ± 9.25 fold increase), on high lysine diet (30.92 ± 11.8 fold increase) and on chow + water diet (33.43 ± 8.95 fold increase) compared to *Dhtkd1*^{+/+}/*Gcdh*^{+/+} mice (figure 10A). In the liver tissue lysates, *Dhtkd1*^{+/+}/*Gcdh*^{-/-} mice showed the same pattern of significant GA accumulation as that seen in the brain tissue lysates ($P \leq 0.05$; two way ANOVA for multiple comparisons; Fisher's LSD). We observed a significant increase in GA levels on standard diet (46.17 ± 12.05 fold increase), on high lysine diet (27.39 ± 15.96 fold increase) and on chow plus

water diet (25.01 ± 16.75 fold increase) when compared to *Dhtkd1^{+/+}/Gcdh^{+/+}* mice (figure 10B). Also, when compared to the *Dhtkd1^{-/-}/Gcdh^{+/+}* mice, *Dhtkd1^{+/+}/Gcdh^{-/-}* mice showed significantly increased GA levels in brain tissue lysates on standard diet (41 ± 6.3 fold increase), high lysine diet (4.5 ± 1.73 fold increase) and chow plus water diet (24.6 ± 6.6 fold increase) (figure 10A). Similarly, in the liver tissue lysates, the *Dhtkd1^{+/+}/Gcdh^{-/-}* mice as compared to the *Dhtkd1^{-/-}/Gcdh^{+/+}* mice showed a significant accumulation on standard diet (12.2 ± 3.2 fold increase), high lysine diet (5.75 ± 3.35 fold increase) and chow plus water diet (9.2 ± 6.15 fold increase) ($P \leq 0.05$; two way ANOVA for multiple comparisons; Fisher's LSD) (figure 10B).

Surprisingly, the *Dhtkd1^{-/-}/Gcdh^{-/-}* mice also showed increased GA concentrations as compared to the *Dhtkd1^{+/+}/Gcdh^{+/+}* mice, similar to that of *Dhtkd1^{+/+}/Gcdh^{-/-}* mice. In brain tissue lysates, we observed a significant accumulation of GA levels ($P \leq 0.05$; two way ANOVA for multiple comparisons; Fisher's LSD) on standard diet (50.57 ± 10.2 fold increase), on high lysine diet (42 ± 9.5 fold increase) and on chow plus water diet (38.5 ± 15.3 fold increase) compared to the *Dhtkd1^{+/+}/Gcdh^{-/-}* mice (figure 10A). Similarly, the liver tissue lysates of *Dhtkd1^{-/-}/Gcdh^{-/-}* mice also showed a significant accumulation of GA levels on standard diet (35.2 ± 8.27 fold increase), on high lysine diet (27.02 ± 13.08 fold increase) and on chow plus water diet (34.27 ± 16.9 fold increase) compared to the *Dhtkd1^{+/+}/Gcdh^{+/+}* mice (figure 10B). These results contradicted our initial idea of exploiting *Dhtkd1* inhibition as novel therapeutic strategy in GA-I.

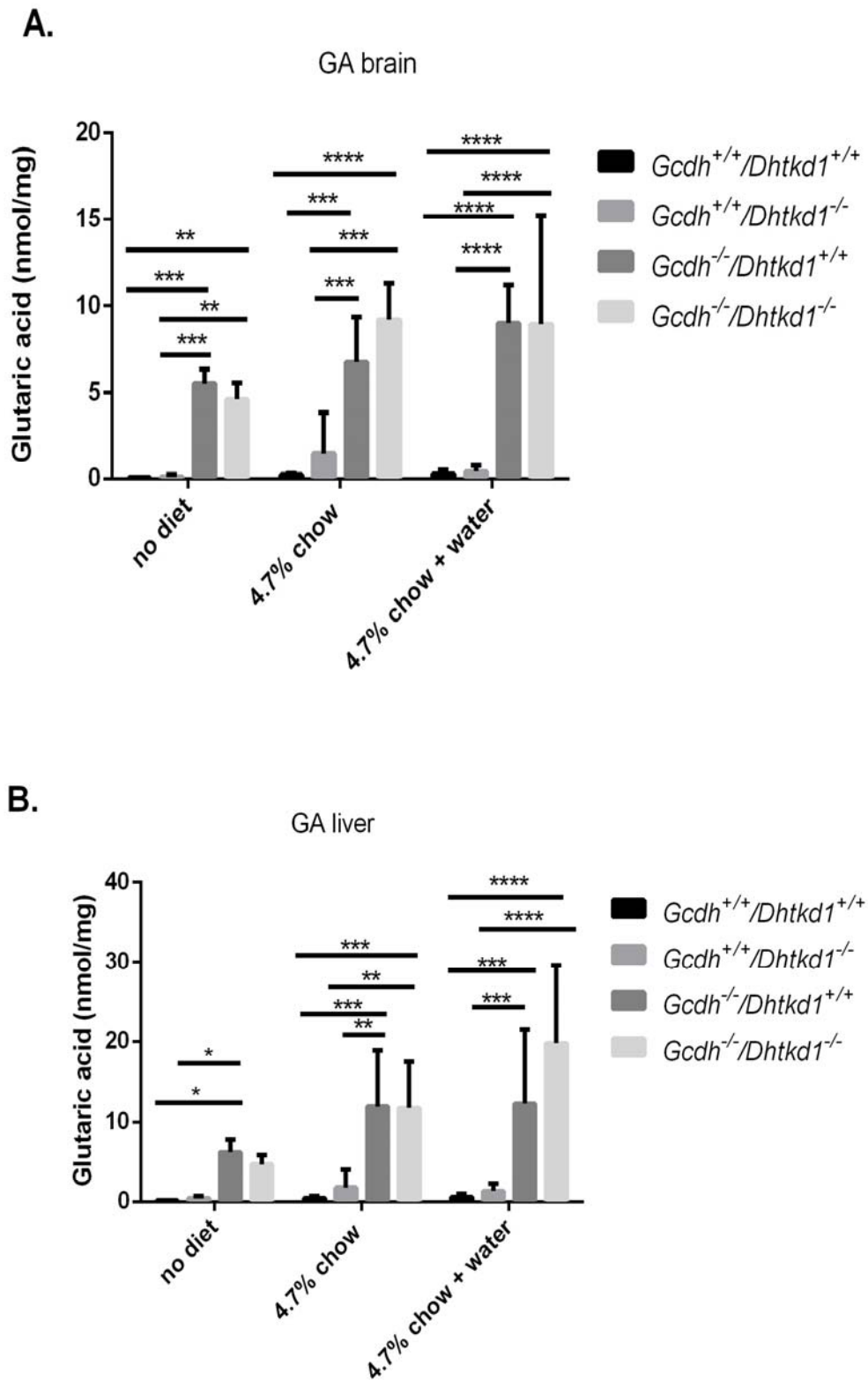


Figure 10: Graphs showing GA levels in brain and liver: Biochemical analyses of GA levels in brain **(A)** and liver tissues **(B)** of double knockout mice (*Dhtkd1*^{-/-}/*Gcdh*^{-/-}), *Dhtkd1* Knockout mice (*Dhtkd1*^{-/-}/*Gcdh*^{+/+}), *Gcdh* Knockout mice (*Dhtkd1*^{+/+}/*Gcdh*^{-/-}) as compared to the control

mice (*Dhtkd1^{+/+}/Gcdh^{+/+}*) on no diet or high-lysine diet or chow + water diet. No diet=standard diet (age of 39.2 days (sd \pm 7.7)); chow 4.7%=high lysine in chow (age of 39.7 days (sd \pm 3.5)); 4.7% chow+water=high lysine in chow and water (age of 36.2 days (sd \pm 4.8)); n \geq 5 for GA; Data is presented as mean and error bars indicate standard deviation (sd) (* represents $P \leq 0.05$; two way ANOVA for multiple comparisons; Fisher's LSD).

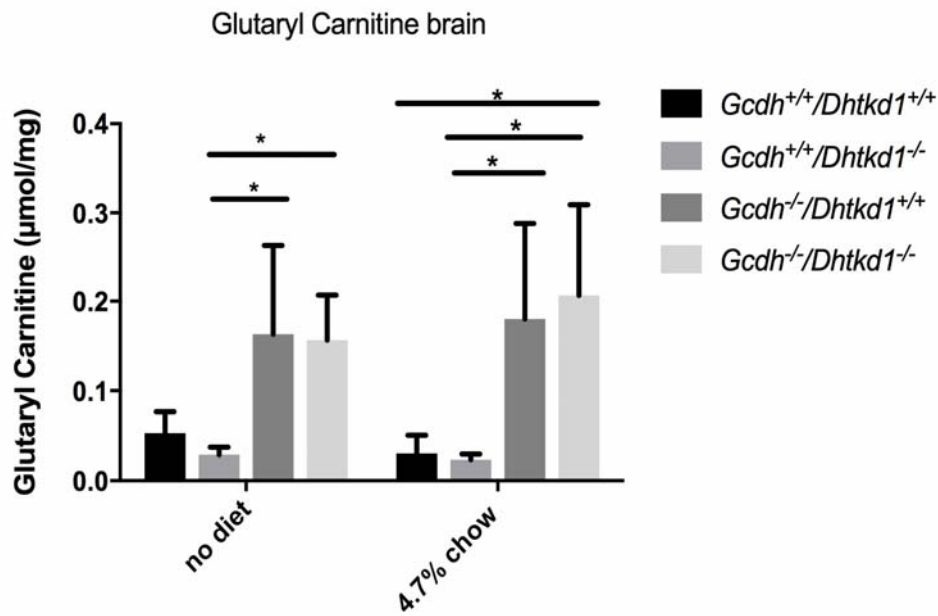
Since we did not observe a reduction in GA levels in the *Dhtkd1^{-/-}/Gcdh^{-/-}* mice, we further aimed to test, if this holds true with respect to glutaryl carnitine (C5DC) levels (n = 4). We did not observe any significant differences ($P \leq 0.05$; two way ANOVA for multiple comparisons; Fisher's LSD) in the CD5 levels of *Dhtkd1^{-/-}/Gcdh^{+/+}* mice when compared to *Dhtkd1^{+/+}/Gcdh^{+/+}* mice under standard diet and high lysine diet conditions in both liver and brain tissue lysates (figure 11 A&B). When we compared the CD5 levels in liver and brain samples of *Dhtkd1^{-/-}/Gcdh^{+/+}* mice to that of *Dhtkd1^{+/+}/Gcdh^{-/-}* mice, we observed a significant rise in CD5 levels of *Dhtkd1^{+/+}/Gcdh^{-/-}* mice under standard diet (brain, 5.6 ± 3.35 fold increase; liver, 23.2 ± 2.4 fold increase) and high lysine diets (brain, 8.34 ± 5 fold increase; liver, 38.6 ± 28.7 fold increase). In the brain tissue lysates of *Dhtkd1^{+/+}/Gcdh^{-/-}* mice, we observed a significant up regulation ($P \leq 0.05$; two way ANOVA for multiple comparisons; Fisher's LSD) of CD5 levels under high lysine diet (5.35 ± 3.21 fold increase) as compared to *Dhtkd1^{+/+}/Gcdh^{+/+}* mice. In case of liver lysates, the *Dhtkd1^{+/+}/Gcdh^{-/-}* mice showed a significant up regulation of CD5 levels in both standard diet and also under high lysine diet (17.45 ± 12.96 fold increase) when compared to the *Dhtkd1^{+/+}/Gcdh^{+/+}* mice (figure 11 A&B).

When we compared the CD5 levels of *Dhtkd1^{+/+}/Gcdh^{+/+}* mice to that of *Dhtkd1^{-/-}/Gcdh^{-/-}* mice, in brain and liver tissue lysates, we found a significant increase ($P \leq 0.05$; two-way ANOVA for multiple comparisons; Fisher's LSD) in CD5 levels upon high lysine diet (brain, 6.03 ± 2.97 fold increase; liver, 12.76 ± 6.24 fold increase), similar to the pattern observed for GA levels. We also observed an increase in CD5 levels significantly in brain lysates of *Dhtkd1^{-/-}/Gcdh^{-/-}* mice (9.4 ± 4.6 fold increase) under high lysine diet and in liver lysates under both standard diet (17.3 ± 8 fold increase) and high lysine diets (28.3 ± 13.8 fold increase) as compared to *Dhtkd1^{-/-}/Gcdh^{+/+}* mice (figure 11 A&B). Similarly, we

also observed a rise in CD5 levels in both *Dhtkd1*^{+/+}/*Gcdh*^{-/-} mice and *Dhtkd1*^{-/-}/*Gcdh*^{-/-} mice in both standard diet and high lysine diet in both the brain and liver tissue samples, replicating the pattern seen for GA levels (figure 11 A&B).

The increase in GA levels in *Dhtkd1*^{-/-}/*Gcdh*^{-/-} mice similar to *Dhtkd1*^{+/+}/*Gcdh*^{-/-} mice shows that the Knockout of *Dhtkd1* in *Gcdh* knockout mice did not rescue the biochemical phenotype of GA-I. The increase in CD5 levels in *Dhtkd1*^{-/-}/*Gcdh*^{-/-} mice compared to *Dhtkd1*^{+/+}/*Gcdh*^{+/+} mice or *Dhtkd1*^{-/-}/*Gcdh*^{+/+} mice further strengthens the idea that *Dhtkd1* may not be an effective therapeutic strategy to treat GA-1 disorder either clinically or biochemically.

A.



B.

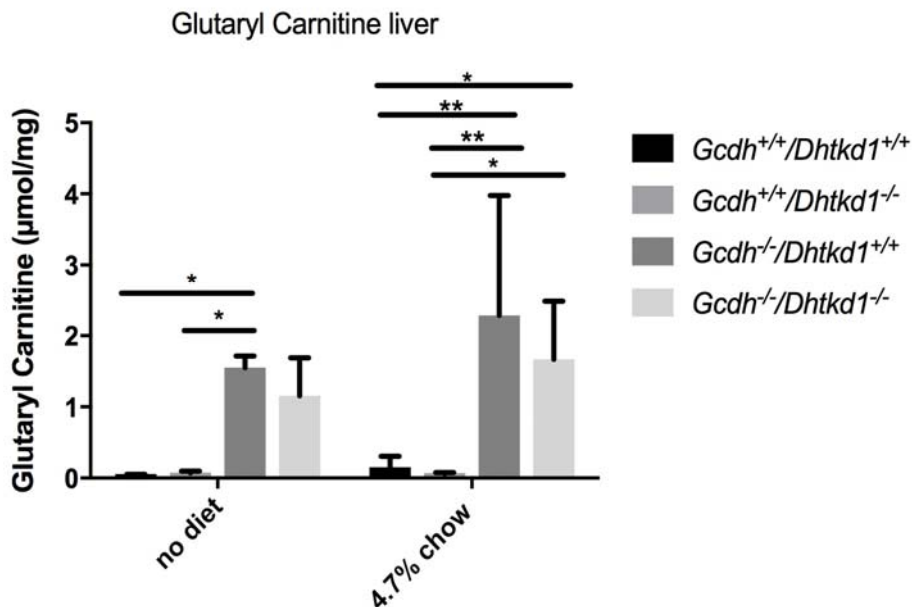


Figure 11: Graphs showing CD5 levels in brain and liver: Biochemical analyses of glutaryl carnitine (CD5) levels in brain **(A)** and liver tissues **(B)** of double knockout mice (*Dhtkd1^{-/-}/Gcdh^{-/-}*), Dhtkd1 Knockout mice (*Dhtkd1^{-/-}/Gcdh^{+/+}*), Gcdh Knockout mice (*Dhtkd1^{+/+}/Gcdh^{-/-}*) as compared to control mice (*Dhtkd1^{+/+}/Gcdh^{+/+}*) on no diet or high-lysine diet or chow + water diet. No diet=standard diet (age of 39.2 days (sd ± 7.7)); chow 4.7%=high lysine in chow (age of 39.7 days (sd ± 3.5)); 4.7% chow+water=high lysine in chow and water (age of 36.2 days (sd ± 4.8)); n=3-4 for CD5; Data is presented as mean and error bars indicate standard deviation (sd) (* represents $P \leq 0.05$; two-way ANOVA for multiple comparisons; Fisher's LSD).

3.2. AADAT as an alternative target for treating GA-1 patients?

Our results clearly indicated that DHTKD1 is not a suitable drug target in GA-I. In the next steps we employed a similar strategy as that followed for DHTKD1, targeting AADAT. To achieve this, we performed siRNA mediated knock down of AADAT on patient fibroblasts, tested the effect of AADAT inhibitor PF-04859989 on patient and control fibroblasts and later moved on to knocking out AADAT in GCDH Knockout cell models by employing CRISPR/Cas9 method.

3.2.1. siRNA mediated knockdown of AADAT

First, we performed siRNA-mediated AADAT knockdown experiments in GA-I patient fibroblast. siRNA transfections were done using electroporation or lipid mediated methods. Fibroblasts did not survive electroporation mediated transfection, however, we were successful in transfecting the fibroblasts, by employing lipofectamine RNAi max method. Different concentrations of siRNA (5 nM, 10 nM, 25 nM, 50 nM) (figure 12) were transfected into fibroblasts, cell lysates were made 72 h after transfection and analyzed by western blot. Surprisingly, we did not observe any reduction in AADAT levels after siRNA knockdown at all concentrations tested (figure 12) compared to the mock control and the non-targeting control.

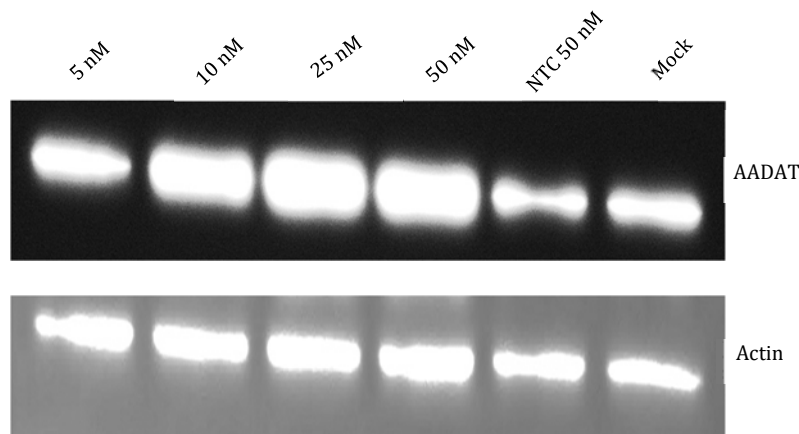


Figure 12: siRNA mediated knock down of AADAT: Western blot showing knock down efficiency of AADAT after transfection with AADAT siRNA (5 nM, 10 nM, 25 nM, 50 nM) in comparison to the non-targeting control (NTC) and mock control. Actin was used as a loading control.

3.2.2. Inhibition of AADAT by PF-04859989 *in vitro*

In the next steps, we aimed to test the activity of AADAT in the presence and absence of PF-04859989 (50 μ M), a known and specific to AADAT/KAT-II inhibitor. To perform this, we took the cell lysates from GA-I patient fibroblasts and incubated them with and without PF-04859989 for different time points (0 h, 0.5 h, 1 h) in AADAT activity assay buffer and 2-oxoadipate levels were measured by GCMS. We observed a significant reduction in AADAT activity in the presence of inhibitor, when compared to the controls at all the time points tested (at 0 h, 0.32 ± 0.07 fold reduction; at 0.5 h, 0.27 ± 0.01 fold reduction; at 1h, 0.27 ± 0.05 fold reduction compared to their respective controls; $P \leq 0.05$; statistical test; students T test) (figure13).

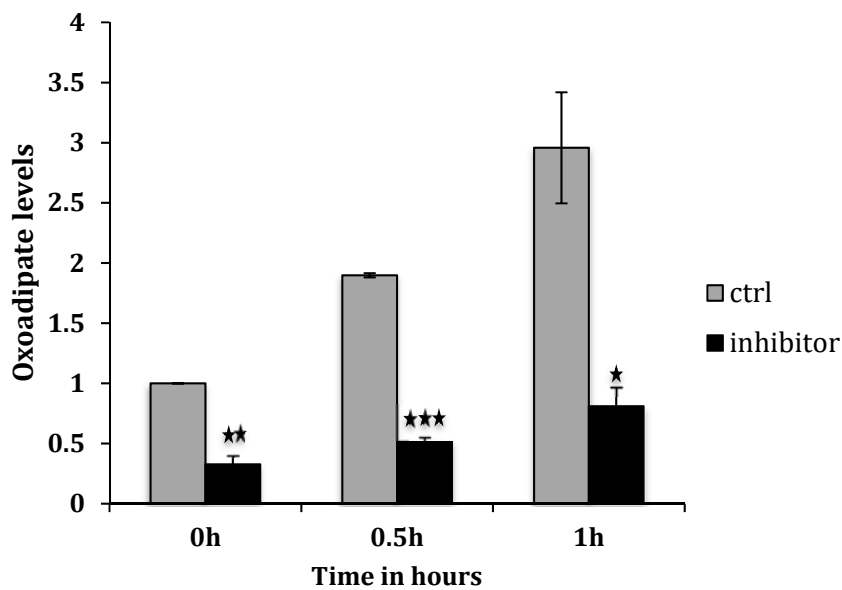


Figure 13: Analysis of 2-oxoadipate levels in the presence and absence of inhibitor at different time points: Data was normalized to control 0 h sample values and error bars indicate standard deviation (sd) * represents $P \leq 0.05$; statistical test: students T test.

3.2.3. Effect of lysine stress induction on GA levels of GA-I patient and control fibroblasts

In the next steps we wanted to establish a cell culture model to further test, if PF-04859989 prevents GA production. To this end we applied GA-I patient-derived fibroblasts. These cells produce only small amounts of GA due to the fact that fibroblasts display a rather slow metabolism and, in addition, their lysine metabolism is virtually inactive under nutrient conditions of standard media. Therefore we tested if we could enhance the biochemical phenotype of patient-derived fibroblasts. Similar to mice experiments, we exposed these cells to high lysine stress. In brief, we first starved the patient and control fibroblasts overnight and put them under lysine (5 mM) stress for next 3 consecutive days, by changing the old medium and replacing with lysine containing medium each day. Finally, the cells were lysed and GA levels using were quantitatively

detected using GCMS. We saw a significant rise in GA levels in both tested patient fibroblasts cell lines (Patient 1, 8268.3 ± 1235.4 fold increase; patient 2, 3.68 ± 0.76 fold increase compared to their respective without lysine treated samples; $P \leq 0.05$; one-way ANOVA for both; Fisher's LSD) compared to the lysine untreated samples. As expected, GA levels in the control cells remained same before and after lysine treatment (figure 14).

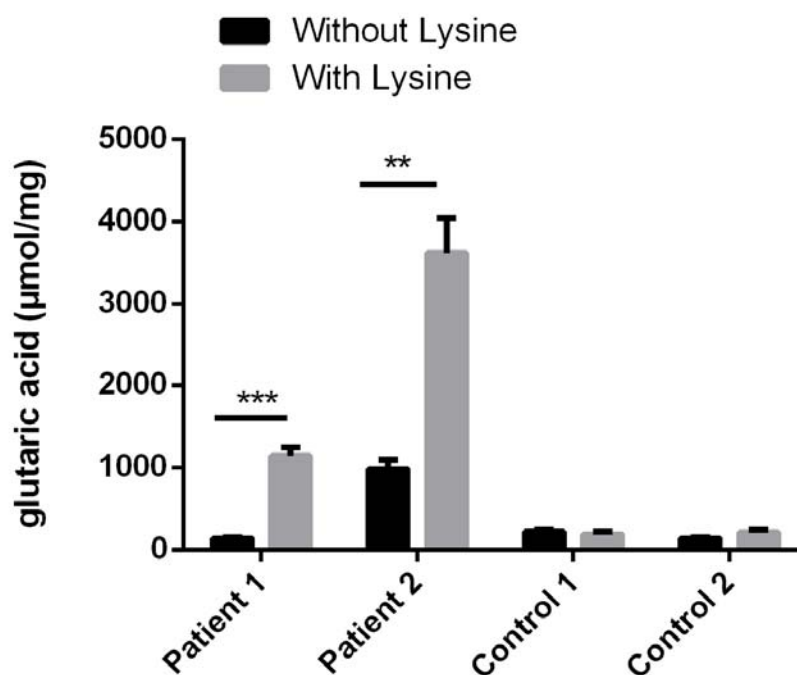
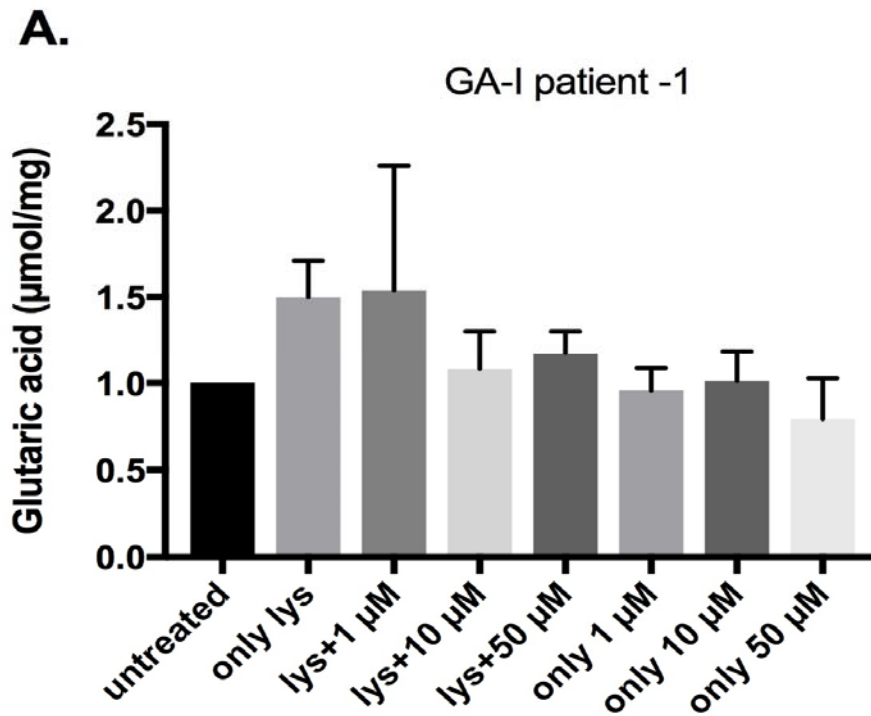


Figure 14: Measurement of GA levels in patient and control fibroblasts: GA levels in patient and control fibroblasts with lysine and without lysine treatment. N=3 independent experiments, Data is presented as mean and error bars indicate standard deviation (SD) * represents $P \leq 0.05$; one-way ANOVA for multiple comparisons; Fisher's LSD test.

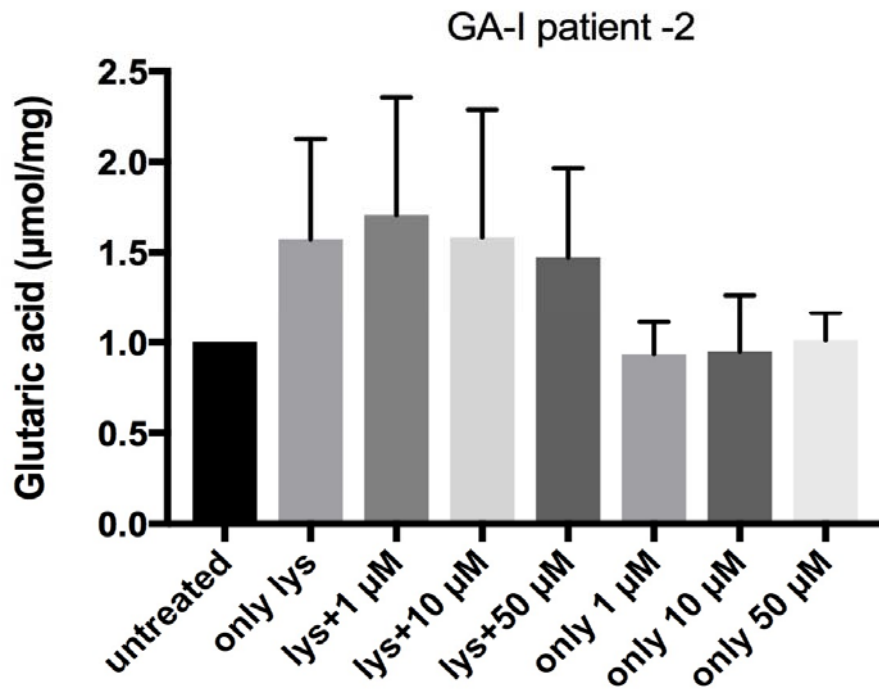
3.2.4. Effect of AADAT inhibitor on GA levels of patient and control fibroblasts

After observing a rise in GA accumulation after lysine treatment in GA-I patient fibroblasts (figure 14), we aimed to inhibit the same (GA accumulation) in both GA-I patient there is no increase in controls by targeting AADAT using PF-0485998. We starved the cells overnight and the following day kept them under lysine (5 mM) stress together with different concentrations of inhibitor along

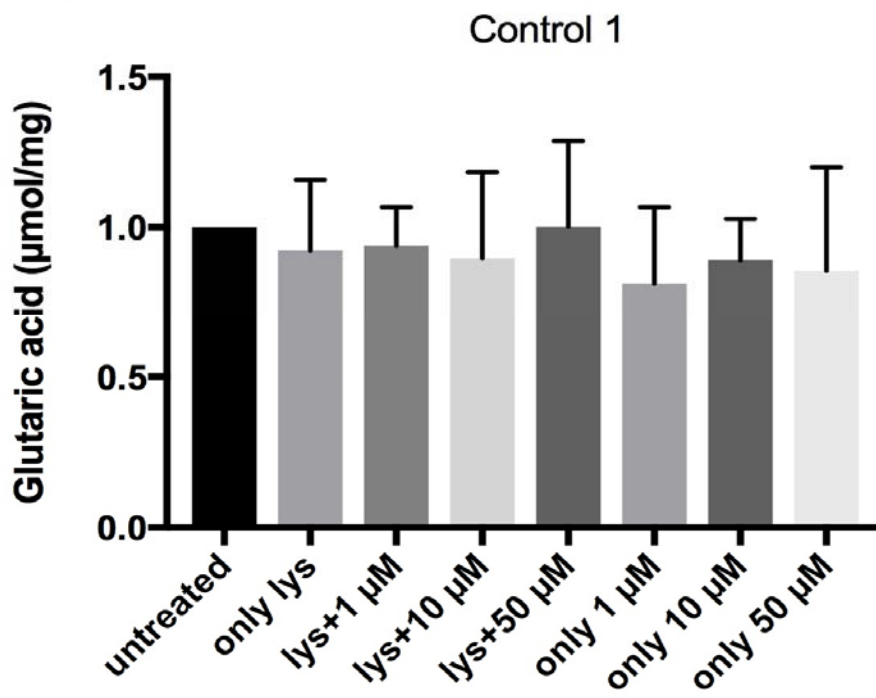
with lysine (lys+1 μM , lys+10 μM , lys+50 μM) or incubating them only with inhibitor without additional lysine in the medium (only 1 μM , only 10 μM , only 50 μM) for the next 3 consecutive days, by adding lysine and inhibitor each day. Cells were then lysed and GA accumulation was observed using GCMS. Unexpectedly, we saw a very poor and non-significant rise in GA levels in both the patient (1&2) fibroblasts (figure 15) after lysine treatment. This poor metabolic response to the applied inhibitor, which is in contrast to our previous study, was reproduced in four independent experiments (n=4). Overall, the instability of the biochemical phenotype of GA-I patient fibroblasts questioned the suitability of this cell system for further inhibitor studies.



B.



C.



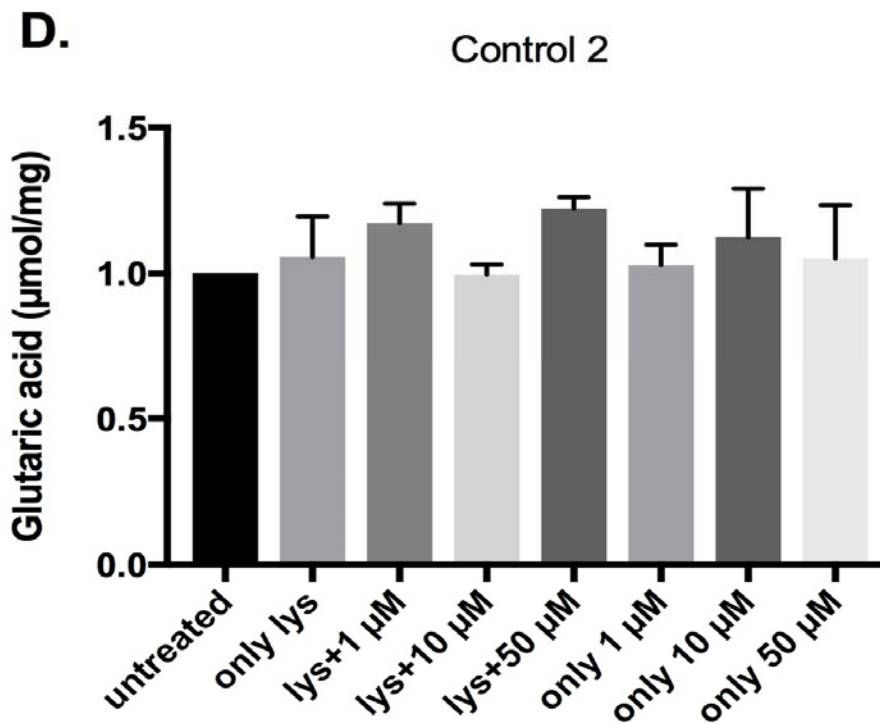


Figure 15: GA levels in patient and control fibroblasts following inhibitor treatment; GA levels after treating with only lysine (only lysine), lysine + inhibitor (lys+1 µM, lys+10 µM, lys+50 µM) and only inhibitor (only 1 µM, only 10 µM, only 50 µM). Figures also show untreated samples; A. patient 1; B. patient 2; C. control 1; D. control 2 Data was normalized to the untreated sample (n=4 independent experiments).

3.3. Generation of alternative GA-I cell culture models

3.3.1. CRISPR/Cas9-mediated generation of knockout cells

In order to successfully simulate the biochemical effect of loss of *GCDH* activity, we aimed to switch to a more suitable cell model. To this end we employed HEK and HeLa cells, which are fast growing and easy to transfect cells. We aimed to generate *GCDH* Knockout, *AADAT* Knockout and double Knockouts (*GCDH*^{-/-}/*AADAT*^{-/-}) in HEK and HeLa cells by utilizing CRISPR/Cas9 methodology. We used PX459 plasmid containing Cas9 gene and puromycin antibiotic resistance gene (figure 16A) to clone gRNAs against *GCDH* or *AADAT*. HEK and HeLa cells were successfully transfected with CRISPR/cas9 plasmids containing gene

specific gRNAs against *GCDH* or *AADAT*. After twenty four hours after transfection, transfected cells were kept under Puromycin antibiotic pressure continuously for four days until all the cells died in mock (transfection reagent was used as mock) transfected conditions. The cells survived under Puromycin antibiotic pressure were further subjected to Western blot analysis. Absence of *GCDH* or *AADAT* expression in knockout samples in comparison to the controls, confirmed the generation of knockouts (figure 16B, C, D). The Knockout cells were further screened for single cell clonal selection (figure 16E). The single cell clones for *GCDH* Knockout were observed to be indeed true Knockouts, as seen by the absence of *GCDH* protein via immunoblotting. From these single cell clones, HeLa 9(4) (figure 16 E) and HEK 6 were used for further experiments. However, for *AADAT*, despite absence of the band for *AADAT* protein in western blot analysis (figure 16C), the single cell clones showed *AADAT* protein and hence were not used for further analysis.

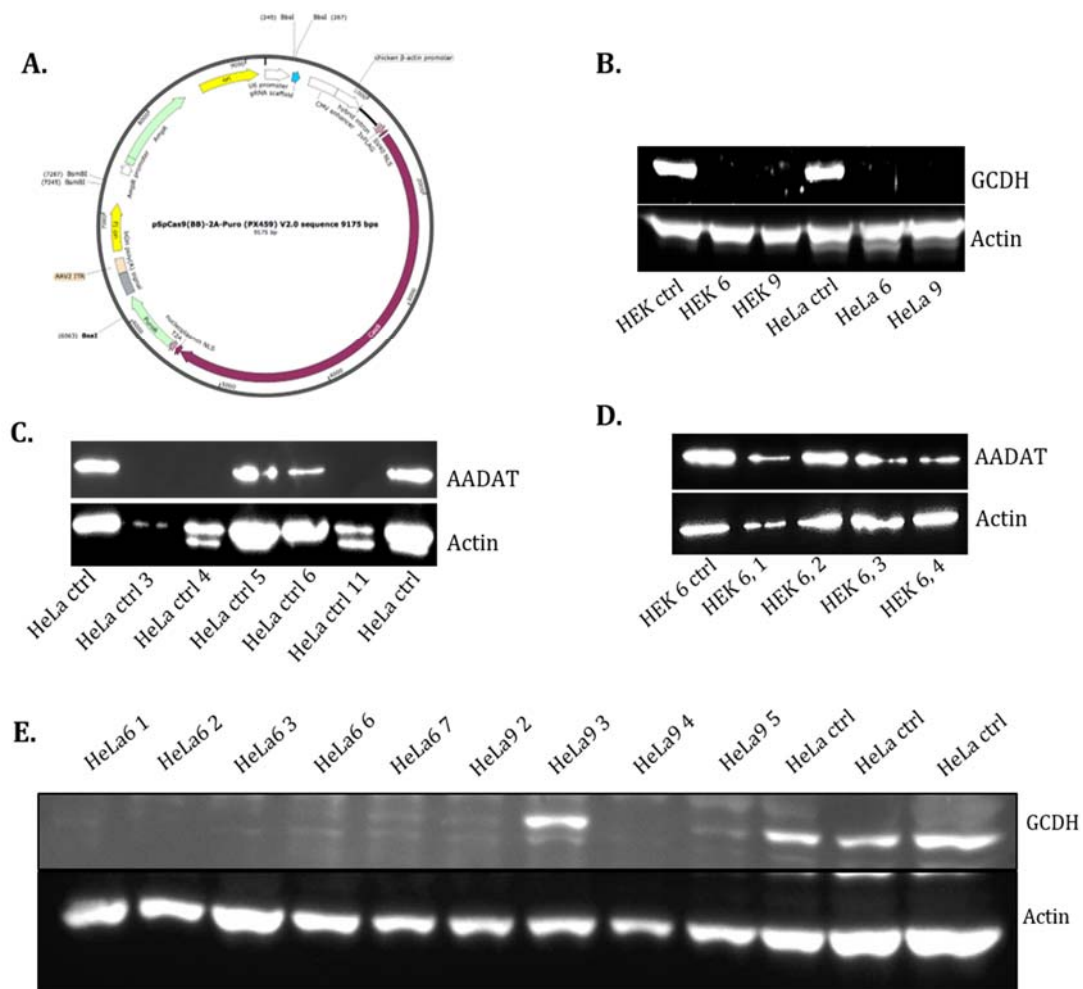


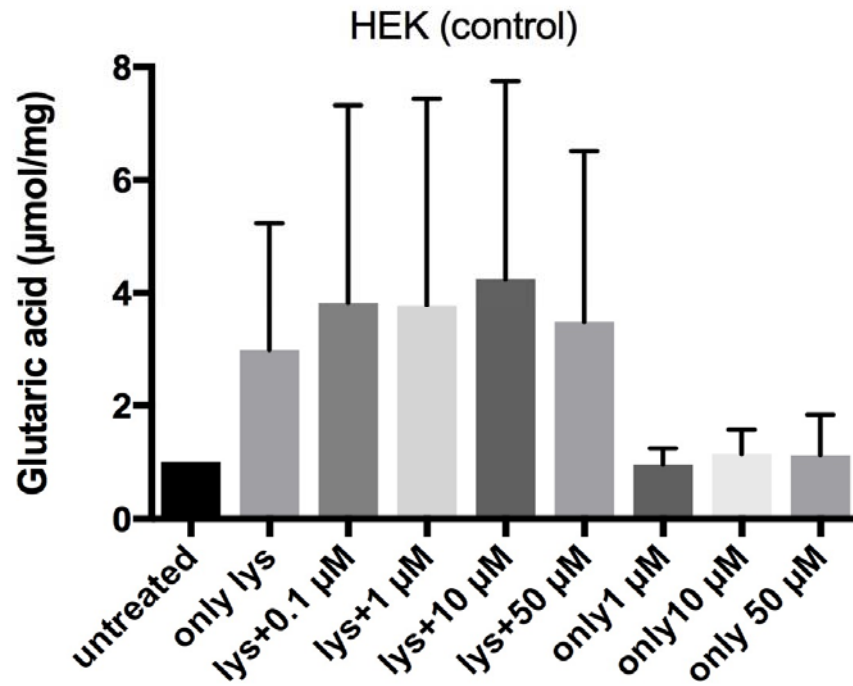
Figure 16: Generation of HEK and HeLa GCDH and AADAT knockout cells A: Schematic representation of PX459 plasmid containing Cas9 gene and Puromycin antibiotic resistance gene B: The upper panel shows GCDH expression only in controls but not in the knockouts and the lower panel represents actin as the loading control. HEK6, HeLa6; HEK9, HeLa9- GCDH knockouts; HEK ctrl, HeLa ctrl- controls. C: The upper panel shows AADAT expression only in HeLa ctrl, HeLa ctrl 5 & 6. In HeLa 4 & 11 no expression of AADAT is seen, showing the presence of knockout. The lower panel represents actin as the loading control. D: The upper panel shows AADAT expression in all samples, but AADAT expression is slightly reduced in HEK 6, 3&4 showing the presence of putative double Knockout. The lower panel represents actin as the loading control (numbering for all the blots is done for internal reference). E. Single cell clones generated from HeLa 6 and HeLa9 GCDH Knockouts (see B). The upper panel showing GCDH knockout, seen clearly in HeLa 6 (1), HeLa 6 (2), HeLa 9 (4). The lower panel represents actin as loading control.

3.3.2. Analysis of GA levels in GCDH Knockout and control cells after inhibitor treatment

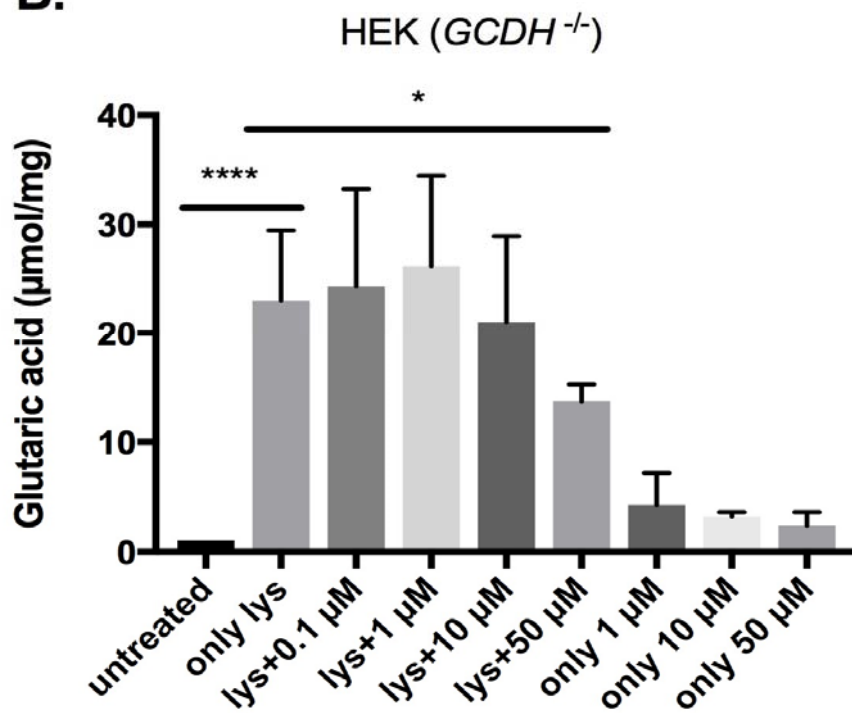
To check the effect of PF-0485998 on GA production levels in GCDH Knockout, GCDH Knockout cells and control cells were treated with and without lysine, along with different concentrations of AADAT inhibitor. As expected in the control HEK and HeLa cells, we did not observe any significant differences in GA production after lysine treatment in comparison to untreated cells (Figure 17A & C; $P \geq 0.05$; one way ANOVA for multiple comparisons; Fisher's LSD). Upon lysine treatment, we observed that GCDH Knockout showed an increase in GA accumulation, in both HEK (21.99 ± 6.4 fold increase; $P \leq 0.05$; one way ANOVA for multiple comparisons; Fisher's LSD, Figure 17C) and HeLa cells (1.2 ± 0.98 fold increase; $P \geq 0.05$; one way ANOVA for multiple comparisons; Fisher's LSD, Figure 17D), when compared to their respective lysine untreated controls. In HEK cells with GCDH knockout, we observed a significant reduction in GA levels when treated with lysine plus 50 μM concentration of AADAT inhibitor (0.59 ± 0.06 fold decrease; $P \leq 0.05$; one way ANOVA for multiple comparisons; Fisher's LSD, Figure 17C) compared with only lysine treated cells. In HeLa GCDH Knockouts, we observed a profound reduction in GA levels upon lysine treatment after addition of even only 1 μM inhibitor (0.39 ± 0.1 fold decrease; one way ANOVA for multiple comparisons; Fisher's LSD, Figure 17D) concentrations of

inhibitor compared with lysine alone treated cells. These results clearly indicate that inhibition of AADAT with PF-0485998 concentration-dependently reduces the GA levels in GCH Knockout conditions.

A.



B.



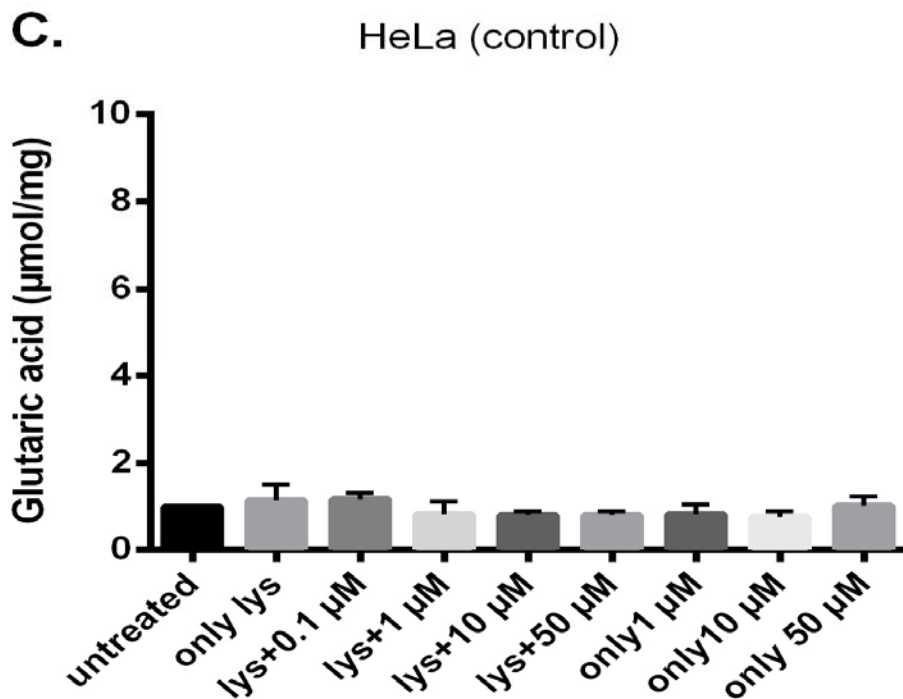
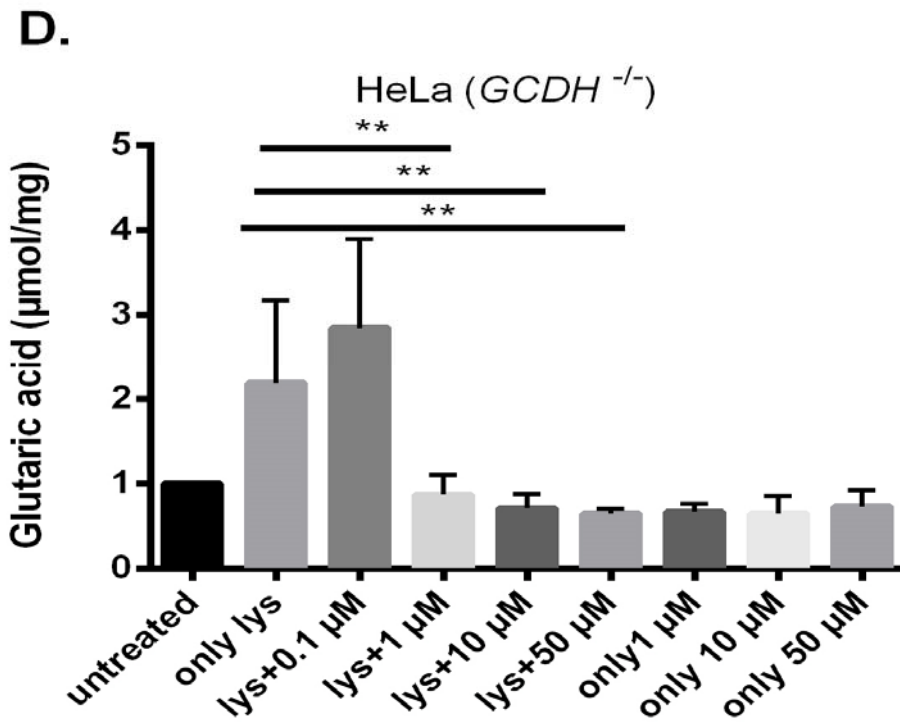


Figure 17: Graphs showing the effect of AADAT inhibitor on GA levels in HEK and HeLa KO cells and controls. Data was normalized to the untreated sample. A, B, C, D represents GA levels in

HEK (control), HEK *GCDH*^{-/-} (HEK GCDH knockout), HeLa (control), HeLa *GCDH*^{-/-} (HeLa GCDH knockout) respectively at different concentrations of inhibitor with lysine (lys+0.1 μM, lys+1 μM, lys+10 μM, lys+50 μM) and only inhibitor (only 0.1 μM, only 1 μM, only 10 μM, only 50 μM) used. Figures also show untreated and only lysine (only lys) treated samples. N=3 independent experiments, (* represents $P \leq 0.05$; one-way ANOVA for multiple comparisons; Fisher's LSD test (for HEK GCDH knockout), Tukey's multiple comparison test (for HeLa GCDH knockout).

4. DISCUSSION

4. Discussion

GA-I is an autosomal recessive cerebral organic aciduria caused by defective GCDH, a key enzyme in the catabolic pathways of lysine, OH-lysine and tryptophan. This disease is complicated by acute or insidious-onset striatal damage precipitated by episodes that are likely to induce catabolism and occurring as a result of the accumulation of the toxic metabolites GA, 3-OH GA and glutaryl-CoA (Stefan Kölker et al., 2011). After early diagnosis via newborn screening (NBS), neonatal start and adherence to the recommended dietary treatment prevents striatal lesions in the majority of patients (Boy, Mengler, et al., 2018). However, several recent clinical follow-up studies raise concern about the efficacy of the current dietary treatment and questions whether this dietary treatment leads to a life long disease-free state in all the affected individuals. The answer seems to be ambiguous, since many patients who are diagnosed early and received proper metabolic and emergency maintenance treatment still suffer from extra-striatal, extra-cerebral and non-neurologic abnormalities like changes in white matter (Tuncel et al., 2018), sub-ependymal mass lesions (Boy, Heringer, et al., 2017; Harting et al., 2015), peripheral polyneuropathy (Herskovitz et al., 2013a) and chronic renal failure (S Kölker, Valayannopoulos, et al., 2015) suggesting that the disease course extends to other organs as well. This in turn clearly highlights the fact that there is an immediate need for employing novel therapeutic interventions, for a disease-free long-term outcome in GA-I patients.

Our current study aims to explore several novel ways to treat patients with GA-I. For the first time, we tested inhibition of enzymatic steps upstream to GCDH step (DHTKD1 and AADAT) to prevent toxic metabolite accumulation in and eventually improving the life at later stages of GA-I patients.

4.1. Inhibiting of DHTKD1 function does not rescue the clinical and biochemical phenotype of *Gcdh*^{-/-} mice

DHTKD1, also called human thiamin diphosphate (ThDP)-dependent 2-oxoadipate dehydrogenase (E1a) (Nemeria et al., 2018), is an E1-like subunit of the 2-oxoglutarate dehydrogenase complex (OGDHc). It has been shown to catalyze the oxidative decarboxylation of 2-oxoadipate (OA) to glutaryl-CoA in the final degradative pathway of L-lysine, OH lysine and L-tryptophan (Danhauser et al., 2012a). DHTKD1 is also reported to have a role in the mitochondrial ATP production and functional integrity as shown by Xu and coworkers (W. Xu et al., 2013). As a first therapeutic target, we focused on blocking DHTKD1. We started our approach simultaneously *in vitro* using DHTKD1 patient-derived dermal fibroblasts and *in vivo* using relevant Knockout mouse models.

In vitro, using control and DHTKD1 patient-derived fibroblasts, we tested the effect of several phosphonate analogs of 2-oxoglutarate on DHTKD1 activity and observed that AP was able to influence the enzymatic function of DHTKD1, as seen by the increased OA levels in control fibroblasts. We also found some surprising observations, namely, increased OA levels in AP-treated DHTKD1 patient-derived fibroblasts. OA levels are higher in DHTKD1 patient cells due to loss of function mutations in *DHTKD1* (Danhauser et al., 2012a), however, here we found that the OA levels in the DHTKD1 patient-derived fibroblasts treated with AP even further increased, whereas other tested compounds (GP, TEGP, TMAP, DEGP) did not show an effect. This observation is best explained by co-expression of other enzymes (isoforms of DHTKD1-like OGDHc, OGDHL as shown in (Goncalves, Bunik, & Brand, 2016; W. Xu et al., 2013)), partially compensating the loss of DHTKD1 function in the lysine degradation pathway. Thus, AP might have blocked these enzymes, in turn leading to a rise in OA levels.

To test our hypothesis *in vivo*, we generated *Dhtkd1*^{-/-} mice using TALENS and crossed these mice with the well-characterized *Gcdh*^{-/-} mice, to generate the *Dhtkd1*^{-/-}/*Gcdh*^{-/-} mice. We tested the clinical and biochemical characteristics of the newly generated knockout mice and compared them with the *Gcdh*^{-/-} and *Dhtkd1*^{+/+}/*Gcdh*^{+/+} mice. *Dhtkd1*^{-/-} mice resembled the patients with 2-aminoadipic 2-oxoadipic aciduria and were presented with a mild or

asymptomatic clinical phenotype and biochemically showed increased AA levels but not GA levels (Biagosch et al., 2017). In *Gcdh*^{-/-} mice, toxic metabolite production and severe neurologic phenotype as that of the affected GA I patients can be induced by giving a high lysine diet (Sauer et al., 2015). Mice with all the four different genotypes (*Dhtkd1*^{-/-}, *Gcdh*^{-/-}, *Dhtkd1*^{-/-}/*Gcdh*^{-/-} and *Dhtkd1*^{+/+}/*Gcdh*^{+/+}) were fed with a high lysine diet (4.7% lysine in chow) and we then checked for phenotypic changes. For evaluation of the therapeutic efficacy of our treatment, weight loss, seizures and finally death were considered as critical clinical parameters and GA accumulation in brain and liver tissues were considered as the biochemical parameters.

According to our hypothesis, because of the knockout of *Dhtkd1*, the toxic metabolite accumulation should be subsided in *Dhtkd1*^{-/-}/*Gcdh*^{-/-} mice. As a result, no apparent clinical changes should occur. To our surprise, we saw that the *Dhtkd1*^{-/-}/*Gcdh*^{-/-} mice exhibited a drastic weight loss of > 15% as well as showed lethargic behavior upon the start of the high lysine diet, thereby clinically resembling *Gcdh*^{-/-} mice. Biochemically, *Dhtkd1*^{-/-} and the *Dhtkd1*^{-/-}/*Gcdh*^{-/-} mice should resemble *DHTKD1* patients and show accumulation of OA and AA with increased dietary lysine, but no GA production. As expected, in both *Dhtkd1*^{-/-} and the *Dhtkd1*^{-/-}/*Gcdh*^{-/-} mice, with respect to the OA levels, we saw a slight increase in liver samples. Also, we observed an increase in AA levels, in brain and liver samples under control diet, in both *Dhtkd1*^{-/-} and the *Dhtkd1*^{-/-}/*Gcdh*^{-/-} mice and this was markedly increased upon high lysine diet. With regard to the GA levels, we found that the *Dhtkd1*^{-/-} mice behaved as expected and no increase in GA levels were seen, but the *Dhtkd1*^{-/-}/*Gcdh*^{-/-} mice, similar to *Gcdh*^{-/-} mice showed an increase in GA levels on control diet which rose profoundly with dietary lysine supply, in both brain and liver samples, contradicting our hypothesis. We also measured the levels of glutaryl carnitine, which is a valuable marker for neonatal and high-risk screening (S. Kölker et al., 2007), and is usually found accumulated in body fluids (plasma, CSF, urine) of GA-I patients. Formation of glutaryl carnitine is a physiological detoxifying mechanism to prevent accumulation of glutaryl -CoA (Stefan Kölker et al., 2011; Sauer et al., 2011; Seccombe, James, & Booth, 1986). Our data showed similar levels of

glutaryl carnitine in both *Gcdh*^{-/-} and *Dhtkd1*^{-/-} / *Gcdh*^{-/-} mice, indicating that glutaryl CoA is the precursor of GA in both the model. Summarizing, genetic knockout of *Dhtkd1* does not rescue the clinical or biochemical phenotype observed in *Gcdh*^{-/-} mice, further raising questions about our current understanding of lysine degradation.

Based on our *in vitro* and *in vivo* derived results, we assume that loss of DHTKD1 activity was compensated by other proteins which facilitate the conversion of 2-OA into glutaryl-CoA. Different studies from the literature report on the existence of isoforms of DHTKD1 namely, 2-oxoglutarate dehydrogenase (OGDH, E1 α ; EC1.2.4.2) and OGDH-like protein (OGDHL, EC 1.2.4) (V. Bunik & Degtyarev, 2008). OGDH is the E1 α subunit of OGDHc, which additionally includes dihydrolipoyl succinyl transferase (DLST, E2; EC 2.3.1.61) and dihydrolipoyl dehydrogenase (DLDH, E3; EC1.8.1.4) as the E2 and E3 subunits respectively and together catalyzes the oxidative decarboxylation of 2-oxoglutarate (α -ketoglutarate; OG) to succinyl-CoA. The protein product of *DHTKD1* and *OGDHL* gene are subunits of an alternative OGDHc with affinities for different but structurally similar substrates like 2-oxoadipate, 2-oxo-4-hydroxyglutarate, products of carbonylase reaction between 2-oxodicarboxylate and acetaldehyde or glyoxalate (V. Bunik & Degtyarev, 2008; V. Bunik, Kaehne, Degtyarev, Shcherbakova, & Reiser, 2008). Also, recent findings from Nemeria and colleagues showed that OGDH accepts both OG and OA as specific substrates, although with a 3 times lower affinity for OA (Nemeria et al., 2017). Little is known about OGDHL. It was shown to be mainly expressed in the brain and favor OG as substrate (V. Bunik et al., 2008). Overall OGDH or OGDHL could compensate for the loss of DHTKD1 activity.

Another source of glutaryl-CoA generation might be succinyl-CoA:glutarate-CoA transferase (SUGCT) or C7Orf10, which adds CoA from Succinyl-CoA to glutarate, thus forming glutaryl-CoA (Sherman et al., 2008). However, GA obtained in this step comes from an yet unknown metabolic pathway or, more likely from gut microbiome (Backes et al., 2002; Baric et al., 1999a; Tomé & Bos, 2007) and can therefore only account for GA accumulation in intracerebral tissue due to the

extremely low permeability of the BBB for this metabolite. In summary, because of the functional similarity of DHTKD1 to other proteins (OGDH, OGDHL), these findings exclude DHTKD1 as a target protein for pharmacological GA-I treatment. Moreover, DHTKD1 mutations have been suggested to play a role in Charcot-Marie-Tooth (CMT) disease, one of the most common subgroups of inherited peripheral neuropathies (Baets, Jonghe, & Timmerman, 2014). Individuals with CMT are characterized by gradually advancing distal neuropathy of hands and legs. CMT is divided into two subtypes, i.e. CMT1, where myelin derived from glia is affected and CMT2, where the nerve axon is affected. A nonsense mutation in DHTKD1 in exon 8 (c.1455T>G (p.Tyr485*)) was reported to be associated with CMT2 leading to inadequate energy production and malfunction of peripheral nerves in a Chinese family of affected individuals Xu et al 2012). The implications of this study remained unclear, since CMT and 2-amino-2-oxoadipic aciduria are clinically distinct disorders and several reports have confirmed mutations in DHTKD1 in patients with the latter disease. However, Xu et al. have shown in a recent study that old DHTKD1-deficient mice develop symptoms of CMT2 (W. Y. Xu et al., 2018). This study provides another argument against inhibiting DHTKD1 as a therapeutic strategy.

4.2. Development of an alternative therapeutic strategy

Next, we targeted aminoadipate aminotransferase (AADAT), which is two enzymatic steps ahead of GCDH in the lysine degradation pathway.

Besides its role in lysine metabolism, AADAT catalyzes the conversion of kynurenine to KYNA in tryptophan catabolism. KYNA is a neuroactive metabolite which was shown to be an antagonist of glutamate receptors, α -7 nicotinic acetylcholine receptor and also N-methyl-D-aspartate (NMDA) receptor, and, thereby is a neuro-modulatory metabolite (Schwarcz & Stone, 2017). KYNA was found to accumulate in several neurocognitive disorders like cerebral ischemia, epilepsy, Alzheimer's, Parkinson's, Huntington's disease (Vamos, Pardutz, Klivenyi, Toldi, & Vecsei, 2009). Interestingly, blocking KYNA generation by pharmacologically targeting AADAT in different animal models (rats, primates)

has been tested as a novel treatment option for neurological, neurodegenerative disorders and psychiatric diseases such as depression and schizophrenia (Koshy Cherian et al., 2014). This approach was shown to be effective in rats and non-human primates with neurological disease symptoms similar to psychiatric disorders like schizophrenia (Dounay, Tuttle, & Verhoest, 2015). Importantly, no disease-causing mutations in AADAT are known suggesting that a loss of AADAT activity is well tolerated being in line with the positive effect of the aforementioned inhibitor on neurotransmission. Aadat knockout (KAT II^{-/-}) in mice was shown to effectively reduce the formation of endogenous KYNA resulting in enhanced cognitive behavior (Potter et al., 2010). Henceforth, we first tested whether PF04859989, which is a potent, irreversible and selective inhibitor of kynurenine deamination via AADAT, will also block the deamination of 2-aminoadipate. Indeed, we could show that PF04859989 concentration-dependently inhibits the enzymatic production of OA. Next, we proceeded to test our hypothesis, i.e., that inhibition of AADAT prevents GA accumulation, in a cell culture model. To test this, we first used GA-I patient-derived fibroblasts. However, GA accumulation in these cells, being a prerequisite for drug testing, was not stable and reproducible. A likely explanation for this observation is the low metabolic activity of fibroblasts that results in GA levels close to the detection limit of our method.

To circumvent this problem, we genetically modified HEK and HeLa cells, that are established as simple and reliable cell models in the scientific community to further delineate the effect of AADAT blockade in GA-I disease. We used CRISPR/Cas9 methodology and successfully generated GCDH knockouts in both HEK and HeLa cell lines. They mimicked the biochemical GA-I phenotype as shown by the increased basal GA levels that could be enhanced by additional lysine treatment. In the next steps, we used these generated GCDH knockout cell lines to test the effect of different concentrations of PF04859989, with or without lysine treatment on GA accumulation. Strikingly, we found a strong reduction in GA levels at an inhibitor concentration of 50 μ M for HEK and at 10 μ M for HeLa GCDH knockout cells. For HeLa cells, GA production was almost abolished. Thus we were able to show that AADAT inhibition indeed can

successfully reduce toxic metabolite production. To compare the efficacy of the tested inhibitor with a complete loss of AADAT, we went on further to knock out AADAT in *GCDH* deficient HEK and HeLa cells. We were successful in cloning AADAT CRISPR constructs and performing transfections of these plasmids into HEK and HeLa control and *GCDH* Knockout cells. Western blot analysis indicated knockout of AADAT in HEK and HeLa after transfection, but no single cell clones could be established. Unfortunately, we also observed that *GCDH* knockout cells did not survive additional AADAT Knockout. Further experiments are to be done, to identify the optimal conditions needed for the generation of a single (AADAT^{-/-}) and double knockouts (*GCDH*^{-/-}/AADAT^{-/-}) in HEK and HeLa cells.

4.3. Outlook 1. Novel mechanism of chronic GA-induced toxicity

A yet poorly understood finding in GA-I patients with chronic disease course in adolescence and adulthood are sub-ependymal mass lesions (Herskovitz et al., 2013b; Korman et al., 2007). The prognostic value and origin of these sub-ependymal cell masses remain elusive, yet it may indicate starting tumorigenesis. Recent studies revealed that accumulating succinate and fumarate levels in Krebs-cycle-deficient hereditary cancer syndromes block the homologous recombination (HR) DNA-repair pathway resulting in increased number of DNA double-strand breaks (DSBs) (Sulkowski et al., 2018). Due to the structural similarity of these metabolites to the toxic metabolite GA, we questioned whether increased levels of GA would act as an endogenous DNA damaging agent, resulting in DNA DSBs formation, further leading to activation of DNA repair pathways. Un repaired DSBs are considered harmful and are enough to trigger cell cycle arrest and cell death, further leading to chromosomal redistribution in turn resulting in activation of oncogenes causing malignancy (Panier & Boulton, 2014). To see if GA is resulting in DNA DSBs, which might further power the malignant transformation, we looked for DNA damage foci in GA-I patient and control fibroblasts. DNA damage foci are chromosomal modifications resulting from DNA damage response proteins like RAD51 recombinase (RAD51), p53 binding protein (53BP1), gamma- histone variant H2AX (γ H2AX) that are recruited to the regions with chromosomal DNA DSBs,

(Rothkamm et al., 2015). Additionally, and as a response to DNA damage, kinases like DNA-dependent protein kinase (DNA-PK), ataxia telangiectasia mutated (ATM) and ATM-Rad3-related (ATR) are activated at the site of DNA damage and in turn phosphorylates the histone variant H2AX, resulting in the formation of γ H2Ax. The formed γ H2Ax binds with other DNA damage signalling elements like 53BP1 and Mediator of DNA damage checkpoint protein 1 (MDC1) (Panier & Boulton, 2014). Since, this process of DNA damage response involving several thousands of histone-related modifications and signalling reactions, is restricted to a particular region of the chromosome involving DNA damage, this region can be detected under a microscope following immunostaining against γ H2Ax as distinct spots, called together as DNA damage foci. This sort of nuclear reprogramming is often associated with diseases like cancer (Rothkamm et al., 2015).

By performing immunofluorescence (IF) analysis on patient and control fibroblasts using γ H2Ax antibody (marker for DSBs), we detected increased levels of DNA damage in patient cells compared to control cells (figure 19), as observed by the significantly increased number of foci, (GA-I patient cells, 10.5 ± 0.8 ; control cells, 3.8 ± 1.3 ; $P \leq 0.005$, Student's T-test). Such an observation probably suggests the underlying DNA damage due to the accumulation of the toxic metabolite GA. However, in GA-I, we need to investigate further, if at all there is a link between the increased number of foci and complications associated with it, especially in the later stages of the disease. This finding eventually gives new insights into the understanding of the mechanism behind GA-I disease toxicity, which might in turn help patients live a long-term disease-free state.

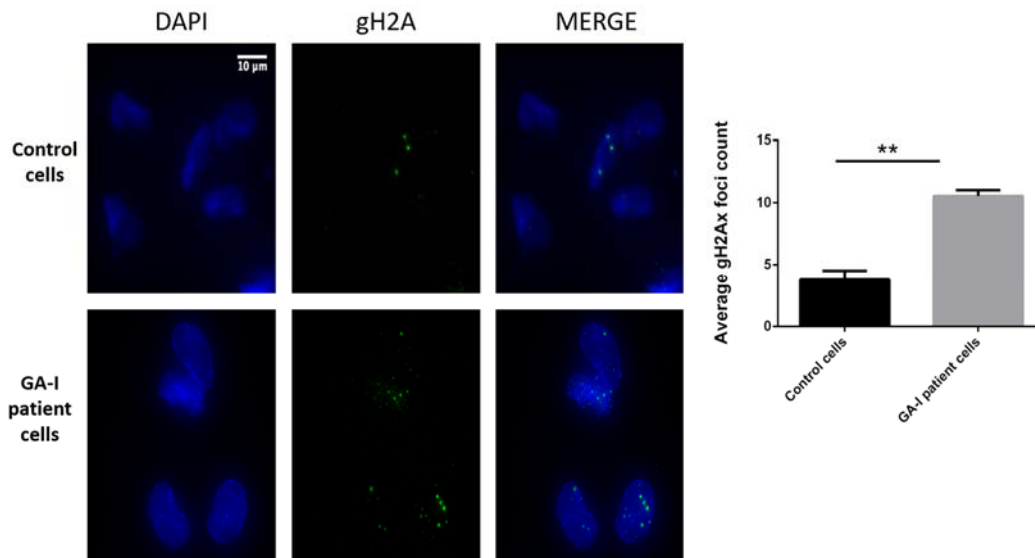


Figure 19: Immunofluorescence staining of control cells (upper panel) and patient cells (lower panel) using gamma H2Ax antibody, shows the foci (green) inside the DAPI stained cells. Quantification of the foci showed the significantly higher number in GA-I patient cells compared to controls (n=3). ** mark represents $P \leq 0.005$, Student's T-test.

4.4. Outlook 2, Role of DHTKD1 in Diabetes

Interestingly, *Dhtkd1* was shown to be up-regulated in diabetes condition by Wu and colleagues via multilayered transcriptome, metabolome and targeted proteomics in BXD genetic reference mouse lines on two different diets (Y. Wu et al., 2014). Also, reports from different groups suggest that *Dhtkd1* might play a role in the regulation of glucose levels and insulin sensitivity via AA in humans as well as in mice, thus influencing the development of diabetes (Wang et al., 2013; Y. Wu et al., 2014; Zhao, Rio, Barrere-Cain, & Yang, 2015). To test this, we performed immunoblot analysis on the liver and kidney tissue samples of streptozotocin (STZ)-induced diabetic mice and control mice (SHAM) to check if there is an upregulation of *Dhtkd1* under diabetes condition. Interestingly, we observed a significant rise (figure 18) in *Dhtkd1* levels in the liver samples of STZ mice when compared to SHAM mice (control mice), implying an overexpression of *Dhtkd1* in the liver tissue under diabetes condition. From this study, we confirm that the role of DHTKD1 in diabetes can be further analyzed and

extrapolated in different areas of diabetic research like contributing to better diagnosis and treatment of diabetes or most likely, its prevention. This will be an interesting focus of future studies and may even be a possible application for DHTKD1 inhibition.

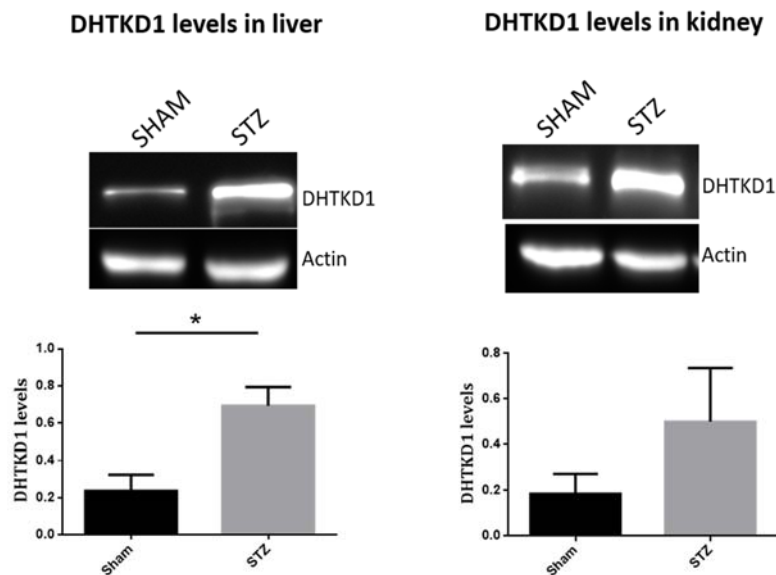


Figure 18: Expression of DHTKD1 in diabetes: Western blot showing expression of DHTKD1 in liver and kidneys of Sham and STZ mouse. Graphs show the quantification of Western blot, DHTKD1 values normalized to Actin. (n=3), bars indicate standard deviation (sd) * mark represents $P \leq 0.05$, Student's T-test.

5. CONCLUSIONS

5. Conclusions

1) From the *in vitro* and *in vivo* experiments performed and the results obtained, we conclude that DHTKD1 is not a suitable target for GA-I treatment due to its multiple isoforms, which can replace its metabolic function. Also, proper delineation of lysine degradation pathway is essential to clearly understand the source of GA production and accumulation. .

2) From the *in vitro* experiments we performed using PF-04859989 in HEK and HeLa GCDH knockout cells, we can reasonably conclude that AADAT can be targeted as a novel therapeutic strategy in GA-I. Furthermore, mouse *in vivo* studies are still to be done to add an additional layer of confidence.

6. REFERENCES

6. References

- Aishah, S., Wahab, A., Yakob, Y., Azimah, N., Azize, A., Yunus, Z., ... Hock, N. L. (2016). Clinical and Mutational Analysis of the GCDH Gene in Malaysian Patients with Glutaric Aciduria Type 1, 2016, 5. <http://doi.org/10.1155/2016/4074365>
- Anthony A. Albanese Selma E. Snyderman Marilyn Lein Emilie M. Smetak Betty Vestal. (1949). The Biological Value of Corn and Wheat Proteins in the Male Infant, with a Note on the Utilization of D-Tryptophan. *The Journal of Nutrition*, 38(2), 215–224.
- Backes, G., Hennig, U., Petzke, K. J., Elsner, A., Junghans, P., Nürnberg, G., & Metges, C. C. (2002). Contribution of intestinal microbial lysine to lysine homeostasis is reduced in minipigs fed a wheat gluten-based diet 1-3. *Am J Clin Nutr*, 76, 1317–1342. Retrieved from <https://academic.oup.com/ajcn/article-abstract/76/6/1317/4689579>
- Baets, J., Jonghe, P. De, & Timmerman, V. (2014). Recent advances in Charcot – Marie – Tooth disease, 27(5), 532–540. <http://doi.org/10.1097/WCO.0000000000000131>
- Bähr, O., Mader, I., Zschocke, J., Dichgans, J., & Schulz, J. B. (2002). Adult onset glutaric aciduria type I presenting with a leukoencephalopathy. *Neurology*, 59(11), 1802–4. Retrieved from <http://www.ncbi.nlm.nih.gov/pubmed/12473778>
- Baric, I., Wagner, L., Feyh, P., Liesert, M., Buckel, W., & Hoffmann, G. F. (1999a). Sensitivity and specificity of free and total glutaric acid and 3-hydroxyglutaric acid measurements by stable-isotope dilution assays for the diagnosis of glutaric aciduria type I. *J Inherit Metab Dis*, 22(8), 867–81.
- Baric, I., Wagner, L., Feyh, P., Liesert, M., Buckel, W., & Hoffmann, G. F. (1999b). Sensitivity and specificity of free and total glutaric acid and 3-hydroxyglutaric acid measurements by stable-isotope dilution assays for the diagnosis of glutaric aciduria type I. *Journal of Inherited Metabolic Disease*, 22(8), 867–81. Retrieved from <http://www.ncbi.nlm.nih.gov/pubmed/10604139>
- Basinger, A. A., Booker, J. K., Frazier, D. M., Koeberl, D. D., Sullivan, J. A., & Muenzer, J. (2006). *Glutaric acidemia type 1 in patients of Lumbee heritage from North Carolina. Molecular Genetics and Metabolism* (Vol. 88).
- Benevenga, N. J., & Blemings, K. P. (2007). Unique Aspects of Lysine Nutrition and Metabolism. *The Journal of Nutrition*, 137(6), 1610S–1615S. <http://doi.org/10.1093/jn/137.6.1610S>
- Bergman, I., Finegold, D., Gartner, J. C., Zitelli, B. J., Claassen, D., Scarano, J., ... Goodman, S. I. (1989). Acute Profound Dystonia in Infants With Glutaric Acidemia. *PEDIATRICS*, 83(2). Retrieved from <http://pediatrics.aappublications.org/content/pediatrics/83/2/228.full.pdf>
- Beslin, A., Vie, M.-P., Blondeau, J.-P., & Francon, J. (1995). Identification by photoaffinity labelling of a pyridine nucleotide-dependent tri-iodothyronine-binding protein in the cytosol of cultured astroglial cells. *Biochem. J*, 305, 729–737. Retrieved from <https://www.ncbi.nlm.nih.gov/pmc/articles/PMC1136320/pdf/biochemj00070-0048.pdf>
- Biagosch, C., Ediga, R. D., Hensler, S. V., Faerberboeck, M., Kuehn, R., Wurst, W., ...

- Prokisch, H. (2017). Elevated glutaric acid levels in Dhtkd1-/Gcdh- double knockout mice challenge our current understanding of lysine metabolism. *Biochimica et Biophysica Acta - Molecular Basis of Disease*, 1863(9), 2220–2228. <http://doi.org/10.1016/j.bbadis.2017.05.018>
- Bjugstad, K. B., Crnic, L. S., Goodman, S. I., & Freed, C. R. (2006). Infant mice with glutaric acidemia type I have increased vulnerability to 3-nitropropionic acid toxicity. *Journal of Inherited Metabolic Disease*, 29(5), 612–619. <http://doi.org/10.1007/s10545-006-0102-9>
- Borsook H, Deasy CL, Haagen-Smit A J, Keighley G, and L. P. (1948). The degradation of α -amino adipic acid in guinea pig liver homogenate. *Journal of Biological Chemistry*, 176, 1383–1393. <http://doi.org/10.1007/978-3-319-05065-2>
- Boy, N., Garbade, S. F., Heringer, J., Seitz, A., Kölker, S., & Harting, I. (2018). Patterns, evolution, and severity of striatal injury in insidious- versus acute-onset glutaric aciduria type 1. *Journal of Inherited Metabolic Disease*.
- Boy, N., Heringer, J., Brackmann, R., Bodamer, O., Seitz, A., Kölker, S., & Harting, I. (2017). Extrastriatal changes in patients with late-onset glutaric aciduria type I highlight the risk of long-term neurotoxicity. *Orphanet Journal of Rare Diseases*, 12(1), 1–13. <http://doi.org/10.1186/s13023-017-0612-6>
- Boy, N., Mengler, K., Thimm, E., Schiergens, K. A., Marquardt, T., Weinhold, N., ... Kölker, S. (2018). Newborn screening: A disease-changing intervention for glutaric aciduria type 1. *Annals of Neurology*. <http://doi.org/10.1002/ana.25233>
- Boy, N., Mühlhausen, C., Maier, E. M., Heringer, J., Assmann, B., Burgard, P., ... vom Dahl, S. (2017). Proposed recommendations for diagnosing and managing individuals with glutaric aciduria type I: second revision. *Journal of Inherited Metabolic Disease*, 40(1), 75–101. <http://doi.org/10.1007/s10545-016-9999-9>
- Bunik, V., & Degtyarev, D. (2008). Structure-function relationships in the 2-oxo acid dehydrogenase family: Substrate-specific signatures and functional predictions for the 2-oxoglutarate dehydrogenase-like proteins. *Proteins: Structure, Function and Genetics*, 71(2), 874–890. <http://doi.org/10.1002/prot.21766>
- Bunik, V. I., Denton, T. T., Xu, H., Thompson, C. M., Cooper, A. J. L., & Gibson, G. E. (2005). Phosphonate analogues of α -ketoglutarate inhibit the activity of the α -ketoglutarate dehydrogenase complex isolated from brain and in cultured cells. *Biochemistry*, 44(31), 10552–10561. <http://doi.org/10.1021/bi0503100>
- Bunik, V., Kaehne, T., Degtyarev, D., Shcherbakova, T., & Reiser, G. (2008). Novel isoenzyme of 2-oxoglutarate dehydrogenase is identified in brain, but not in heart. *FEBS Journal*, 275(20), 4990–5006. <http://doi.org/10.1111/j.1742-4658.2008.06632.x>
- Busquets, C., Merinero, B., & Christensen, E. (2000). Glutaryl-CoA Dehydrogenase Deficiency in Spain: Evidence of Two Groups of Patients, Genetically, and Biochemically Distinct, 48(3).
- Campistol, J., Ribes, A., Alvarez, L., Christensen, E., & Millington, D. S. (1992). Glutaric aciduria type I' Unusual biochemical presentation. *Pediatrics*, 121(1). Retrieved from https://ac.els-cdn.com/S002234760582548X/1-s2.0-S002234760582548X-main.pdf?_tid=3cbba34a-0fac-460e-b11a-

d2682942e2d3&acdnat=1526218966_90d8bca330a1da6f535b8df82221a6
fa

- CARSON, N. A. J., SCALLY, B. G., NEILL, D. W., & CARRÉ, I. J. (1968). Saccharopinuria: a New Inborn Error of Lysine Metabolism. *Nature*, 218. Retrieved from <http://www.nature.com/articles/218679a0.pdf>
- Casey, R. E., Zaleski, W. A., Philp, M., Mendelson, I. S., & MacKenzie, S. L. (1978). Biochemical and clinical studies of a new case of α -amino adipic aciduria, 1(4), 129–135.
- Chace, D. H., Kalas, T. A., & Naylor, E. W. (2003). Use of Tandem Mass Spectrometry for Multianalyte Screening of Dried Blood Specimens from Newborns. *Clinical Chemistry*, 49(11), 1797–1817. <http://doi.org/10.1373/clinchem.2003.022178>
- Chalmers, R. A., Bain, M. D., & Zschocke, J. (2006). Riboflavin-responsive glutaryl CoA dehydrogenase deficiency. *Molecular Genetics and Metabolism*, 88(1), 29–37. <http://doi.org/10.1016/j.ymgme.2005.11.007>
- Chang, Y. (1976). PIPECOLIC ACID PATHWAY: THE MAJOR LYSINE METABOLIC ROUTE IN THE RAT BRAIN. *BIOCHEMICAL AND BIOPHYSICAL RESEARCH COMMUNICATIONS*, 69(1), 174–180.
- Chang, Y. (1978). Lysine Metabolism in the Rat Brain: the Pipecolic Acid-Forming Pathway. *Journal of Neurochemistry*, 30(2), 347–354. <http://doi.org/10.1111/j.1471-4159.1978.tb06536.x>
- Christensen, E., Ribes, A., Merinero, B., & Zschocke, J. (2004a). Correlation of genotype and phenotype in glutaryl-CoA dehydrogenase deficiency, 27, 861–868.
- Christensen, E., Ribes, A., Merinero, B., & Zschocke, J. (2004b). Correlation of genotype and phenotype in glutaryl-CoA dehydrogenase deficiency. *J. Inherit. Metab. Dis*, 27, 861–868. Retrieved from <https://link.springer.com/content/pdf/10.1023/B:BOLI.0000045770.93429.3c.pdf>
- Dancis, J., Hutzler, J., Ampola, M. G., Shih, V. E., Van Gelderen, H. H., Kirby, L. T., & Woody, A. N. C. (1983). The prognosis of hyperlysinemia: an interim report. *Am J Hum Genet*, 35, 438–442. Retrieved from <https://www.ncbi.nlm.nih.gov/pmc/articles/PMC1685659/pdf/ajhg00351-0108.pdf>
- Dancis, J., Hutzler, J., Woody, N. C., & Cox, R. P. (1976). Multiple enzyme defects in familial hyperlysinemia. *Pediatric Research*, 10(7), 686–691. <http://doi.org/10.1203/00006450-197607000-00011>
- Danhauser, K., Sauer, S. W., Haack, T. B., Wieland, T., Staufner, C., Graf, E., ... Kölker, S. (2012a). DHTKD1 mutations cause 2-amino adipic and 2-oxoadipic aciduria. *American Journal of Human Genetics*, 91(6), 1082–1087. <http://doi.org/10.1016/j.ajhg.2012.10.006>
- Danhauser, K., Sauer, S. W., Haack, T. B., Wieland, T., Staufner, C., Graf, E., ... Kölker, S. (2012b). REPORT DHTKD1 Mutations Cause 2-Amino adipic and 2-Oxoadipic Aciduria. *The American Journal of Human Genetics*, 91, 1082–1087. <http://doi.org/10.1016/j.ajhg.2012.10.006>
- Danks, D. M., Tippett, P., Adams, C., & Campbell, P. (1975). Cerebro-hepato-renal syndrome of Zellweger. *Journal of Pediatrics*, 86(3), 382–387.
- Dasgupta, A., Wahed, A., Dasgupta, A., & Wahed, A. (2014). Inborn Errors of Metabolism. In *Clinical Chemistry, Immunology and Laboratory Quality*

- Control* (pp. 213–228). Elsevier. <http://doi.org/10.1016/B978-0-12-407821-5.00012-7>
- Divry, P., Vianey-Liaud, C., & Mathieu, M. (1991). [Inborn errors of lysine metabolism]. *Annales de Biologie Clinique*, 49(1), 27–35. Retrieved from <http://www.ncbi.nlm.nih.gov/pubmed/1904694>
- Dounay, A. B., Anderson, M., Bechle, B. M., Campbell, B. M., Claffey, M. M., Evdokimov, A., ... Verhoest, P. R. (2012). Discovery of brain-penetrant, irreversible kynurenine aminotransferase ii inhibitors for schizophrenia. *ACS Medicinal Chemistry Letters*, 3(3), 187–192. <http://doi.org/10.1021/ml200204m>
- Dounay, A. B., Tuttle, J. B., & Verhoest, P. R. (2015). Challenges and Opportunities in the Discovery of New Therapeutics Targeting the Kynurenine Pathway. *Journal of Medicinal Chemistry*, 58(22), 8762–8782. <http://doi.org/10.1021/acs.jmedchem.5b00461>
- du Moulin, M., Thies, B., Blohm, M., Oh, J., Kemper, M. J., Santer, R., & Mühlhausen, C. (2017). Glutaric Aciduria Type 1 and Acute Renal Failure : Case Report and Suggested Pathomechanisms. *JIMD Reports*. <http://doi.org/10.1007/8904>
- Duran, M., Beemer, F. A., Wadman, S. K., Wendel, U., & Janssen, B. (1984). A patient with alpha-ketoadipic and alpha-amino adipic aciduria. *Journal of Inherited Metabolic Disease*, 7(2), 61. Retrieved from <http://www.ncbi.nlm.nih.gov/pubmed/6434826>
- Epelbaum, S., Mcdevitt, R., & Falco, S. C. (1997). Lysine-ketoglutarate reductase and saccharopine dehydrogenase from *Arabidopsis thaliana*: nucleotide sequence and characterization. *Plant Molecular Biology*, 35, 735–748. Retrieved from <https://link.springer.com/content/pdf/10.1023%2FA%3A1005808923191.pdf>
- Fellows, F. C., & Lewis, M. H. (1973). Lysine metabolism in mammals. *The Biochemical Journal*, 136(2), 329–34. Retrieved from <http://www.ncbi.nlm.nih.gov/pubmed/4774398>
- Fondi, M., Brilli, M., Emiliani, G., Paffetti, D., & Fani, R. (2007). The primordial metabolism: an ancestral interconnection between leucine, arginine, and lysine biosynthesis. *BMC Evolutionary Biology*, 7(Suppl 2), S3. <http://doi.org/10.1186/1471-2148-7-S2-S3>
- Friedman, M. (1996). Nutritional Value of Proteins from Different Food Sources . A Review. *Journal of Agricultural and Food Chemistry*, 44, 6–29. <http://doi.org/10.1021/jf9400167>
- Gatfield, P. D., Taller, E., Hinton, G., Wallace, A., Abdelnour, G., & Haust, M. (1968). Hyperpipecolatemia : A New Metabolic Disorder Associated with Neuropathy and Hepatomegaly : A case study. *The Canadian Medical Association Journal*, 99(25), 1215–1233.
- Gelderen, H. H. V. A. N., & Teijema, H. L. (1973). Hyperlysinaemia Harmless inborn error of metabolism ?, 892–895.
- Gholsoi, R. K., Sanders, D. C., & Henderson, L. M. (1959). GLUTARIC ACID: A PRODUCT OF TRYPTOPHAN METABOLISM. *Biochemical and Biophysical Research Communications*, 1(2), 98–100.
- Goh, D. L. M., Patel, A., Thomas, G. H., Salomons, G. S., Schor, D. S. M., Jakobs, C., & Geraghty, M. T. (2002). Characterization of the human gene encoding alpha-

- aminoadipate aminotransferase (AADAT). *Molecular Genetics and Metabolism*, 76(3), 172–80. Retrieved from <http://www.ncbi.nlm.nih.gov/pubmed/12126930>
- Gomes, B., Fendrich, G., & Abeles, R. H. (1981). Mechanism of Action of Glutaryl-CoA and Butyryl-CoA Dehydrogenases. Purification of Glutaryl-CoA Dehydrogenase. *Biochemistry Methods Enzymol. J. Biol. Chem. Biochemistry J. Am. Chem. Soc. Biochemistry J. Isot. Eff Enzyme-Catal. React. J. Biol. Chem. J. J. Am. Chem. Soc. Biochemistry J. Am. Chem. Soc.*, 20, 1481–1490. Retrieved from <https://pubs.acs.org/doi/pdf/10.1021/bi00509a012>
- Goncalves, R. L. S., Bunik, V. I., & Brand, M. D. (2016). Production of superoxide/hydrogen peroxide by the mitochondrial 2-oxoadipate dehydrogenase complex. *Free Radical Biology and Medicine*, 91, 247–255. <http://doi.org/10.1016/j.freeradbiomed.2015.12.020>
- Goodman, S. I., & Kohlhoff, J. G. (1975). Glutaric aciduria: Inherited deficiency of glutaryl-CoA dehydrogenase activity. *Biochemical Medicine*, 13(2), 138–140. [http://doi.org/10.1016/0006-2944\(75\)90149-0](http://doi.org/10.1016/0006-2944(75)90149-0)
- Goodman, S. I., Markey, S. P., Moe, P. G., Miles, B. S., & Teng, C. C. (1975a). Glutaric Aciduria; A “New” Disorder of Amino Acid Metabolism. *BIOCHEMICAL MEDICINE*, 12, 12–21. Retrieved from https://ac.els-cdn.com/0006294475900915/1-s2.0-0006294475900915-main.pdf?_tid=spdf-8b15c704-e6fd-49d2-9619-dc33844533d1&acdnat=1519819752_9cac5ea93035cd59789988590e09bfe0
- Goodman, S. I., Markey, S. P., Moe, P. G., Miles, B. S., & Teng, C. C. (1975b). Glutaric aciduria; A “new” disorder of amino acid metabolism. *Biochemical Medicine*, 12(1), 12–21. [http://doi.org/10.1016/0006-2944\(75\)90091-5](http://doi.org/10.1016/0006-2944(75)90091-5)
- Greenberg, B. L., & Glick, M. (2012). LETTERS SCREENING FOR UNIDENTIFIED INCREASED SYSTEMIC DISEASE RISK IN A DENTAL SETTING. *American Journal of Public Health*, 102. <http://doi.org/10.2105/AJPH.2012.300729>
- Greenberg, C. R., Duncan, A. M. V., Gregory, C., Singal, R., & Goodman, S. I. (1994). Assignment of human glutaryl-CoA dehydrogenase gene (GCDH) to the short arm of chromosome 19 (19p13.2) by in situ hybridization and somatic cell hybrid analysis. *Genomics*, 21(1), 289–290.
- Greenberg, C. R., Prasad, A. N., Dilling, L. A., Thompson, J. R. G., Haworth, J. C., Martin, B., ... Siddiqui, M. (2002a). Outcome of the first 3-years of a DNA-based neonatal screening program for glutaric acidemia type 1 in Manitoba and northwestern Ontario, Canada. *Molecular Genetics and Metabolism*, 75(1), 70–8. <http://doi.org/10.1006/mgme.2001.3270>
- Greenberg, C. R., Prasad, A. N., Dilling, L. A., Thompson, J. R. G., Haworth, J. C., Martin, B., ... Siddiqui, M. (2002b). Outcome of the first 3-years of a DNA-based neonatal screening program for glutaric acidemia type 1 in Manitoba and northwestern Ontario, Canada. *Molecular Genetics and Metabolism*, 75(1), 70–8. <http://doi.org/10.1006/mgme.2001.3270>
- Grove, J., & Henderson, L. (1968). The metabolism of d- and l-lysine in the intact rat, perfused liver and liver mitochondria*. *Biochimica et Biophysica Acta*, 27, 113–120.
- Hagen, J., te Brinke, H., Wanders, R. J. A., Knegt, A. C., Oussoren, E., Hoogeboom, A. J. M., ... Houten, S. M. (2015). Genetic basis of alpha-aminoadipic and alpha-ketoadipic aciduria. *Journal of Inherited Metabolic Disease*, 38(5), 873–879.

- <http://doi.org/10.1007/s10545-015-9841-9>
- HALDANE, J. B. S. (1957). Graphical Methods in Enzyme Chemistry. *Nature*, 179(4564), 832–832. <http://doi.org/10.1038/179832b0>
- Hallen, A., Jamie, J. F., & Cooper, A. J. L. (2013). Lysine metabolism in mammalian brain: an update on the Importance of Recent Discoveries. *Amino Acids*, 45(6), 1–37. <http://doi.org/10.1007/s00726-013-1590-1>.
- Han, Q., Robinson, H., Cai, T., Tagle, D. a, & Li, J. (2009). Biochemical and structural properties of mouse kynurenine aminotransferase III. *Molecular and Cellular Biology*, 29(3), 784–93. <http://doi.org/10.1128/MCB.01272-08>
- Hanes, C. S. (1932). Studies on plant amylases: The effect of starch concentration upon the velocity of hydrolysis by the amylase of germinated barley. *Biochemical Journal*, 26, 1406–1421.
- Harting, I., Boy, N., Heringer, J., Seitz, A., Bendszus, M., Pouwels, P. J. W., & Kölker, S. (2015). ¹H-MRS in glutaric aciduria type 1: impact of biochemical phenotype and age on the cerebral accumulation of neurotoxic metabolites. *Journal of Inherited Metabolic Disease*, 38(5), 829–838. <http://doi.org/10.1007/s10545-015-9826-8>
- Harting, I., Neumaier-Probst, E., Seitz, A., Maier, E. M., Assmann, B., Baric, I., ... Kö, S. (2009). Dynamic changes of striatal and extrastriatal abnormalities in glutaric aciduria type I. *Brain*, 132, 1764–1782. <http://doi.org/10.1093/brain/awp112>
- Heringer, J., Boy, S. P. N., Ensenauer, R., Assmann, B., Zschocke, J., Harting, I., ... Kölker, S. (2010). Use of guidelines improves the neurological outcome in glutaric aciduria type I. *Annals of Neurology*, 68(5), 743–52. <http://doi.org/10.1002/ana.22095>
- Heringer, J., Valayannopoulos, V., Lund, A. M., Wijburg, F. A., Freisinger, P., Barić, I., ... Kölker, S. (2016). Impact of age at onset and newborn screening on outcome in organic acidurias. *Journal of Inherited Metabolic Disease*. <http://doi.org/10.1007/s10545-015-9907-8>
- Herskovitz, M., Goldsher, D., Sela, B.-A., & Mandel, H. (2013a). Subependymal mass lesions and peripheral polyneuropathy in adult-onset glutaric aciduria type I. *Neurology*, 81(9), 849–50. <http://doi.org/10.1212/WNL.0b013e3182a2cbf2>
- Herskovitz, M., Goldsher, D., Sela, B.-A., & Mandel, H. (2013b). Subependymal mass lesions and peripheral polyneuropathy in adult-onset glutaric aciduria type I. *Neurology*, 81(9), 849–50. <http://doi.org/10.1212/WNL.0b013e3182a2cbf2>
- Higashino, K., Fujioka, M., Aoki, T., & Yamamura, Y. (1967). Metabolism of lysine in rat liver. *Biochemical and Biophysical Research Communications* *Biophys Res Commun*, 29(1), 95–100.
- Higashino, K., Tsukada, K., & Lieberman, I. (1965). Saccharopine, a product of lysine breakdown by mammalian liver. *Biochemical and Biophysical Research Communications* *Biophys Res Commun*, 20(3), 285–290.
- Hoffmann, G. F. (2006). Cerebral Organic Acid Disorders and Other Disorders of Lysine Catabolism.
- Hoffmann, G. F., Athanassopoulos, S., Burlina, A. , Duran, M., de Klerk, J. B. C., Lehnert, W., ... Christensen, E. (1996). Clinical Course , Early Diagnosis , Treatment , and Prevention of Disease in Glutaryl-CoA Dehydrogenase Deficiency. *Neuropediatrics*, 27, 115–123.

- Hoffmann, G. F., & Zschocke, J. (1999). Glutaric aciduria type I : From clinical, biochemical and molecular diversity to successful therapy. *J. Inher. Metab. Dis*, 22, 381–391. Retrieved from <https://link.springer.com/content/pdf/10.1023/A:1005543904484.pdf>
- Hoffmann, Trefz, F. K., Barth, P. G., Bohles, H. J., Biggemann, B., Bremer, H. J., ... U., W. (1991). Glutaryl-coenzyme A dehydrogenase deficiency: A distinct encephalopathy. *Pediatrics*, 88(6), 1194–1203. Retrieved from <http://ovidsp.ovid.com/ovidweb.cgi?T=JS&PAGE=reference&D=emed2&NEWS=N&AN=1992029708>
- Houten, S. M., Te Brinke, H., Denis, S., Ruiten, J. P. N., Knecht, A. C., De Klerk, J. B. C., ... Duran, M. (2013). Genetic basis of hyperlysinemia. *Orphanet Journal of Rare Diseases*, 8(1), 1–8. <http://doi.org/10.1186/1750-1172-8-57>
- Hutzler, J., & Dancis, J. (1968). Conversion of lysine to saccharopine by human tissues. *Biochimica et Biophysica Acta (BBA) - General Subjects*, 158(1), 62–69. [http://doi.org/10.1016/0304-4165\(68\)90072-X](http://doi.org/10.1016/0304-4165(68)90072-X)
- Hutzler, J., & Dancis, J. (1975). Lysine-ketoglutarate reductase in human tissues. *Biochimica et Biophysica Acta*, 377(1), 42–51. Retrieved from <http://www.ncbi.nlm.nih.gov/pubmed/235294>
- Jafari, P., Braissant, O., Bonafé, L., & Ballhausen, D. (2011). The unsolved puzzle of neuropathogenesis in glutaric aciduria type I. *Molecular Genetics and Metabolism*, 104(4), 425–437. <http://doi.org/10.1016/j.ymgme.2011.08.027>
- Jansen, G. R. (1962). Lysine in Human Nutrition. *Journal of Nutrition*, 76(1), 1–35. http://doi.org/10.1093/jn/76.2_Suppl.1
- Kaminski, M. M., Sauer, S. W., Klemke, C.-D., Süß, D., Okun, J. G., Krammer, P. H., & Gülow, K. (2010). Mitochondrial reactive oxygen species control T cell activation by regulating IL-2 and IL-4 expression: mechanism of ciprofloxacin-mediated immunosuppression. *Journal of Immunology (Baltimore, Md. : 1950)*, 184(9), 4827–41. <http://doi.org/10.4049/jimmunol.0901662>
- Kasé, Y., Kataoka, M., Miyata, T., & Okano, Y. (1973). Pipecolic acid in the dog brain. *Life Sciences*, 13(7), 867–873. [http://doi.org/10.1016/0024-3205\(73\)90077-5](http://doi.org/10.1016/0024-3205(73)90077-5)
- Kasé, Y., Takahama, K., Hashimoto, T., Kaisaku, J., Okano, Y., & Miyata, T. (1980). Electrophoretic study of pipecolic acid, a biogenic imino acid, in the mammalian brain. *Brain Research*, 193(2), 608–613. [http://doi.org/10.1016/0006-8993\(80\)90199-7](http://doi.org/10.1016/0006-8993(80)90199-7)
- Kobashi, N., Makoto, N., & Tanokura, M. (1999). Alpha-amino adipate pathway for the biosynthesis of lysine in lower eukaryotes. *Critical Reviews in Microbiology*, 181(6), 1–6.
- Koeller, D. M., DiGiulio, K. A., Angeloni, S. V., Dowler, L. L., Frerman, F. E., White, R. A., & Goodman, S. I. (1995). Cloning, structure, and chromosome localization of the mouse Glutaryl-CoA dehydrogenase gene. *Genomics*. <http://doi.org/10.1006/geno.1995.1182>
- Koeller, D. M., Woontner, M., Crnic, L. S., Kleinschmidt-DeMasters, B., Stephens, J., Hunt, E. L., & Goodman, S. I. (2002). Biochemical, pathologic and behavioral analysis of a mouse model of glutaric acidemia type I. *Human Molecular Genetics*, 11(4), 347–357. <http://doi.org/10.1093/hmg/11.4.347>
- Kölker, S., Cazorla, A. G., Valayannopoulos, V., Lund, A. M., Burlina, A. B., Sykut-

- Cegielska, J., ... Burgard, P. (2015). The phenotypic spectrum of organic acidurias and urea cycle disorders. Part 1: the initial presentation. *Journal of Inherited Metabolic Disease*, 38(6), 1041–1057. <http://doi.org/10.1007/s10545-015-9839-3>
- Kölker, S., Christensen, E., Leonard, J. V., Greenberg, C. R., Burlina, A. B., Burlina, A. P., ... Burgard, P. (2007). Guideline for the diagnosis and management of glutaryl-CoA dehydrogenase deficiency (glutaric aciduria type I). *Journal of Inherited Metabolic Disease*, 30(1), 5–22. <http://doi.org/10.1007/s10545-006-0451-4>
- Kölker, S., Christensen, E., Leonard, J. V., Greenberg, C. R., Boneh, A., Burlina, A. B., ... Burlina, A. P. (2011). Diagnosis and management of glutaric aciduria type I – revised recommendations. *J Inherit Metab Dis*, 34, 677–694. <http://doi.org/10.1007/s10545-011-9289-5>
- Kölker, S., Garbade, S. F., Boy, N., Maier, E. M., Meissner, T., Mühlhausen, C., ... Hoffmann, G. F. (2007). Decline of acute encephalopathic crises in children with glutaryl-CoA dehydrogenase deficiency identified by newborn screening in Germany. *Pediatric Research*, 62(3), 357–363. <http://doi.org/10.1203/PDR.0b013e318137a124>
- Kölker, S., Garbade, S. F., Greenberg, C. R., Leonard, J. V., Saudubray, J., Ribes, A., ... Hoffmann, G. F. (2006). Natural History, Outcome, and Treatment Efficacy in Children and Adults with Glutaryl-CoA Dehydrogenase Deficiency. *Pediatric Research*, 59(6), 840–847. <http://doi.org/10.1203/01.pdr.0000219387.79887.86>
- Kölker, S., Koeller, D. M., Okun, J. G., & Hoffmann, G. F. (2004). Pathomechanisms of neurodegeneration in glutaryl-CoA dehydrogenase deficiency. *Annals of Neurology*, 55(1), 7–12. <http://doi.org/10.1002/ana.10784>
- Kölker, S., Sauer, S. W., Hoffmann, G. F., Müller, I., Morath, M. A., & Okun, J. G. (2008). Pathogenesis of CNS involvement in disorders of amino and organic acid metabolism. *Journal of Inherited Metabolic Disease*, 31(2), 194–204. <http://doi.org/10.1007/s10545-008-0823-z>
- Kölker, S., Sauer, S. W., Okun, J. G., Hoffmann, G. F., & Koeller, D. M. (2006). Lysine intake and neurotoxicity in glutaric aciduria type I: Towards a rationale for therapy? [1]. *Brain*, 129(8). <http://doi.org/10.1093/brain/awl137>
- Kölker, S., Sauer, S. W., Surtees, R. a H., & Leonard, J. V. (2006). The aetiology of neurological complications of organic acidaemias—a role for the blood-brain barrier. *Journal of Inherited Metabolic Disease*, 29(6), 701–704; discussion 705–706. <http://doi.org/10.1007/s10545-006-0415-8>
- Kölker, S., Valayannopoulos, V., Burlina, A. B., Sykut-Cegielska, J., Wijburg, F. A., Leão Teles, E., ... Kölker, S. (2015). The phenotypic spectrum of organic acidurias and urea cycle disorders. Part 2: the evolving clinical phenotype. *J Inherit Metab Dis*, 38, 1059–1074. <http://doi.org/10.1007/s10545-015-9840-x>
- Korman, S. H., Jakobs, C., Darmin, P. S., Gutman, A., van der Knaap, M. S., Ben-Neriah, Z., ... Salomons, G. S. (2007). Glutaric aciduria type 1: Clinical, biochemical and molecular findings in patients from Israel. *European Journal of Paediatric Neurology*, 11(2), 81–89. <http://doi.org/10.1016/j.ejpn.2006.11.006>
- Koshy Cherian, A., Gritton, H., Johnson, D., Young, D., Kozak, R., & Sarter, M. (2014). A systemically-available kynurenine aminotransferase II (KAT II)

- inhibitor restores nicotine-evoked glutamatergic activity in the cortex of rats Ajeesh, *10*(7), 552–554.
<http://doi.org/10.1016/j.neuropharm.2014.03.004>. A
- Külkens, S., Harting, I., Sauer, S., Zschocke, J., Hoffmann, G. F., Gruber, S., ... Kölker, S. (2005). Late-onset neurologic disease in glutaryl- CoA dehydrogenase deficiency. *NEUROLOGY*, *64*, 2142–2144. Retrieved from
<http://n.neurology.org/content/neurology/64/12/2142.full.pdf>
- Kvittingen, E. A., Bergan, A., & Berger, R. (1993). Hereditary tyrosinemia type I . Self-induced correction of the fumarylacetoacetase defect . Find the latest version :, *91*(4), 1816–1821.
- Kyllerman, M., Skjeldal, O., Christensen, E., Hagberg, G., Holme, E., Lönnquist, T., ... von Döbeln, U. (2004). Long-term follow-up, neurological outcome and survival rate in 28 Nordic patients with glutaric aciduria type 1. *European Journal of Paediatric Neurology*, *8*(3), 121–129.
<http://doi.org/10.1016/j.ejpn.2003.12.007>
- Lanouette, S., Mongeon, V., Figeys, D., & Couture, J.-F. (2014). The functional diversity of protein lysine methylation. *Mol Syst Biol*, *10*.
<http://doi.org/10.1002/msb.134974>
- Linderholm, K. R., Alm, M. T., Larsson, M. K., Olsson, S. K., Goiny, M., Hajos, M., ... Engberg, G. (2016). Inhibition of kynurenine aminotransferase II reduces activity of midbrain dopamine neurons. *Neuropharmacology*, *102*, 42–47.
<http://doi.org/10.1016/j.neuropharm.2015.10.028>
- Lindstedt, S., Holme, E., Lock, E. A., Hjalmarsen, O., & Strandvik, B. (1992). Treatment of hereditary tyrosinaemia type I by inhibition of 4-hydroxyphenylpyruvate dioxygenase. *The Lancet*, *340*(8823), 813–817.
[http://doi.org/10.1016/0140-6736\(92\)92685-9](http://doi.org/10.1016/0140-6736(92)92685-9)
- Lock, E. A., Ellis, M. K., Gaskin, P., Robinson, M., Auton, T. R., Provan, W. M., ... Lee, D. L. (1998). From toxicological problem to therapeutic use: The discovery of the mode of action of 2-(2-nitro-4-trifluoromethylbenzoyl)-1,3-cyclohexanedione (NTBC), its toxicology and development as a drug. *Journal of Inherited Metabolic Disease*, *21*(5), 498–506.
<http://doi.org/10.1023/A:1005458703363>
- Lowry, O. H., Rosebrough, N. J., Farr, A. L., & Randall, R. J. (1951). PROTEIN MEASUREMENT WITH THE FOLIN PHENOL REAGENT*. *The Journal of Biological Chemistry*.
- Markovitz, P. J., & Chuang, D. T. (1987). The Bifunctional Amino adipic Semialdehyde Synthase in Lysine Degradation. *Journal of Biological Chemistry*, *262*(19), 9353–9358.
- Markovitz, P. J., Chuang, D. T., & Cox, R. P. (1984). Familial hyperlysinemias. Purification and characterization of the bifunctional amino adipic semialdehyde synthase with lysine-ketoglutarate reductase and saccharopine dehydrogenase activities. *Journal of Biological Chemistry*, *259*(19), 11643–11646.
- Mason, M. (1954). THE KYNURENINE TRANSAMINASE OF RAT KIDNEY*. *The Journal of Biological Chemistry*. Retrieved from
<http://www.jbc.org/content/211/2/839.full.pdf>
- Matsuda, M., & Ogur, M. (1969). Separation and Transaminase * Specificity of the Yeast. *The Journal of Biological Chemistry*, *244*(12), 3352–3358.
- Matsumoto, S., Yamamoto, S., Sai, K., Maruo, K., Adachi, M., Saitoh, M., & Nishizaki,

- T. (2003). Pipecolic acid induces apoptosis in neuronal cells. *Brain Research*, 980(2), 179–184. [http://doi.org/10.1016/S0006-8993\(03\)02869-5](http://doi.org/10.1016/S0006-8993(03)02869-5)
- Meister, A. (1962). [120] Δ^1 -Piperideine-2-carboxylate and Δ^1 -pyrroline-2-carboxylate reductase: Δ^1 -Piperideine-2-carboxylate + DPNH + H⁺ → L-Pipecolate + DPN+ Δ^1 -pyrroline-2-carboxylate + DPNH + H⁺ → L-Proline + DPN+. *Methods in Enzymology*, 5, 878–882. [http://doi.org/10.1016/S0076-6879\(62\)05332-X](http://doi.org/10.1016/S0076-6879(62)05332-X)
- Mihalik, S.J., Rhead, W. J. (1991). Species variation in organellar location and activity of L-pipecolic acid oxidation in mammals. - PubMed - NCBI. *Journal of Comparative Physiology.B, Biochemical, Systemic and Environmental Physiology*. Retrieved from <https://www.ncbi.nlm.nih.gov/pubmed/2045546>
- Mihalik, S. J., Moser, H. W., Watkins, P. A., Danks, D. M., Poulos, A., & Rhead, W. J. (1989). Peroxisomal l-pipecolic acid oxidation is deficient in liver from zellweger syndrome patients. *Pediatric Research*, 25(5), 548–552. <http://doi.org/10.1203/00006450-198905000-00024>
- Mihalik, S. J., & Rhead, W. J. (1989). L-pipecolic acid oxidation in the rabbit and cynomolgus monkey. Evidence for differing organellar locations and cofactor requirements in each species. *The Journal of Biological Chemistry*, 264(5), 2509–17. Retrieved from <http://www.ncbi.nlm.nih.gov/pubmed/2914918>
- Miller, I. L., Tsuchida, M., & Adelberg, E. A. (1953). THE TRANSAMINATION OF KYNURENINE. *The Journal of Biological Chemistry*. Retrieved from <http://www.jbc.org/content/203/1/205.full.pdf>
- Monavari, A., & Naughten, E. R. (2000). Prevention of cerebral palsy in glutaric aciduria type 1 by dietary management, 82, 67–70.
- Mori, J.-I., Suzuki, S., Kobayashi, M., Inagaki, T., Komatsu, A., Takeda, T., ... Hashizume, K. (2002). Nicotinamide Adenine Dinucleotide Phosphate-Dependent Cytosolic T 3 Binding Protein as a Regulator for T 3 -Mediated Transactivation. Retrieved from https://watermark.silverchair.com/endo1538.pdf?token=AQECAHi208BE490oan9kkhW_Ercy7Dm3ZL_9Cf3qfKAc485ysgAAAb8wggG7BgkqhkiG9w0B BwagggGsMIIBqAIBADCCAaEGCSqGSib3DQEHATAeBgIghkgBZQMEAS4wEQQMb5xJoZGKsn5Zfx7BAGeQgIIBcgx5v8258QuW2ndlu3_YuEDlub5lxG5sQT17hCOgWy13ac
- Mühlhausen, C., Christensen, E., Schwartz, M., Muschol, N., Ullrich, K., & Lukacs, Z. (2003). CASE REPORT Severe phenotype despite high residual glutaryl-CoA dehydrogenase activity: A novel mutation in a Turkish patient with glutaric aciduria type I. *J. Inherit. Metab. Dis*, 26, 713–714. Retrieved from <https://link.springer.com/content/pdf/10.1023%2FB%3ABOLI.0000005604.90621.e2.pdf>
- Murthy, S. N., & Janardanasarma, M. K. (1999). Identification of L-amino acid/L-lysine α -amino oxidase in mouse brain. *Molecular and Cellular Biochemistry*, 197, 13–23. Retrieved from <https://link.springer.com/content/pdf/10.1023/A:1006906505745.pdf>
- Nakatani, Y., Fujioka, M., & Higashino, K. (1970). α -AMINOADIPATE AMINOTRANSFERASE OF RAT LIVER MITOCHONDRIA. *Biochimica et Biophysica Acta*. Retrieved from <https://ac.els-cdn.com/0005274470900549/1-s2.0-0005274470900549->

main.pdf?_tid=0b727839-3e6a-4a1d-b7de-
f1846d0c4475&acdnat=1525774721_811a6cc81907be5d9215d0e7d5a9e3
72

- Naughten, E. R., Mayne, P. D., Monavari, A. A., Goodman, S. I., Sulaiman, G., & Croke, D. T. (2004). Glutaric aciduria type I: outcome in the Republic of Ireland. *Journal of Inherited Metabolic Disease*, *27*(6), 917–20.
<http://doi.org/10.1023/B:BOLI.0000045777.82784.74>
- Nematollahi, A., Sun, G., Jayawickrama, G. S., Hanrahan, J. R., & Church, W. B. (2016). Study of the activity and possible mechanism of action of a reversible inhibitor of recombinant human KAT-2: A promising lead in neurodegenerative and cognitive disorders. *Molecules*, *21*(7).
<http://doi.org/10.3390/molecules21070856>
- Nemeria, N. S., Gerfen, G., Guevara, E., Nareddy, P. R., Szostak, M., & Jordan, F. (2017). The human Krebs cycle 2-oxoglutarate dehydrogenase complex creates an additional source of superoxide/hydrogen peroxide from 2-oxoadipate as alternative substrate. *Free Radical Biology and Medicine*, *108*, 644–654. <http://doi.org/10.1016/j.freeradbiomed.2017.04.017>
- Nemeria, N. S., Gerfen, G., Nareddy, P. R., Yang, L., Zhang, X., Szostak, M., & Jordan, F. (2018). The mitochondrial 2-oxoadipate and 2-oxoglutarate dehydrogenase complexes share their E2 and E3 components for their function and both generate reactive oxygen species. *Free Radical Biology and Medicine*, *115*(December 2017), 136–145.
<http://doi.org/10.1016/j.freeradbiomed.2017.11.018>
- Neuberger, A., & Sanger, F. (1943). The Availability of the Acetyl Derivatives of Lysine for Growth, 37. Retrieved from
<https://www.ncbi.nlm.nih.gov/pmc/articles/PMC1257953/pdf/biochemj00972-0074.pdf>
- Neuberger, A., & Webster, T. A. (1945). The Lysine Requirements of the Adult Rat, 39, 200–202. Retrieved from
<https://www.ncbi.nlm.nih.gov/pmc/articles/PMC1258198/pdf/biochemj00963-0093.pdf>
- Panier, S., & Boulton, S. J. (2014). Double-strand break repair: 53BP1 comes into focus. *Nature Reviews Molecular Cell Biology*, *15*(1), 7–18.
<http://doi.org/10.1038/nrm3719>
- Papes, F., Kemper, E. L., Cord-Neto, G., Langone, F., & Arruda, P. (1999). Lysine degradation through the saccharopine pathway in mammals: involvement of both bifunctional and monofunctional lysine-degrading enzymes in mouse. *The Biochemical Journal*, *344 Pt 2*(2), 555–63.
<http://doi.org/10.1042/BJ3440555>
- Papes, F., Surpili, M. J., Langone, F., Trigo, J. R., & Arruda, P. (2000). The essential amino acid lysine acts as precursor of glutamate in the mammalian central nervous system, *488*, 34–38.
- Papes, F., Surpili, M. J., Langone, F., Trigo, J. R., & Arruda, P. (2001). The essential amino acid lysine acts as precursor of glutamate in the mammalian central nervous system. *FEBS Letters*, *488*(1–2), 34–38.
[http://doi.org/10.1016/S0014-5793\(00\)02401-7](http://doi.org/10.1016/S0014-5793(00)02401-7)
- Pierson, T. M., Nezhad, M., Tremblay, M. A., Lewis, R., Wong, D., Salamon, N., & Sicotte, N. (2015). Adult-onset glutaric aciduria type I presenting with white matter abnormalities and subependymal nodules. *Neurogenetics*, *16*(4),

- 325–328. <http://doi.org/10.1007/s10048-015-0456-y>
- Potter, M. C., Elmer, G. I., Bergeron, R., Albuquerque, E. X., Guidetti, P., Wu, H.-Q., & Schwarcz, R. (2010). Reduction of Endogenous Kynurenic Acid Formation Enhances Extracellular Glutamate, Hippocampal Plasticity, and Cognitive Behavior. *Neuropsychopharmacology*, *35*, 1734–1742. <http://doi.org/10.1038/npp.2010.39>
- Przyrembel, H., Bachmann, D., Lombeck, I., Becker, K., Wendel, U., Wadman, S. K., & Bremer, H. J. (1975). Alpha-ketoadipic aciduria, a new inborn error of lysine metabolism; biochemical studies. *Clinica Chimica Acta; International Journal of Clinical Chemistry*, *58*(3), 257–69. Retrieved from <http://www.ncbi.nlm.nih.gov/pubmed/1112064>
- Ran, F. A., Hsu, P. D. P., Wright, J., Agarwala, V., Scott, D. a, & Zhang, F. (2013). Genome engineering using the CRISPR-Cas9 system. *Nature Protocols*, *8*(11), 2281–2308. <http://doi.org/10.1038/nprot.2013.143>. Genome
- Ranganath, L. R., Jarvis, J. C., & Gallagher, J. A. (2013). Recent advances in management of alkaptonuria (invited review; Best practice article). *Journal of Clinical Pathology*, *66*(5), 367–373. <http://doi.org/10.1136/jclinpath-2012-200877>
- Rao, V. V., & Chang, Y.-F. (1990). l-Pipecolic acid metabolism in human liver: detection of l-pipecolate oxidase and identification of its reaction product. *Biochimica et Biophysica Acta (BBA) - Protein Structure and Molecular Enzymology*, *1038*(3), 295–299. [http://doi.org/10.1016/0167-4838\(90\)90240-G](http://doi.org/10.1016/0167-4838(90)90240-G)
- Rao, V. V., Pan, X., & Chang, Y. F. (1992). Developmental changes of l-lysine-ketoglutarate reductase in rat brain and liver. *Comparative Biochemistry and Physiology -- Part B: Biochemistry And*, *103*(1), 221–224. [http://doi.org/10.1016/0305-0491\(92\)90435-T](http://doi.org/10.1016/0305-0491(92)90435-T)
- Rao, V. V., & Chang, Y.-F. (1992). Assay for L-pipecolate oxidase activity in human liver: detection of enzyme deficiency in hyperpipecolic acidemia. *Biochimica et Biophysica Acta*, *1139*, 189–195.
- Rao, V. V., Tsai, M. J., Pan, X., & Chang, Y.-F. (1993). L-Pipecolic acid oxidation in rat: subcellular localization and developmental study. *Biochimica et Biophysica Acta*, *1164*, 29–35.
- Rothkamm, K., Barnard, S., Moquet, J., Ellender, M., Rana, Z., & Burdak-Rothkamm, S. (2015). DNA damage foci: Meaning and significance. *Environmental and Molecular Mutagenesis* *56*:491–504 (2015) Review, *56*, 491–504. <http://doi.org/https://doi.org/10.1002/em.21944>
- Rothstein, M., & Miller, L. (1954a). THE CONVERSION OF LYSINE TO PIPECOLIC ACID IN THE RAT*. *Journal of Biological Chemistry*, 851–858.
- Rothstein, M., & Miller, L. L. (1954b). THE CONVERSION OF LYSINE TO PIPECOLIC ACID IN THE RAT*. Retrieved from <http://www.jbc.org/content/211/2/851.full.pdf>
- Sacksteder, K. A., Biery, B. J., Morrell, J. C., Goodman, B. K., Geisbrecht, B. V, Cox, R. P., ... Geraghty, M. T. (2000). Identification of the alpha-amino adipic semialdehyde synthase gene, which is defective in familial hyperlysinemia. *American Journal of Human Genetics*, *66*(6), 1736–43. <http://doi.org/10.1086/302919>
- Sauer, S. W., Okun, J. G., Fricker, G., Mahringer, A., Müller, I., Crnic, L. R., ... Kler, S. (2006). Intracerebral accumulation of glutaric and 3-

- hydroxyglutaric acids secondary to limited flux across the blood-brain barrier constitute a biochemical risk factor for neurodegeneration in glutaryl-CoA dehydrogenase deficiency. *Journal of Neurochemistry*, 97(3), 899–910. <http://doi.org/10.1111/j.1471-4159.2006.03813.x>
- Sauer, S. W., Okun, J. G., Fricker, G., Mahringer, A., Müller, I., Crnic, L. R., ... Kölker, S. (2006). Intracerebral accumulation of glutaric and 3-hydroxyglutaric acids secondary to limited flux across the blood-brain barrier constitute a biochemical risk factor for neurodegeneration in glutaryl-CoA dehydrogenase deficiency. *Journal of Neurochemistry*, 97(3), 899–910. <http://doi.org/10.1111/j.1471-4159.2006.03813.x>
- Sauer, S. W., Okun, J. G., Schwab, M. A., Crnic, L. R., Hoffmann, G. F., Goodman, S. I., ... Kölker, S. (2005). Bioenergetics in glutaryl-coenzyme A dehydrogenase deficiency: A role for glutaryl-coenzyme A. *Journal of Biological Chemistry*, 280(23), 21830–21836. <http://doi.org/10.1074/jbc.M502845200>
- Sauer, S. W., Opp, S., Hoffmann, G. F., Koeller, D. M., Okun, J. G., & Kölker, S. (2011). Therapeutic modulation of cerebral l-lysine metabolism in a mouse model for glutaric aciduria type I. *Brain*, 134(1), 157–170. <http://doi.org/10.1093/brain/awq269>
- Sauer, S. W., Opp, S., Komatsuzaki, S., Blank, A. E., Mittelbronn, M., Burgard, P., ... Kölker, S. (2015). Multifactorial modulation of susceptibility to l-lysine in an animal model of glutaric aciduria type I. *Biochimica et Biophysica Acta - Molecular Basis of Disease*, 1852(5), 768–777. <http://doi.org/10.1016/j.bbadis.2014.12.022>
- Sauer, S. W., Opp, S., Mahringer, A., Kamiński, M. M., Thiel, C., Okun, J. G., ... Kölker, S. (2010). Glutaric aciduria type I and methylmalonic aciduria: Simulation of cerebral import and export of accumulating neurotoxic dicarboxylic acids in in vitro models of the blood–brain barrier and the choroid plexus. *BBA - Molecular Basis of Disease*, 1802, 552–560. <http://doi.org/10.1016/j.bbadis.2010.03.003>
- Scannone, H., Wellner, D., & Novogrodsky, A. (1964). A Study of Amino Acid Oxidase Specificity, Using a New Sensitive Assay*. *Biochemistry*, 3(11). Retrieved from <https://pubs.acs.org/doi/pdf/10.1021/bi00899a027>
- Schulze, A., Lindner, M., Kohlmü, D., Olgemö, K., Mayatepek, E., & Hoffmann, G. F. (2003). Expanded Newborn Screening for Inborn Errors of Metabolism by Electrospray Ionization-Tandem Mass Spectrometry: Results, Outcome, and Implications. *Pediatrics*, 111(6). Retrieved from <http://pediatrics.aappublications.org/content/pediatrics/111/6/1399.full.pdf>
- Schwarcz, R., & Stone, T. W. (2017). The kynurenine pathway and the brain: Challenges, controversies and promises. *Neuropharmacology*, 112, 237–247. <http://doi.org/10.1016/j.neuropharm.2016.08.003>
- Schwartz, M., Christensen, E., Niels, A. S., & Brandt, J. (1998). The human glutaryl-CoA dehydrogenase gene : report of intronic sequences and of 13 novel mutations causing glutaric aciduria type I. *Human Genetics*, 102(4), 452–458.
- Seccombe, D. W., James, L., & Booth, F. (1986). L-carnitine treatment in glutaric aciduria type I. *Neurology*, 36(2), 264–7. Retrieved from <http://www.ncbi.nlm.nih.gov/pubmed/3945396>
- Sherman, E. A., Strauss, K. A., Tortorelli, S., Bennett, M. J., Knerr, I., Morton, D. H., & Puffenberger, E. G. (2008). Genetic Mapping of Glutaric Aciduria, Type 3,

- to Chromosome 7 and Identification of Mutations in C7orf10. *American Journal of Human Genetics*, 83(5), 604–609.
<http://doi.org/10.1016/j.ajhg.2008.09.018>
- Slyke, D. D. Van, & Sinext, F. M. (1958). THE COURSE OF HYDROXYLATION OF LYSINE TO FORM HYDROXYLYSINE IN COLLAGEN*. Retrieved from
<http://www.jbc.org/content/232/2/797.full.pdf>
- Soda, K., Misono, H., & Yamamoto, T. (1968). L-Lysine- α -Ketoglutarate Aminotransferase. I. Identification of a Product, Δ 1-Piperideine-6-carboxylic Acid. *Biochemistry*, 7(11), 4102–4109.
<http://doi.org/10.1021/bi00851a045>
- Stemmer, M., Thumberger, T., Del Sol Keyer, M., Wittbrodt, J., & Mateo, J. L. (2015). CCTop: An intuitive, flexible and reliable CRISPR/Cas9 target prediction tool. *PLoS ONE*, 10(4), 1–11.
<http://doi.org/10.1371/journal.pone.0124633>
- Strauss, K. A., Brumbaugh, J., Duffy, A., Wardley, B., Robinson, D., Hendrickson, C., ... Morton, D. H. (2011). Safety, efficacy and physiological actions of a lysine-free, arginine-rich formula to treat glutaryl-CoA dehydrogenase deficiency: Focus on cerebral amino acid influx. *Molecular Genetics and Metabolism*, 104(1–2), 93–106. <http://doi.org/10.1016/j.ymgme.2011.07.003>
- Strauss, K. A., Donnelly, P., & Wintermark, M. (2010). Cerebral haemodynamics in patients with glutaryl-coenzyme A dehydrogenase deficiency. *Brain*, 133, 76–92. <http://doi.org/10.1093/brain/awp297>
- Strauss, K. A., Lazovic, J., Wintermark, M., & Morton, D. H. (2007). Multimodal imaging of striatal degeneration in Amish patients with glutaryl-CoA dehydrogenase deficiency. *Brain*, 130(7), 1905–1920.
<http://doi.org/10.1093/brain/awm058>
- Strauss, K. A., & Morton, D. H. (2003). Type I glutaric aciduria, part 2: A model of acute striatal necrosis. *American Journal of Medical Genetics*, 121C(1), 53–70.
<http://doi.org/10.1002/ajmg.c.20008>
- Strauss, K. A., Puffenberger, E. G., Robinson, D. L., & Morton, D. H. (2003). Type I glutaric aciduria, part 1: Natural history of 77 patients. *American Journal of Medical Genetics*, 121C(1), 38–52. <http://doi.org/10.1002/ajmg.c.20007>
- Struys, E. A., Jansen, E. E. W., & Salomons, G. S. (2014). Human pyrroline-5-carboxylate reductase (PYCR1) acts on Δ 1-piperideine-6-carboxylate generating L-pipecolic acid. *Journal of Inherited Metabolic Disease*, 37(3), 327–332. <http://doi.org/10.1007/s10545-013-9673-4>
- Sulkowski, P. L., Sundaram, R. K., Oeck, S., Corso, C. D., Liu, Y., Noorbakhsh, S., ... Glazer, P. M. (2018). Krebs-cycle-deficient hereditary cancer syndromes are defined by defects in homologous-recombination DNA repair. *Nature Genetics*, 50(August), 1–7. <http://doi.org/10.1038/s41588-018-0170-4>
- Superti-Furga, A. (1997). Glutaric aciduria type 1 (glutaryl-CoA-dehydrogenase deficiency): advances and unanswered questions. *European Journal of Pediatrics*, 156, 821–828.
- Tan, M., Peng, C., Anderson, K. A., Chhoy, P., Xie, Z., Dai, L., ... Zhao, Y. (2014). Lysine glutarylation is a protein posttranslational modification regulated by SIRT5. *Cell Metabolism*, 19(4), 605–17.
<http://doi.org/10.1016/j.cmet.2014.03.014>
- Tapias, A., Wang, Z.-Q., & Yang, Y.-G. (2017). Lysine Acetylation and Deacetylation in Brain Development and Neuropathies, 15, 19–36.

- <http://doi.org/10.1016/j.gpb.2016.09.002>
- Thomas B. Osborne, L. B. M. E. L. F., & Wakeman, A. J. (1914). Amino acids in nutrition and growth. *Journal of Biological Chemistry*, 17(February), 325–349.
- Tobes, M. C., & Mason, M. (1975). L-KYNURENINE AMINOTRANSFERASE AND L-~-AMINOADIPATE AMINOTRANSFERASE. I. EVIDENCE FOR IDENTITY, 62(2), 19–5. Retrieved from https://ac.els-cdn.com/S0006291X75801513/1-s2.0-S0006291X75801513-main.pdf?_tid=7184b34a-f5c6-49b4-bd18-3a45bf69e3e3&acdnat=1525775050_96f21efafcbf2e26b2bcfce3dcf8ce8b
- Tobes, M. C., & Mason, M. (1977). α -Amino adipate aminotransferase and kynurenine aminotransferase. Purification, characterization, and further evidence for identity. *THE JOURNAL OF BIOLOGICAL CHEMISTRY*, 252(13), 4591–4599. Retrieved from <http://www.jbc.org/content/252/13/4591.full.pdf>
- Tomé, D., & Bos, C. (2007). Lysine Requirement through the Human Life Cycle 1,2. *J. Nutr*, 137, 1642–1645. Retrieved from <http://jn.nutrition.org/content/137/6/1642S.full.pdf>
- Tondo, M., Calpena, E., Arriola, G., Sanz, P., Martorell, L., Ormazabal, A., ... Artuch, R. (2013). Clinical, biochemical, molecular and therapeutic aspects of 2 new cases of 2-amino adipic semialdehyde synthase deficiency. *Molecular Genetics and Metabolism*, 110(3), 231–236. <http://doi.org/10.1016/j.ymgme.2013.06.021>
- Trijbels, J. M., Monnens, L. A., Bakkeren, J. A., Van Raay-Selten, A. H., & Corstiaensen, J. M. (1980). Biochemical studies in the cerebro-hepato-renal syndrome of Zellweger: a disturbance in the metabolism of pipercolic acid. *Journal of Inherited Metabolic Disease*, 2(2), 39–42. Retrieved from <http://www.ncbi.nlm.nih.gov/pubmed/6796759>
- Tuncel, A. T., Boy, N., Morath, M. A., Hörster, F., Mütze, U., & Kölker, S. (2018). Organic acidurias in adults: late complications and management. *Journal of Inherited Metabolic Disease*, 1–12. <http://doi.org/10.1007/s10545-017-0135-2>
- Vamos, E., Pardutz, A., Klivenyi, P., Toldi, J., & Vecsei, L. (2009). The role of kynurenines in disorders of the central nervous system: Possibilities for neuroprotection. <http://doi.org/10.1016/j.jns.2009.02.326>
- van der Watt, G., Owen, E. P., Berman, P., Meldau, S., Watermeyer, N., Olpin, S. E., ... Henderson, H. (2010). Glutaric aciduria type 1 in South Africa-high incidence of glutaryl-CoA dehydrogenase deficiency in black South Africans. *Molecular Genetics and Metabolism*, 101(2–3), 178–182. <http://doi.org/10.1016/j.ymgme.2010.07.018>
- VanderJagt, D. J., Garry, P. J., & Hunt, W. C. (1986). Ascorbate in plasma as measured by liquid chromatography and by dichlorophenolindophenol colorimetry. *Clinical Chemistry*, 32(6). Retrieved from <http://clinchem.aaccjnl.org/content/32/6/1004.long>
- Varadkar, S., & Surtees, R. (2004). Glutaric aciduria type I and kynurenine pathway metabolites: A modified hypothesis. *Journal of Inherited Metabolic Disease*, 27(6), 835–842. <http://doi.org/10.1023/B:BOLI.0000045767.42193.97>
- Vaz, F. M., & Wanders, R. . . . A. (2002). Carnitine biosynthesis in mammals.

- Biochem. J*, 361, 417–429.
- vd Heiden, C., Brink, M., de Bree, P. K., v Sprang, F. J., Wadman, S. K., de Pater, J. M., & van Biervliet, J. P. (1978). Familial hyperlysinaemia due to L-lysine alpha-ketoglutarate reductase deficiency: results of attempted treatment. *Journal of Inherited Metabolic Disease*, 1(3), 89–94. Retrieved from <http://www.ncbi.nlm.nih.gov/pubmed/116084>
- Versmold, H. ., Bremer, H. J., Herzog, V., Siegel, G., Bassewitz, D. B. ., Irle, U., ... Brauser, B. (1997). A Metabolic Disorder Similar to Zellweger Syndrome with Hepatic Acatlasia and Absence of Peroxisomes, Altered Content and Redox State of Cytochromes, and Infantile Cirrhosis with Hemosiderosis. *European Journal of Pediatrics*, 124, 261–275. <http://doi.org/10.1007/BF00477550>
- Wanders, R. J. ., Romeyn, G. ., Roermund van, C. W. ., Scutgens, R. B. ., Bosch, V. den, & Tager, J. . (1988). Identification of L-pipecolate oxidase in human liver and its deficiency in the Zellweger syndrome. *Biochemical and Biophysical Research Communications*, 154, 33–38.
- Wanders, R. J. A., Romeyn, G. ., Schutgens, R. ., & Tager, J. . (1989). L-PIPECOLATE OXIDASE: A DISTINCT PEROXISOMAL ENZYME IN MAN. *Biochemical and Biophysical Research Communications*, 164(1). Retrieved from https://ac.els-cdn.com/0006291X89917543/1-s2.0-0006291X89917543-main.pdf?_tid=73a135cd-70e9-454c-a07d-684099ccf713&acdnat=1525621652_b54e18a32b8dda168f852800a78552d5
- Wang, T. J., Ngo, D., Psychogios, N., Dejam, A., Larson, M. G., Vasan, R. S., ... Gerszten, R. E. (2013). 2-Amino adipic acid is a biomarker for diabetes risk. *The Journal of Clinical Investigation*, 123, 4309. Retrieved from <http://www.jci.org>
- Wass, C., Klammer, D., Katsarogiannis, E., Pålsson, E., Svensson, L., Fejgin, K., ... Rembeck, B. (2011). L-lysine as adjunctive treatment in patients with schizophrenia: a single-blinded, randomized, cross-over pilot study. *BMC Medicine*, 9, 40. <http://doi.org/10.1186/1741-7015-9-40>
- Weissman, N., & Schoenheimer, R. (1941). The relative stability of l(+)-lysine in rats studied with deuterium and heavy nitrogen. *Journal of Biological Chemistry*, 779–795.
- WOODY, N. C. (1964). HYPERLYSINEMIA. *American Journal of Diseases of Children (1960)*, 108, 543–53. Retrieved from <http://www.ncbi.nlm.nih.gov/pubmed/14209691>
- Woody, N. C., & Pupene, M. B. (1970). Excretion of pipecolic acid by infants and by patients with hyperlysinemia. *Pediatric Research*, 4(1), 89–95. <http://doi.org/10.1203/00006450-197001000-00011>
- Wu, G. (2010). *Amino Acids: Biochemistry and Nutrition*. Retrieved from <https://books.google.de/books?id=Sj6Xrc78LKUC&printsec=frontcover&dq=aminoacids&hl=en&sa=X&ved=0ahUKEwj3ZzC80HaAhUBkBQKHS1uCwoQ6AEINzAC#v=onepage&q=aminoacids&f=false>
- Wu, Y., Williams, E. G., Dubuis, S., Mottis, A., Jovaisaite, V., Houten, S. M., ... Aebbersold, R. (2014). Multilayered Genetic and Omics Dissection of Mitochondrial Activity in a Mouse Reference Population. *Cell*, 158(6), 1415–1430. <http://doi.org/10.1016/j.cell.2014.07.039>
- Xu, W.-Y., Zhu, H., Shen, Y., Wan, Y.-H., Tu, X.-D., Wu, W.-T., ... Wang, Z.-G. (2018).

- DHTKD1 Deficiency Causes Charcot-Marie-Tooth Disease in Mice. *MOLECULAR AND CELLULAR BIOLOGY*, 38(13). Retrieved from <http://mcb.asm.org/content/38/13/e00085-18.full.pdf>
- Xu, W., Zhu, H., Gu, M., Luo, Q., Ding, J., Yao, Y., ... Wang, Z. (2013). DHTKD1 is essential for mitochondrial biogenesis and function maintenance. *FEBS Letters*, 587(21), 3587–3592. <http://doi.org/10.1016/j.febslet.2013.08.047>
- Young, R. (1994). Plant proteins in relation to human and amino acid nutrition1 ' 2 whereas. *The American Journal of Clinical Nutrition*, 59, 1203s–12s.
- Yu, P., Di Prospero, N. A., Sapko, M. T., Cai, T., Chen, A., Melendez-Ferro, M., ... Tagle, D. A. (2004). Biochemical and phenotypic abnormalities in kynurenine aminotransferase II-deficient mice. *Molecular and Cellular Biology*, 24(16), 6919–30. <http://doi.org/10.1128/MCB.24.16.6919-6930.2004>
- Zabriskie, T. M., & Jackson, M. D. (2000). Lysine biosynthesis and metabolism in fungi. *Natural Product Reports*, (July 1999), 85–97.
- Zhang, N., Zhou, Y., Huang, T., Zhang, Y.-C., Li, B.-Q., Chen, L., ... Permyakov, E. A. (2014). Discriminating between Lysine Sumoylation and Lysine Acetylation Using mRMR Feature Selection and Analysis, 9(9). <http://doi.org/10.1371/journal.pone.0107464>
- Zhao, Y., Rio, •, Barrere-Cain, E., & Yang, • Xia. (2015). Nutritional systems biology of type 2 diabetes. *Genes Nutrition*. <http://doi.org/10.1007/s12263-015-0481-3>
- Zinnanti, W. J., & Lazovic, J. (2010). Mouse model of encephalopathy and novel treatment strategies with substrate competition in glutaric aciduria type I. *Molecular Genetics and Metabolism*, 100(SUPPL.), S88–S91. <http://doi.org/10.1016/j.ymgme.2010.02.022>
- Zinnanti, W. J., Lazovic, J., Wolpert, E. B., Antonetti, D. A., Smith, M. B., Connor, J. R., ... Cheng, K. C. (2006). A diet-induced mouse model for glutaric aciduria type I. *Brain*, 129(4), 899–910. <http://doi.org/10.1093/brain/awl009>
- Zschocke, J., Quak, E., Guldborg, P., & Hoffmann, G. F. (2000). Mutation analysis in glutaric aciduria type I. *Journal of Medical Genetics*, 37, 177–181.

7. ORIGINAL PUBLICATIONS

7. Original Publications

1. Komatsuzaki S, **Ediga RD**, Okun JG, Kölker S, Sauer SW.

'Impairment of astrocytic glutaminolysis in glutaric aciduria type I'.

J Inherit Metab Dis. 2018 Jan;41(1):91-99. [doi: 10.1007/s10545-017-0096-5](https://doi.org/10.1007/s10545-017-0096-5).

2. Biagosch C, **Ediga RD***, Hensler SV, Faerberboeck M, Kuehn R, Wurst W, Meitinger T, Kölker S, Sauer S, Prokisch H.

'Elevated glutaric acid levels in Dhtkd1-/Gcdh- double knockout mice challenge our current understanding of lysine metabolism'.

Biochim Biophys Acta. 2017 Sep;1863(9):2220-2228. [doi: 10.1016/j.bbadis.2017.05.018](https://doi.org/10.1016/j.bbadis.2017.05.018)

*** Equal contribution**

3. Staufner C, Haack TB, Feyh P, Gramer G, **Raga DE**, Terrile C, Sauer S, Okun JG, Fang-Hoffmann J, Mayatepek E, Prokisch H, Hoffmann GF, Kölker S.

'Genetic cause and prevalence of hydroxyprolinemia'.

J Inherit Metab Dis. 2016 Sep;39(5):625-632. [doi: 10.1007/s10545-016-9940-2](https://doi.org/10.1007/s10545-016-9940-2)

8.

ACKNOWLEDGEMENTS

8. Acknowledgements

I am grateful to Prof. Dr. med. Stefan Kölker for giving me the opportunity to work on this project. His timely advice, criticism and praise have truly made the project, as well as me, as a scientist much better. I thank him for believing in me and supporting me financially. I would like to acknowledge Prof. Dr. Marc Freichel for his support as a member of my thesis advisory committee and as the first referee of my thesis. I would like to also thank Prof. Dr. Matina Muckenthaler for her support as a member of my thesis advisory committee. I offer my deep sense of gratitude to P.D. Dr. Sven Sauer, my mentor for his constant presence and for his fundamental support personally and professionally during each and every stage of my PhD journey. Thank you Sven for being there with me through out the whole process. I offer my gratitude to Dr. Juergen Ökun and Dr. Claus Deiter Langhans , who enabled me to use the Mass spectrometry facility. I would like to thank the technical support offered by Mr. Kratzer Frank and Katherine Schmidt for all the mass spectrometric measurements. I am indebted to Dr. Obulreddy Bandapalli, Dr. med. Kerstin Grund and Prof. Dr. Andreas Kulozik for indirectly playing a major role in building my personal and professional life. I am very thankful to Dr. Ashish Goyal for being so kind and helping me out with few CRISPR experiments. I acknowledge the funding provided by DFG grant. I express a big thank you to my colleagues Monica, Amol, Jidnyasa, Sonja Exner, Sonja, Steffi, Dorothea, Bianca, Virginia, Dr. Dominic Lenz, Prof. Peter Burgard, Sabine, Michelle, Mohammad, Tim, Prof. Verena Peters, Katherine Jeltsch, for making this journey easy and fun. I would like to also thank my friends Shanmukh, Santosh, Venu, Mahesh, Lavanya, Priyanka for creating a homely stay in Heidelberg. I would like to express my deep sense of love for my German families of Sib, Oscar, Lilo, Simone and of Michael Machado, Evelyn, Sharel and Jupp for being there with me always. Lastly, I am hugely indebted to Jagadeesh, my mother, father, sisters and grandfather, without whom I am nowhere.